

USE OF PRESTRESSED CONCRETE PANELS AS ROOFING ELEMENTS

624.183
1991
MAI

A thesis

by

MAINUDDIN AHMED



Submitted to the Department of Civil Engineering of Bangladesh
University of Engineering and Technology, Dhaka
in partial fulfillment of the requirements for the degree
of

MASTER OF SCIENCE IN CIVIL ENGINEERING



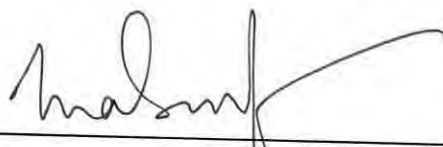
#82253#

August 1991.

USE OF PRESTRESSED CONCRETE PANELS AS ROOFING ELEMENTS


A thesis
by
MAINUDDIN AHMED

Approved as to style and content by:



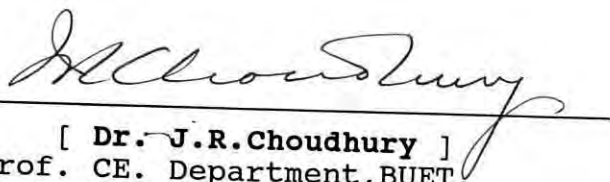
[**Dr. M . A . Rouf**]
Prof. CE. Department, BUET.

Chairman.



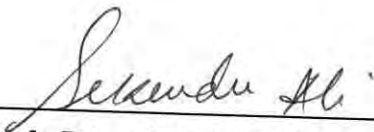
[**Dr. M. Feroze Ahmed**]
Prof. and Head, CE. Department, BUET.

Member.



[**Dr. J.R. Choudhury**]
Prof. CE. Department, BUET.

Member.



[**Dr. SK. Sekender Ali**]
Assoc. Prof. CE. Department, BUET.

Member.



[**Dr. Mizanul Haq**]
House No. 59, Road No. 3/A.
Dhanmondi R/A, Dhaka.

Member
(External).

SYNOPSIS

Results of multi-beam precast prestressed concrete slab panels with cold-drawn low-carbon steel as prestressing reinforcement are reported in this thesis. The multi-beam slab system is attractive for construction of a flat two-dimensional structure. The system combines the ease of fabrication of one-dimensional elements with bi-directional efficiency of the plate. There are two types of multi-beam slabs namely, a) composite slab, and b) pseudo-slab.

In this study a total of 19 slab panels divided into four types were constructed for carrying out laboratory test. The slab type-I, slab without shearkeys without topping, comprised only one slab panel and slab was loaded with uniformly distributed load by piling the iron blocks on it.

Each of other three types comprised six pieces of prestressed concrete slab panels of width 25 inch and length 102 inch. The slab panels were jointed together by filling gaps between two adjacent slab panels forming a complete slab, so that, the imposed loads on slab were distributed in two perpendicular directions.

To test these types of slabs a reaction frame of capacity 720 psf. was fabricated in concrete laboratory of BUET, Dhaka. Water pressure bag had been utilized to exert uniformly distributed load on the slabs. The tests had been conducted to investigate the deflection pattern, cracking and ultimate load

capacity, crack patterns and mode of failure of slab system.

The experimental load-deflection curve of slab without shear keys without topping is identical with the calculated deflection curve computed by using $M-\phi$ curve in elastic as well as plastic ranges.

It was observed that the first hair cracks of the slab with shear keys without topping designed as Type-II, slab without shear keys with topping, Type-III and slab with shear keys with topping, Type-IV, were visualized in the joints (shearkeys) rather than in the maximum moment region. Thereafter cracks propagated along the joints to the supports causing separation of the slab panels from one another.

It was also observed that behavior of the slab with shear keys and without topping, Type-II, was closely represented by the behavior of a one-way slab system.

Within service load, the slab without shear keys and with topping, Type-III and slab with shear keys and with topping, Type-IV, were observed to behave neither like a one-way nor a two-way slab system but their behavior lie in between the two systems.

In four types of slabs the first cracks appeared in the region of maximum moment at a load closes to that estimated by the elastic theory. Almost four types of slabs were found to attain the failure loads near to the values obtained by the ultimate strength theory.

ACKNOWLEDGEMENT

The author wishes to express his heartfelt gratitude and sincerest indebtedness to Dr. M. A. Rouf, Professor, Department of Civil Engineering, Bangladesh University of Engineering and Technology, Dhaka for his guidance, encouragement and constant supervision at all stages of this research.

Sincere gratitude is due to Dr. Alamgir M. Haque, Professor of Department of Civil Engineering BUET, Dr. Shamim Z. Bousunia, Professor and Dean of Civil Engineering, BUET and Dr. J. R. Choudhury, Professor of Department of Civil Engineering for their kind interest and encouragement. Their valuable suggestions and constant encouragement have brought this to the brink of manifestation.

The author wishes to thank Dr. Alamgir Habib, Professor of Civil Engineering Department and Dr. Humayun Kabir, Professor of Civil Engineering Department for their encouragement and help at different stages of this research project.

Sincere appreciation is expressed to acknowledge the valuable service rendered by Messrs. Barkattulla, A. Karim, B. Rozario, A. Barek and other staff members of the laboratories of BUET and Messrs. Md. Abul Hossain, Md. Abdur Rahman and Md. Mosharraf of Housing & Building Research Institute, Dhaka.

The author is also grateful to his family members and his colleagues for their considerate attitude and profuse inspiration without which this study could have never materialized.

Heartiest thanks are expressed to Engr. Md. Abdus Salam, Research Engineer of Housing & Building Research Institute for helping in editing and printing the thesis, to Messrs. Abdur Rahim Khan and Abdul Alim for typing the thesis and to Mr. Mostafizur Rahman for drawing the figures.

CONTENTS

Description	Page
Synopsis.	i
Acknowledgement.	iii
Contents.	iv
List of Figures.	viii
List of Tables.	x
Notation.	xi

Chapter-1:	INTRODUCTION.	1
1.1.	General.	1
1.2.	Historical Background.	2
1.3.	Process of Cold-drawing of Low-carbon Steel.	3
1.4.	Present State of Art of the Research Topic.	5
1.5.	Objectives.	8
1.6.	Justification.	9
1.7.	Brief Description on the Procedure/ Methodology.	11

Chapter-2:	REVIEW OF LITERATURE.	12
2.1.	General.	12
2.2.	Conventional Prestressed Concrete Slab.	12
2.2.1.	Study of Magnel's approach.	12
2.2.2.	Investigation performed by Scordelies, Pister and Lin.	13

2.3.	Metz's Investigation on Conventional Reinforced Concrete Slabs.	15
2.4.	Chinese Approach of Evaluating Cold-drawn Low-carbon Steel Prestressed Concrete Elements.	16
Chapter-3:	AVAILABLE THEORIES AND DESIGN METHODS.	17
3.1.	General.	17
3.2.	Simply Supported Prestressed Concrete.	17
3.3.	Flexural Behavior and Strength of Prestressed Concrete Slab.	18
3.3.1.	Introduction.	18
3.3.2.	Behavior of prestressed concrete slab.	18
3.3.3.	Elastic theory in designing the slab.	19
3.3.4.	Prasado Rao's approach.	21
3.3.5.	Metz's approach.	22
3.3.6.	Somayaji's approach.	23
3.3.7.	Morris' approach.	26
3.4.	Multi-beam Slab, Method of Analysis.	28
3.4.1.	Introduction.	28
3.4.2.	Duberg, Khachaturian & Fradinger's method.	29
3.4.3.	Lee's method of analysis.	34
3.5.	Deflections of slab elements.	37
3.5.1.	Deflection of one-way floor system.	37
3.5.2.	Short-time deflections.	38
3.5.3.	Deflection of two-way floor system.	41
3.6.	Distribution of flexural stresses in simply supported Rectangular Prestressed slab.	44

Chapter-4:	LABORATORY INVESTIGATION.	46
4.1.	General.	46
4.2.	Properties of Cement.	48
4.3.	Properties of Aggregates.	49
4.3.1.	Coarse aggregate.	49
4.3.2.	Fine aggregate.	50
4.4.	Design of Concrete Mix.	51
4.5.	Compressive Strength and Modulus of Elasticity of Concrete.	52
4.6.	Split Cylinder Test.	54
4.7.	Properties of Reinforcement.	54
4.8.	Construction of Test Slabs.	56
4.9.	Fabrication of Testing Platform.	58
4.10.	Testing of Slab.	61
4.11.	Testing of Cylinders.	63
Chapter-5:	TEST RESULTS.	66
5.1.	General.	66
5.2.	Test Results.	66
5.3.	Load Deflection Record.	67
5.4.	Cracking Pattern.	68
Chapter-6:	ANALYSIS AND DISCUSSION OF TEST RESULTS.	72
6.1.	General.	72
6.2.	Moment-curvature Relationship.	72
6.3.	Load-deflection Characteristics.	74
6.3.1.	Theoretical calculation of deflection for one-way slab.	75
6.3.2.	Theoretical calculation of deflection for two-way slab.	77

6.4.	Load-deflection Behavior of Slab Type-I.	77
6.5.	Load-deflection Behavior of Slab Type-II.	81
6.6.	Load-deflection Behavior of Slab Type-III.	85
6.7.	Load-deflection Behavior of Slab Type-IV.	90
6.8.	Discussion on Deflection Profile of Test Slabs.	93
6.9.	Cracking Load Characteristics.	100
6.10.	Ultimate Load Characteristics.	103
6.11.	Cracking Pattern.	105
6.12.	Mode of Failure.	105
Chapter 7:	CONCLUSIONS AND RECOMMENDATIONS FOR FUTURE STUDIES.	106
7.1.	Conclusions.	106
7.2.	Recommendations for Future Studies.	108
	List of References.	109
	Appendix 1.	112
	Appendix 2.	114
	Appendix 3.	119
	Appendix 4.	123
	Appendix 5.	127
	Appendix 6.	138

LIST OF FIGURES

Fig. No.	Description	Page
1.1	The metallographic photograph of wire.	3
1.2	Stress-strain curve of coil rod.	4
1.3	Relation between the total percentage reduction and properties of steel.	5
3.1	Interaction diagrams for one and two critical sections.	24
3.2	Design space diagram.	27
3.3	Idealized structure.	31
3.4	Typical section of composite slabs.	32
3.5	Typical section of pseudo slabs.	32
3.6	System of labeling panels and joints.	34
3.7	Positive directions for forces & displacements.	35
3.8	Stress and strain distribution immediately after application of the prestressing force.	38
3.9	Variation of curvature with span.	40
3.10	Deflection versus time due to prestress and load.	40
3.11	Stress distribution in concrete by the elastic theory.	45
4.1	Types of slab panels used in laboratory investigation.	45
4.2	Stress-strain curve of concrete.	53
4.3	Stress-strain curve of cold-drawn steel.	55
4.4	Plan of reaction frame for testing the slabs.	59
4.5	Section of reaction frame.	60
4.6	Setup arrangement of slab Type-I.	61
4.7	Photograph of test setup of slab Type-I.	62
4.8	Photograph of test setup of slab Types II, III & IV.	64
4.9a	Locations of deflectometers for slab Type-I.	64
4.9b	Locations of deflectometers for slab Types II, III & IV.	65

5.1	Crack patterns of slab Type-I.	69
5.2	Crack patterns of slab Type-II.	70
5.3	Crack patterns of slab Type-III.	70
5.4	Crack patterns of slab Type-IV.	71
6.1	Moment-curvature curve.	74
6.2	Load-deflection curve of slab Type-I (calculated by elastic method).	78
6.3	Load-deflection curve of slab Type-I (calculated from M- ϕ curve).	79
6.4	Loading and unloading cycle of slab Type-I.	80
6.5	Load-deflection curve for the point 1,3,7,8 of slab Type-II.	82
6.6	Load-deflection curve for the points 2,6 of slab Type-II.	83
6.7	Load-deflection curve for the points 4,5, of slab Type-II.	85
6.8	Load-deflection curve for the points 1,3,7,8 of slab Type-III.	87
6.9	Load-deflection curve for the points 2,6 of slab Type-III.	88
6.10	Load-deflection curve for the points 4,5 of slab Type-III.	89
6.11	Load-deflection curve for the points 1,3,7,8 of slab Type-IV.	91
6.12	Load-deflection curve for the points 2,6 of slab Type-IV.	92
6.13	Load-deflection curve for the points 4,5 of slab Type-IV.	94
6.14	Deflection profile of slab Type-I.	95
6.15	Deflection profile of short span of slab Type-II.	96
6.16	Deflection profile of long span of slab Type-II.	96
6.17	Deflection profile of short span of slab Type-III.	97
6.18	Deflection profile of long span of slab Type-III.	98
6.19	Deflection profile of short span of slab Type-IV.	99
6.20	Deflection profile of long span of slab Type-IV.	99

LIST OF TABLES

Table No.	Description	Page
4.1	Some physical properties of cement.	48
4.2	Grading of coarse aggregate.	49
4.3	Some physical properties of coarse aggregate.	50
4.4	Grading of fine aggregate.	50
4.5	Some physical properties of fine aggregate.	51
4.6	Cylinder crushing strength.	52
5.1	Properties test slabs.	67
5.2	Some properties of concrete of test slabs.	67
5.3	Observed cracking & ultimate loads of slabs.	67

Notations

A	cross sectional area in general.
A_{ps}	cross-sectional area of prestressing steel.
A_c	net cross-sectional area of concrete.
a	lever arm.
b	width of cross-section of slab.
C	center of compressive force.
c	distance from c.g. of concrete to extreme fiber.
c_b, c_t	c for bottom (top) fibers.
d	depth of slab.
E	modulus of elasticity in general.
E_c	modulus of elasticity of concrete.
E_{ps}	modulus of elasticity of prestressing steel.
e	eccentricity.
F, F_e	total effective prestress after deducting losses.
F_i	total initial prestress before transfer.
F_o	total prestress, just after transfer.
f	unit stress in general.
f_r	modulus of rupture of concrete.
f_c	unit stress in concrete.
f'_c	ultimate unit stress in concrete.
f'_{ci}	ultimate unit stress in concrete, at transfer.
f_i	initial unit prestress in steel before transfer.
f_o	unit prestress in steel, just after transfer.
f_e	effective unit prestress in steel after deducting losses.
f_{pu}	ultimate unit prestress in steel.
f_t, f_b	fiber stress at top (bottom) fibers.
G	shear modulus of elasticity .

h	thickness of slab.
I	moment of inertia of cross-section.
J	torsion constant.
K^w, K^θ	kernel function co-efficient.
k_t, k_b	top (bottom) kern distances.
L	span length.
M	moment in general.
M_{cr}	cracking moment.
M_L	moment due to total live load only.
M_G	moment due to girder load.
M_T	moment due to total load.
n	modular ratio.
P	total distributed load.
p_j	load on element j .
q	distributed load.
S_t, S_b	section modulus.
s	slope / unit impulse torque.
T	total tension in prestressed steel.
t	torque in general.
V	total shear.
w	deflection of slab.
ϵ	unit strain in concrete.
ϵ_t	top fiber strain.
ϵ_b	bottom fiber strain.
∇_r	backward difference operator.
θ	rotation.
σ	stress.
ϕ	curvature.

CHAPTER 1

INTRODUCTION



1.1 General:

Prestressing of concrete is a technique, by which the permanent internal stresses are introduced in members in order to neutralize, to a desired degree, the undesirable stresses for the purpose of improving its behavior and strength. Conventional prestressed concrete combines high strength steel and high strength concrete in an active manner. This is achieved by tensioning the steel and holding it against the concrete, thus putting the concrete into compression.

One of the best definitions of Prestressed Concrete is given by the ACI Committee on Prestressed Concrete:-

"Concrete in which there have been introduced internal stresses of such magnitude and distribution that the stresses resulting from given external loadings are counteracted to a desired degree. In reinforced concrete member the prestress is commonly introduced by tensioning the steel reinforcements".

The basic principle of prestressing was applied to construction perhaps centuries ago, when ropes or metal bands were wound around wooden staves to form barrels. When the bands were tightened they were under tensile prestress which in turn created compressive prestress between the staves and enabled them to resist hoop tension produced by internal liquid pressure.

1.2. Historical Background:

The principle of prestressing was not applied to concrete until about 1886, when P.H. Jackson, an engineer of San-Francisco, California, obtained patents for tightening steel tie rods in the artificial stones and concrete arches to serve as floor slabs. In 1888, C.E.W. Doehring of Germany independently secured a patent for concrete reinforced with metal that had tensile stress applied to it before the slab was loaded.

It was E. Freyssinet of France who made the first specific contribution to prestressing, in 1928, as it is today. After studying creep and shrinkage of concrete he understood the essence of losses of prestress in reinforcement and began to use high-tensile wires as prestressing steel.

Instead of using high tensile steel as tensioned reinforcement, mild steel having low-carbon has been adopted, since 1965 in Peoples' Republic of China, as tensioned reinforcement for prefabricated prestressed concrete members of medium and small building elements after slight modification of steel wire by cold-drawing system [2]. It has been widely

applied in Zhejiang, Jiangsu, Sichuan, Shandong and Guangdong provinces of China both in urban and rural construction, especially for residential buildings.

1.3. Process of Cold-drawing of Low-carbon Steel:

The process of cold-drawing of steel is one of the techniques of cold process. Through this process, the steel can be strengthened. Plastic deformation of steel takes place after cold processing, which enables its crystals to arrange in fibrous form along the direction of processing, and at the same time, the strength of the steel under process can be enhanced due to the increase of dislocation density. As the process takes place, the steel is subjected to tension in longitudinal direction and compression in radial direction, thus, its crystals are lengthened. The above phenomenon can be found from the metallographic photographs as shown in Fig.1.1.



Before Cold Drawing



After Cold Drawing

Fig.1.1. The metallographic photograph of wire(amplification 200) [2].

Owing to the change of crystal structure in steel, great changes in properties of the steel would happen. The process would result in the enhancement of strength and reduction of plasticity of steel. The typical stress-strain curve is shown in Fig. 1.2.

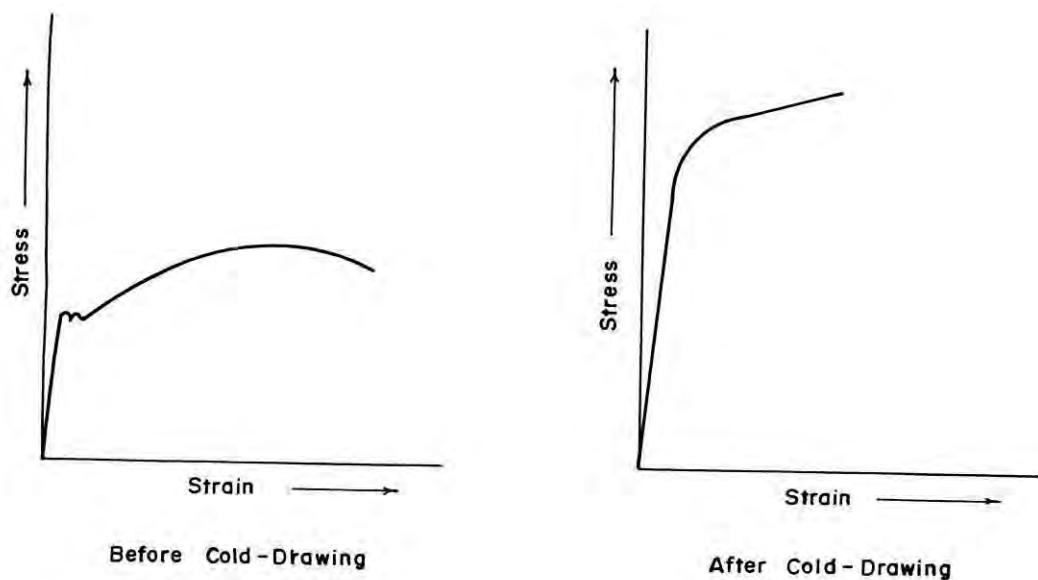


Fig.1.2. Stress-strain curves of coil rod.

The changes of properties of steel, after cold-drawing process, is closely related to the total percentage reduction of steel area. The higher the total percentage reduction, the greater the changes of properties of steel. The relation between the physical properties of steel and the total percentage reduction of area of steel is shown in the Fig.1.3.

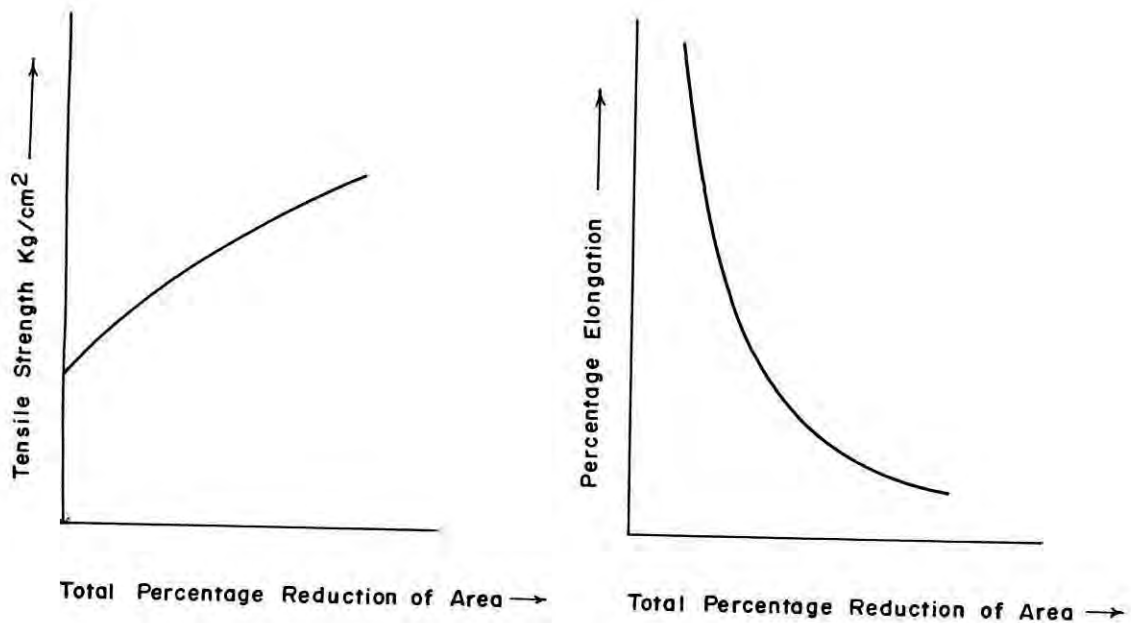


Fig.1.3.Relation between the total percentage reduction and the properties of steel.

1.4. Present State of Art of the Research Topic:

On the basis of trial performance for a considerable period in several provinces and municipalities in China, 'Tentative Code on Cold-Drawn Low-carbon Steel Wire Prestressed Concrete Members of Medium/Small Size' was documented and published in 1977 [2]. It was thoroughly revised in 1982, and was approved by the Ministry of Urban-Rural Construction and Environmental Protection of People's Republic of China in May, 1983 [2]. At present, this is a document on designing, manufacturing and constructing the cold-drawn low-carbon steel wires prestressed concrete members in China.

A book on 'Design and construction of cold-drawn steel wire Prestressed Concrete Members' was published in the year of 1980

[as referred in reference 2]. In this text, comprehensive recommendations on relevant problems in the design and construction of cold-drawn low-carbon prestressed concrete members are furnished.

A hand book on 'A Compilation of Standard (Typical) Drawings for Cold-Drawn Steel Wire Prestressed Concrete Members' was published in China [as referred in reference 2]. The typical and standard drawings of the structural members of hollow-cored slab, lintel, rafter, plates, gutter, channel shaped slab, folded plate, saddle shell, door and window frame, pole and roof slab were compiled and documented in this text. By using these typical and standard drawings the design work is simplified.

The results obtained from laboratory tests and field investigations of cold-drawn low-carbon steel wire prestressing members in various fields such as building materials, properties of members, design, construction and manufacturing were compiled in the text on 'Selected Research Reports on Cold-drawn low-carbon Steel Wire Prestressed Concrete Technology' [as referred in reference 2].

All of these documents and information have played an important role in developing the cold-drawn low-carbon steel wire prestressing technology.

The technique of prestressed concrete had been introduced in bridges and precast prestressed concrete piles in Roads & Highways Department since pre-liberation period in this country.

Recently, Bangladesh Power Development Board is using prestressed concrete poles for electrification network.

In building construction, the following projects were completed, using prestressed concrete slab and other members:

- a. Karnaphuly Rayon Mill, Chittagong H.T.,
- b. Public Works Department Prestressed Concrete Workshop, Dhaka,
- c. Dhaka Medical College Hospital renovation work, Dhaka,
- d. A six-storied residential building of Housing & Settlement office at Baddah, Dhaka, as an experimental project,
- e. Jagannath College Hostel, Dhaka,
- f. Delta Tobacco Redrying Company Ltd., Kushtia,
- g. A rural model house, presented in Rural Housing Exhibition, 1990, Dhaka.
- h. Eurosol Industries Ltd., Rupshi, Narayanganj,
- i. Gardener sheds, Ramna park, Dhaka,
- j. Prestressed concrete piles for seven storied commercial building, Sonargaon road, Dhaka.
- k. An office building of Bangladesh Institute of Distant Education, Dhaka.

In the construction of last five projects, mentioned above, low carbon steel were used as prestressing reinforcement for slabs, beams, purlins, rafters and piles.

Advantages like high crack-resistance and stiffness, light weight, high durability, and low cost are observed in projects using prestressed concrete slab with low-carbon steel as prestressing reinforcement and people now-a-days are coming

forward to adopt the technology in their building construction. However, extensive studies are required for fruitful recommendations but so far, a few research work in this field had been carried out in this country. Housing & Building Research Institute, Mirpur, Dhaka has an extensive program in its hand for research, experimentation and implementation of prestressed concrete technology, particularly the strip slab, using low-carbon steel wire as prestressing reinforcement.

1.5. Objectives:

Housing is a great problem in Bangladesh for ever increasing population and for frequent natural disasters in two or three forms. About seven million new dwelling units to be constructed annually within the year of 2000 to meet the housing demand in Bangladesh [*Proceedings of the seminar on 'Low cost housing' held at Housing and Building Research Institute, Dhaka, on 2nd. Nov. 1983*]. The prices of the conventional construction materials like cement, steel, CGI sheets, timbers, bamboo etc. are increasing rapidly. In this situation the prestressed concrete using low carbon steel as prestressing reinforcement can play an important role by optimizing the use of available materials.

The main objective of the research work is to study the behavior of prestressed concrete strip slab using low-carbon steel as prestressing reinforcement.

1.6. Justification:

The low-carbon steel is easily available in the local market, and the cost of the low-carbon mild steel is cheaper as compared with the high strength steel which is imported one. Low-carbon mild steel, however, needs modification by cold-drawing process. This process would result in the enhancement of strength almost double than as the original strength of mild steel. From tensile test result of wire, after cold process, an average value of ultimate strength of 1,25,000 psi may be obtained. This is about 50% of the ultimate value of high strength steel.

Prestressed concrete is subjected to losses mainly due to creep, shrinkage of the concrete and relaxation of the steel. The creep of concrete and relaxation of steel are greatly related to the magnitude of prestressing force applied. As the applied allowable prestressing force is relatively lower in case of members prestressed with low-carbon steel, the creep of the concrete and relaxation of steel would be low and thus the loss of prestress would be smaller than members prestressed with high tension steel. It was therefore decided that the low-carbon steel is justified as prestressing reinforcement.

The strip slab consists of a number of prefabricated identical prismatic prestressed concrete slabs placed side by side. The connected points of two adjacent slabs have the same vertical displacement as well as same rotation with negative sign.

To transfer the shear from one strip to another, shear connectors (keys) are provided. The longitudinal shear keys are provided along the longitudinal side of the slab elements. The cross-section of shear keys are shown in the figures in chapter 3. According to Morley [21] the shears can be distributed through the negative reinforcement for any reinforcement orientation with respect to the sides of the two-way slab. In similar way shears may be distributed by providing the transverse reinforcement placed across connecting points.

The strip slabs are prefabricated identical prismatic prestressed concrete slabs, have advantages over the conventional prestressed two-way slab, such as:

- a. combines the ease of fabrication of one-dimensional element with bi-directional efficiency of the plate.
- b. construction process is very simple, i.e. ease of casting.
- c. the mould or formwork can be used repeatedly, thus saving supporting materials like timber, bamboo etc.
- d. quality can be controlled & ensured by providing all necessary measures.
- e. proper dimension can be maintained as the same mould with right dimension is used for casting the elements.
- f. all of the raw materials are available in the local markets.
- g. simplicity of equipments and devices for production.
- h. high crack resistance and stiffness, producing almost no crack under service load, thus the wires are well protected against corrosion.
- i. light in weight. Owing to greater stiffness of prestressing concrete members, the dimension of the cross-section can be

- reduced accordingly. This results not only in a reduction of concrete volume but also of the dead weight of the element.
- j. dead weight of the element being smaller, it can be carried and erected manually.
 - k. low-cost, since prestressed concrete elements have high stiffness, a reduction of cross-section of members are possible. A considerable amount of concrete can be saved. And hence work including transportation, handling and erection can be reduced.
 - l. may be provided for housing sectors as well as for industrial buildings.

To get the two-directional efficiency of plates, the experimental study to be carried out by the one-dimensional strip slab element. Hence it is justified to experiment with the strip slab.

1.7. Brief Description on the Procedure / Methodology:

- a. A few number of full scale prestressed concrete slab strips (2'-1" wide) of different thickness will be constructed using cold-drawn low carbon mild steel as prestressing steel.
- b. The slab panels will then be tested in the laboratory to study their load-displacement behavior, crack patterns and load carrying capacity.
- c. The experimental results obtained will then be presented along with other experimental & the numerical analysis available.

CHAPTER 2

REVIEW OF LITERATURE

2.1. General:

A review of literature reveals that significant attempts have been made to understand the pattern of stress distribution in conventional prestressed concrete flexural members under service load condition and to study the behavior and crack patterns of such members under ultimate load condition. Most of these efforts, however, concern prestressed flexural members having stone chips as coarse aggregate and high tensile steels as reinforcement but few number of study were performed on prestressed concrete slab having low-carbon steel as reinforcement and crushed stone as coarse aggregates. Until now, no study has been found concerned with prestressed concrete slabs, beams having crushed brick chips as coarse aggregate.

2.2. Conventional Prestressed Concrete Slab:

2.2.1 *Study of Magnel's [3] approach :*

The test was performed by Magnel [3], to determine the validity of the mathematical theory of elasticity for predicting the load at which the first crack would appear. The 70 mm thick slab was 3.50 m square, and was supported on roller-bearings along end sides so that the clear spans, parallel to the sides, were each 3.20 m apart. At each of the corners of the slab, weights were placed to prevent the corners lifting. The slab was prestressed

by 5 mm ϕ wires, in groups of four, at intervals of 15.0 cm along the sides.

The loads were applied by hydraulic jack over two areas, each 30 cm square, on an axis of symmetry parallel to one of the edges and equidistant from the center. Strain gauges were placed at frequent intervals on the lower surface of the slab near points of critical stresses. Other gauges were placed directly below the centers of the loads, at the middle of the slab.

The test was performed upto the ultimate failure of the test slab, and the following were concluded :

- As in simple and continuous beam, in prestressed slabs the theory of elasticity led to very accurate predictions of loads causing cracking.
- In elastic range the theory agreed very closely with the test.
- At loads near that causing cracking, it was expected that the agreement would be less favorable due to the presence of local yielding. But the load at which the cracks were evident to the eye were very close to the predicted load for cracking.
- The behavior of prestressed two-way slabs was in no way fundamentally different from that of ordinary reinforced concrete slabs.

2.2.2. Investigation performed by Scordelies, Pister and Lin [7]

The investigation of conventional prestressed concrete lift-slab method of construction considered the fundamental case of a square slab simply supported at the four corners under uniformly

distributed loads. The purpose of the investigation was to determine the behavior of slab through and beyond the elastic range.

The overall dimensions of the test slab was 15'-0" by 15'-0" in plan and was 5.0" in thick. Supports at the four corners were on 14.0' centers in both directions. A steel plate with a bearing area of 4.0" by 8.0" was used at each support. A rocker and roller arrangement was adopted to permit the necessary rotations and horizontal movement at the supports so that no restraint was introduced at these points.

Twenty four strain gauges were employed, 16 being placed on the bottom surface and 8 on the top surface of the slab to measure the deflections of respective places. The slab was uniformly loaded with air pressure acting against a steel frame. Air pressure from a compressed air system of the laboratory was introduced to the plastic bags resting on the test slab.

The test was performed until the ultimate failure of the test slab occurred. After performing the test they concluded:

- Prior to cracking of the slab, the classical elastic theory could be applied to obtain slab deflections and distribution of bending moments across the slab, as well as the stresses and strains in the concrete. Deflections and strains are based on some estimated value of the modulus of elasticity of concrete as obtained by cylinder tests.

- Cracking load for the slab could be predicted by the elastic theory within an accuracy of about 10 % , using the modulus of rupture obtained from beam specimens provided that the state of stress at the critical point was nominally uni-axial. Deflection, and strain readings indicated possible minute cracking of concrete sooner it than could be detected visually by magnifying glasses.

2.3. Metz's [8] Investigation on Conventional Reinforced Concrete Slabs:

The aim of the tests performed by Metz [8] was to compare the ultimate failure loads and failure patterns obtained from test results with those predicted by theory. A total of 16 model slabs of 0.875" thick were tested . The model slabs varied from a 12.0" square simply supported slab to a 24.0" by 36.0" simply supported rectangular concrete slab.

The testing machine used in the tests consisted of three lever bars. Loads were applied at the ends of the levers. These loads were transmitted to the slab through loading heads made up of simple beam levers pinned in the center, so that all point loads were equal and would follow the deflections of slab as the load was applied. The points were 0.75" round, 1.0" long wooden dowels spaced 3.0" each way to exert a uniform load approximately on the slab.

From the test results it was concluded :

- The failure crack patterns obtained from the tests were quite identical to the computed crack patterns.
- The ultimate failure loads of the slabs as compared to those predicted by theory were high and were a little scattered.

- Since there is no mathematical proof of validity of a yield-line pattern, a test would be very useful in doubtful cases.
- Even the most complex slab could be solved without too much difficulty, if the location of the yield - lines is known.

2.4. Chinese Approach [2] of Evaluating Cold-drawn Low-carbon Steel Prestressed Concrete Elements:

The purpose of the evaluation, essentially associated with the load tests, is to determine the quality of prestressed concrete elements. The load tests should be made to examine structural properties of members. The method of load tests are divided into three stages:

Test preparation involves random sampling to get the test sample; collection of the original data; inspection of the exterior appearance of test sample and positioning the test samples on supports.

Test program involves the loading, the samples are loaded either with jack for concentrated loads or iron blocks for uniform loads; for measuring deflections the strain gauges are placed on the bottom surface of sample at critical zones.

Test process involves the four stages of loading from preloading to ultimate failure of test sample.

After destruction of the test sample the experimental data are analysed and expressed in test report form. The test results are then compared with the test index for the individual test type.

CHAPTER 3

AVAILABLE THEORIES AND DESIGN METHODS

3.1. General:

The behavior of conventional prestressed concrete members, with high tensioned wire as reinforcement, under both service and ultimate load conditions are relatively better understood as compared to cold-drawn low-carbon steel wire prestressed concrete members. Numerous text books on conventional prestressed concrete design give theories for analysis and methods for designing the members. On the other hand, provision of empirical methods of design for members by cold-drawn wire for prestressing in the Chinese Code of Practice is a relatively recent development. Some of theories and design practices available in the literature are presented in the following articles.

3.2. Simply Supported Prestressed Slabs:

Prestressed concrete slabs used in civil engineering structures are of many types, to provide flat, useful surfaces such as for floors, roofs, decks etc. In its most basic form, a slab is a plate, the thickness of which is small relative to its length and width. Usually the thickness is constant. The slab may be supported by walls, concrete beams, structural steel beams or directly by columns with no beams or girders.

Wall or beam supported slabs may be supported along two opposite edges only, in which the structural action is essentially one-way. Loads applied to the surface are carried by the slab spanning in the direction perpendicular to the supporting edges. On the other hand, there may be supports on all four sides of the slab panel, so that, two-way action is obtained. These are known as simply supported prestressed slabs when they are pretensioned and rested freely on the supports, that is, not monolithically supported.

3.3. Flexural Behavior and Strength of Prestressed Concrete Slab:

3.3.1. Introduction:

In designing a simply supported slab, one of the following methods may be adopted. The methods are: (a) elastic analysis; (b) plastic (limit) analysis on the basis of an assumed yield-line mechanism (upper-bound method) or (c) plastic (limit) design on the basis of an assumed equilibrium system (lower-bound method).

3.3.2. Behavior of prestressed concrete slabs [13]:

In order to establish a reasonable basis for design of a prestressed concrete slab, it is necessary to know the relationship between the load and the resulting deformations for the entire range of load.

For a given slab and type of load, the relationship between the load and a particular deformation when the acting load varies

from zero to the magnitude corresponding to the complete collapse of the slab is a measure of the behavior of the slab. The term behavior of the slab, therefore, refers to the variation of deformations in the slab as the load is increased and at a certain point the slab fails in a particular way.

There are several ways in which a prestressed concrete member can fail. It can fail in the region of pure moment, or, in the region of combined stresses where the both shear and moment are present.

For prestressed concrete slab the failure is, generally, initiated in the region of pure moment. The failure in the region of pure moment can be controlled more accurately, and more strength and ductility may be obtained.

The behavior of prestressed concrete slabs varies with load. For low magnitudes of load the relationship between load and deformation is linear. As the load is increased beyond that corresponding to the cracking load, the properties of the slab section become a function of load, and the relationship between load and deformation becomes non-linear.

3.3.3. Elastic theory in designing the slabs :

According to Muspratt [14], if the design is based on elastic analysis and a permissible stress criterion, the analysis consists of the solution of the bi-harmonic equation for specified boundary conditions. Tedious calculations and curvilinear principal moment trajectories are obvious

disadvantages of this approach. However, the use of computers and piece-wise linearization of moment trajectories partially overcomes these difficulties.

The difficulties in designing by elastic theory are partially simplified by Lin [1]. In his approach, the method of preliminary design is based on the fact that the section is governed by two controlling values of external bending moment : the total moment considering the dead and live loads, which controls the stresses under the action of the working load (service load), and the girder load moment considering dead load only, which determines the location of the c.g of steel and the stresses at transfer.

From the law of static, the internal resisting moment in prestressed member, must equal the external moment. The internal moment can be represented by a couple, C and T, where T is the tensile prestress force in the steel and C is the compressive force at the center of compression on the concrete.

In the actual design of prestressed concrete sections, a certain amount of trial and error is inevitable.

Lin [1] concluded that three variables came into consideration in designing prestressed concrete members by elastic analysis. These variables are : (a) the general layout of the structure which must be chosen as a start but which may be modified as the process of design develops. (b) the dead weight of the member which influences the design but which must be assumed before embarking on the moment calculations. (c) the approximate shape

of the concrete section, governed by both practical and theoretical considerations, which must be assumed for the trial.

Because of these variables, it has been found that the best procedure is one of trial and error, guided by known relations which enables the final results to be obtained without excessive work.

3.3.4. *Prasado Rao's [15] approach:*

The approach gives a direct method for the design of short-span prestressed concrete members with or without fillets and having either straight or curved wires or tendons. It neither employed the usual trial and error techniques nor the curves of the efficiency factors. The solution given by Rao exactly satisfies the permissible stresses at transfer and service load stages. For the assumed or given values of the beam depth, the web width and the top and bottom flange thickness, Rao's method gives a section that employed minimum concrete area and hence employed minimum prestressing force also. This method utilizes the principles developed by Guyon [24], Chetty [25] and Saether [26], which give a minimum weight section using iterative techniques. On the other hand, Rao's method directly gives the sectional dimensions without any iterations. Moreover, there is a scope to simplify the expressions developed in his approach which may reduce the computational work. By employing this method the section so obtained gives minimum concrete area which reduces weight of the member, brings saving in the

erection and transportation costs, and thus leads to a minimum cost design.

3.3.5. Metz's [8] approach :

In designing the slabs Metz chose the yield-line theory, because this theory offers a method which is relatively simple, involve nothing more complex than algebra and simple partial differentiation. The algebraic equations may at times become cumbersome, but this can generally be overcome by approximate solutions. In solution of a given slab, a yield-line pattern is assumed and the slab is analyzed either by the equilibrium equations or work equations. The solution obtained from this analysis is correct if the assumed yield-line pattern is the correct failure pattern.

As a two-way slab is progressively loaded, yielding will initiate in the region of maximum moment, and yield-line will start to form. As the loading continues, the yield-lines lengthen, and a pattern is formed known as the yield-line pattern. When this yield-line pattern spreads to the edges of the slab, the slab fails with the slab parts rotating about the supports and the yield-lines acting as hinges.

The general shape of possible yield-line patterns may be determined from the following criteria : (a) individual slab parts are assumed to remain plane, (b) the yield-lines must be straight to maintain continuity between the slab parts, (c) the yield-line between two slab parts must pass through the

intersection of their axes of rotation, (d) an axis of rotation will usually lie in a line of support or pass through a column.

As the load on a slab is increased the steel yields in the region of maximum moment, the neutral axis rises, and the compression increases in the concrete until a secondary failure takes place in compression zone after large rotations occurs in the yield- lines.

3.3.6. Somayaji's [16] approach:

The design of prestressed concrete flexural member for service load criteria consists essentially of selecting the cross-sectional dimensions, location and amount of prestressing force such that the stresses at any point and at any stage are within the allowable limits. Somayaji's approach differs, in the sense that no preliminary estimation of the prestressing force or sectional dimensions is necessary, and the range of prestress is determined prior to determining the cross-sectional dimensions or section modulus. The use of the design equations requires a preliminary assumption of eccentricity ratio. Different equations are derived for different types of cross-sections for estimation of their thickness or section modulus.

In the proposed method of designing prestressed concrete flexure members, the suggested procedure for the determination of prestressing force and eccentricity requires the knowledge of construction and use of interaction diagrams.

The interaction diagram represented by the two variables namely prestress at transfer forms the Y-axis of the diagram and the product of prestress at transfer and the eccentricity ratio forms the X-axis of the interaction diagram. The slope of a line, such as OE drawn (Fig. 3.1) from the origin O, is called S-line. The line corresponds to a certain eccentricity ratio (e/h) for every point along this line. The permissible eccentricity ratio (e/h) can be computed, for an assumed or given cross-section, by knowing the minimum concrete cover. Using this computation a permissible S-line (as OF) can be drawn. If the S-line falls outside ABCD (as OF') and towards the X-axis the entire area bounded by points A, B, C, and D represents the valid domain. But, if the S-line falls inside area ABCD (as OF) and intersects the stress constraint lines at

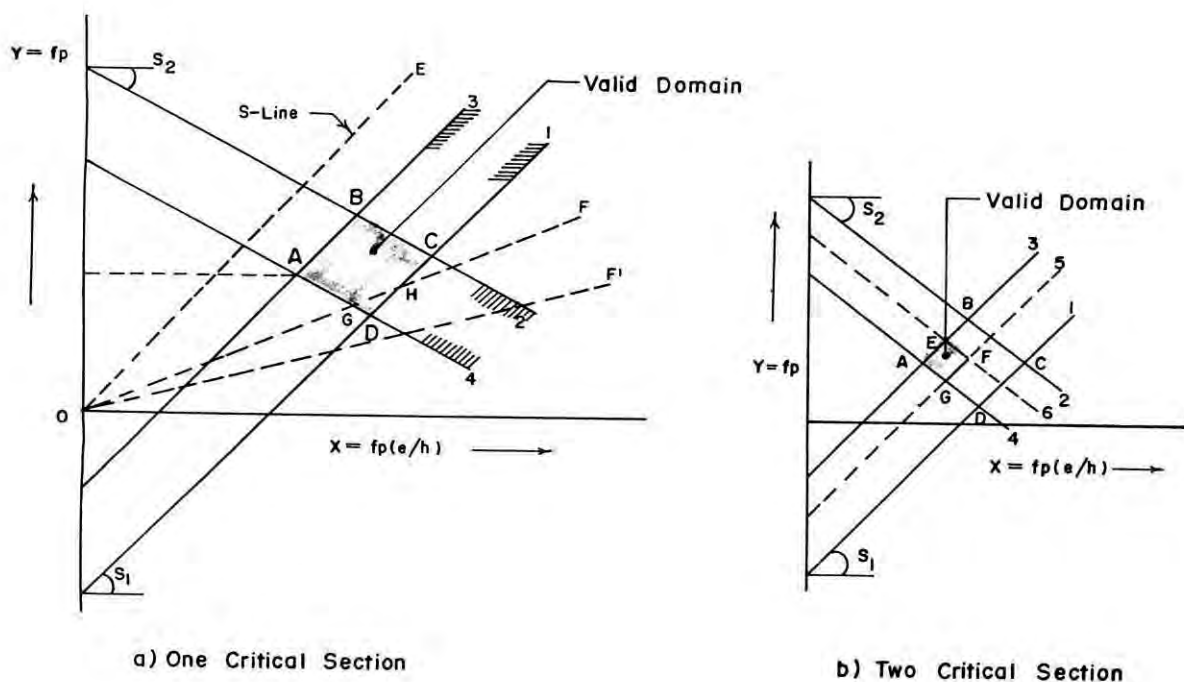


Fig.3.1. Interaction diagrams for one and two critical sections[16].

points G and H, the valid domain is reduced to that bound by points A,B,C,H, and G. But, on the other hand, if this line falls outside area ABCD and towards the Y-axis (as OE), it indicates that for the chosen cross-section there is no valid domain and has no practical solution. For a given or assumed prestress at transfer, f_o , one can draw a horizontal line as shown in Fig.3.1 to intersects the valid domain at points, such as A and H. The slopes of the S-lines that pass through these points give the lower and upper limits of eccentricity ratio. In addition, if the member consists of more than one critical section, the stress constraint equations for all critical sections can be drawn on the same interaction diagram.

The suggested method of design is aimed to determine a number of safe combinations of prestressing force and eccentricity. This procedure, common for all types of cross sections, involves the following:

- Determination of the prestress at transfer, f_p ,
- Estimation of thickness or section modulus from the stress constraint equations
- Calculation of stress range,
- Drawing of the interaction diagram, and identify the valid domain,
- Using the valid domain, various combinations of f_o and e/h can be determined and then corresponding F_i and e can be found out.

3.3.7. Morris' [17] approach:

The design of prestressed concrete members is relatively complex procedure that involves multiple loading conditions, time-dependent material behavior and service range plus ultimate strength investigations as discussed in the previous articles.

The purpose of Morris' study was to present a simple, direct and readily available linear programming solution to the most common prestress design problems. This is the determination of the adequacy of a given trial section, the termination of the minimum necessary prestressing force, and with the selection of the actual prestressing tendons, determination of the permissible prestressing zone. These solutions will be based on working stress, ultimate strength, and limiting reinforcement criteria.

In service load, flexural working stresses in a prestressed member must, in general, lie within the permissible limits set forth by design regulations these are :

$$f_{ci} \geq F_i/A - F_i e/S_t + M_G/S_t \geq - f_u \dots \dots \dots [3.1]$$

$$f_{ci} \geq F_i/A + F_i e/S_b - M_G/S_b \geq - f_u \dots \dots \dots [3.2]$$

$$f_c \geq F/A - Fe/S_t + M_T/S_t \geq - f_t \dots \dots \dots [3.3]$$

$$f_c \geq F/A + Fe/S_b - M_T/S_b \geq - f_t \dots \dots \dots [3.4]$$

To ensure that cross sections are not over-stressed, the prestressing force is limited by the specifications to :

$$A_{ps} f_{pu} \leq 0.30 bdf'_c \dots \dots \dots [3.5]$$

The flexural design requirements for both the working stress and the ultimate strength criteria are contained in the nonlinear relationship. If the properties of the trial concrete section are known and the loading criteria, allowable stresses, and performance factors are specified, then the remaining terms in these expressions are the prestressing forces, F and F_i and the eccentricity e .

We know that $F_i = F/\eta$ in which η is a specified ratio coefficient, then the unknown design variables can be reduced to F and e . If these are used to plot the preceding constraints, diagrams as shown in Fig.3.2a and Fig.3.2b will result.

It is evident from the Fig.3.2 that construction of curvilinear relationships and search for an optional solution can be a tedious task. Thus the graphical solution offers no advantage over conventional design procedures.

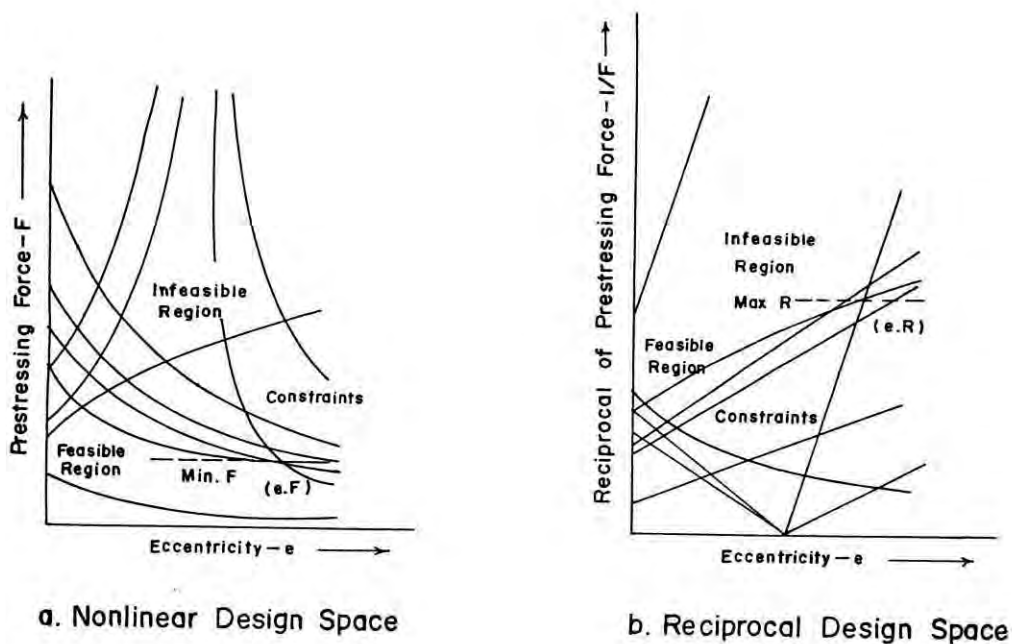


Fig.3.2. Design space diagram.

This problem can be solved by non-linear mathematical programming techniques. In this technique not only the concrete cross section can be determined but also the minimum necessary prestressing force and the permissible zone for the proposed or given force can be evaluated. Morris' method suggests a format for further design refinement to accommodate discrete component sizes, standardized geometric arrangements and other loading conditions. The unique nature of the working stress relationships, in terms of the unknown prestressing force and its eccentricity, allows for the design constraints to be linearized through the use of the reciprocal value of the prestressing force. The ultimate flexural strength and limiting percentage of reinforcement constraints are converted to low degree, non-linear functions by the substitution of reciprocal value.

3.4. Multi - beam Slab, Method of Analysis:

3.4.1. Introduction:

A multi-beam slab consists of a number of prefabricated identical prismatic reinforced or prestressed concrete slab panels placed side by side and connected by longitudinal shear connectors as shown in Fig. 3.3. Such a system is attractive for construction of a flat two-dimensional structure. It combines the ease of fabrication of the one-dimensional element with the bi-directional efficiency of the plate. There exist two types of slab systems :

Composite slab: The composite slab is one made of separate precast beams (with or without some form of shear key) with a continuous covering of in-situ concrete as shown in Fig. 3.4.

Pseudo-slab: The pseudo-slab is composed of separate precast beams, and transverse load distribution is obtained by means of concrete shearkeys and mild steel shear connectors or transverse prestressing as shown in the Fig.3.5. According to Cusens and Pama [20] the composite slab possesses more inherent transverse stiffness than the pseudo-slab.

The connecting points of two adjacent slab panels have the same vertical displacement as well as the same rotation with negative sign. To transfer the shear from one panel to another, shear keys are provided along the longitudinal sides of the slab elements. The details of shear keys are shown in the Figs. 3.3, 3.4 and 3.5. According to Morley [21] the shears can be distributed through the negative reinforcement for any reinforcement orientation with respect to the sides of the two-way slab. In similar way shears may be distributed by providing the transverse reinforcement placed across connecting points.

3.4.2. *Duberg, Khachaturian and Fradinger's [18] method:*

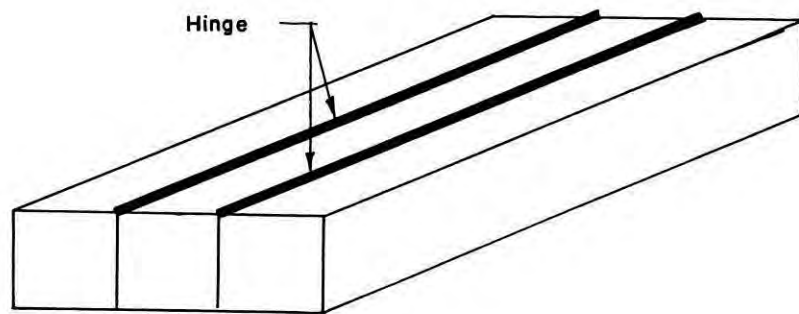
In the development of the theory for analysis of multi-beam slab the authors made following assumptions.

- The slab consisted of beam elements placed side by side and connected to each other along the span by hinges at the

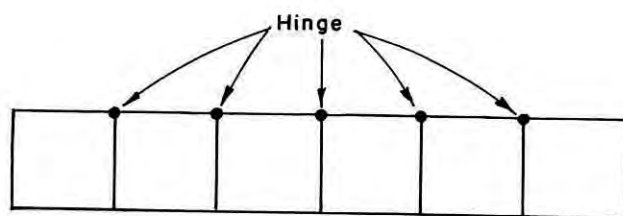
corners of the cross-section at the level of top fiber as shown in Fig. 3.3.

- The point of connection of any two adjacent beam elements would be a joint.
- Although the joints moved, at the components of movement and the rotation of each element at a joints were equal to those of adjacent element at the same joint.
- The slab was subjected to downward loads ,the beam elements deflected downward and rotated about the hinges causing a separation of elements at all points except at the hinge.
- The beam elements were made of a homogeneous, isotropic and elastic material.
- The shear strains were small could be neglected.
- The cross-section of each element was rigid.
- The beam elements were prismatic.

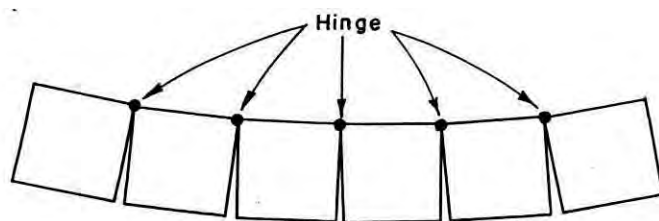
Considering an intermediate beam element, designated by j , between elements $j-1$ and $j+1$. The element j was subjected to the external load p_j as well as to statically indeterminate distributed forces which act on the element at joints j and $j-1$.



Oblique View

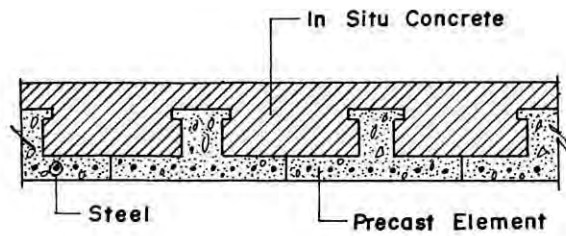


Cross Section

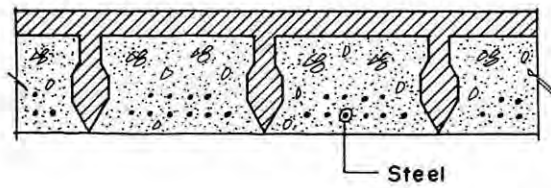


Deflected Shape

Fig.3.3. Idealized structure [18].

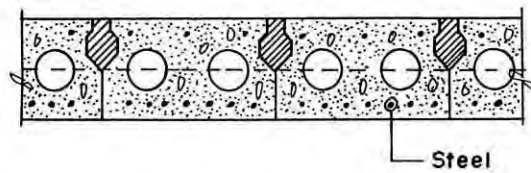


a) Inverted T Sections Forming A Composite Slab.

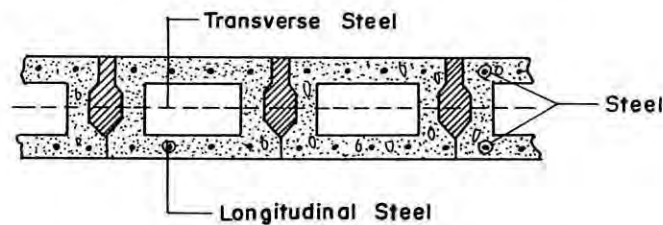


b) Rectangular Sections Forming A Composite Slab.

Fig.3.4. Typical section of composite slabs.



a) AASHTO Standard Beams Forming A Pseudo Slab.



b) Hollow Box Section Forming A Pseudo Slab.

Fig.3.5. Typical section of pseudo slabs.

According to usual engineering theory of bending and restrained torsion, the differential equations for the deflection of element j can be expressed as follows :

$$EI_{xy} \frac{d^4 w_{jz}}{dx^4} = p_{jz} \dots \dots \dots [3.6]$$

$$EI_{xz} \frac{d^4 w_{jy}}{dx^4} = 0 \dots \dots \dots [3.7]$$

$$-Ec \frac{d^4 \phi_j}{dx^4} + GJ \frac{d^2 \phi_j}{dx^2} = -t_j \dots [3.8]$$

$$EA \frac{du_j}{dx} = 0 \dots \dots \dots [3.9]$$

Only vertical concentrated loads were taken into account and it was pointed out that Eqs. 3.6 through 3.9 could be applied to beam elements of any cross-sectional shape [18]. The only external load acting on beam element j is the concentrated load p_j . In beam elements of solid or hollow square section, c, the torsion-bending constant, is small or zero so that the first term on the left side of the Eq.3.8 can be neglected.

In order to determine the normal and shearing stresses in each element, it is necessary to calculate the moments, shear, and torque which are carried by each beam element.

Authors concluded that the influence lines for moments about neutral plane in two-element and three-element multi-beam structures indicated the load was distributed almost uniformly among the elements. As one element was loaded all elements in

the bridge deflected almost same amount and they pointed out that two-element and three-element structures had no practical significance.

3.4.3. Lee's method of analysis:

To establish the mathematical model of multi-panel slab Lee [19] considered a multi-panel slab made up of m identical prismatic panels. Denoting the slab panels and joints by the discrete variable r as shown in Fig.3.6. Let the positive directions for the forces and displacements of the r -th slab panel be as shown in Fig.3.7. The equations of vertical deflection and torsion are given by

$$w(r,z) = [P(r,s) + \nabla_r V(r,s)]k^w(z,s)ds \dots \dots \dots [3.10]$$

$$\phi(r,z) = [M(r,s) + e(\nabla_r - 2)V(r,s)]k^\phi(z,s)ds \dots \dots \dots [3.11]$$

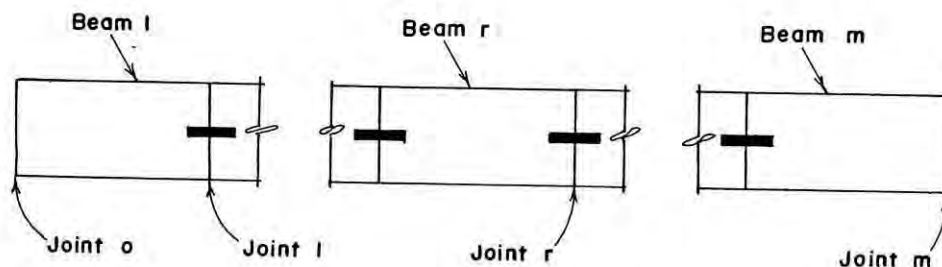


Fig.3.6. System of labeling panels and joints [19].

Where $k^w(z,s)$ is the deflection at z due to a unit impulse load at s and $k^\phi(z,s)$ is the rotation at z due to a unit impulse torque at s and also ∇_r is the first backward difference operator. It is necessary to expand the various force and displacement functions into infinite series and then

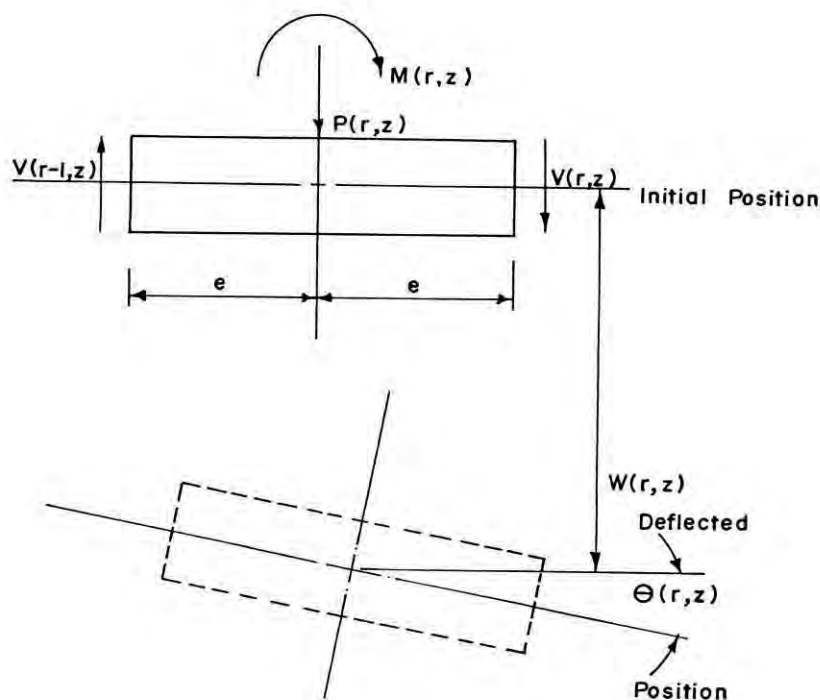


Fig.3.7. Positive directions for forces & displacements.

substituting the series into Eqs.3.10 and 3.11 give the force-deformation relations, in terms of co-efficient of infinite series as in Eqs.3.12 and 3.13.

$$w_i(r) = (Lk^w_i/2) [P_i(r) + \nabla_r V_i(r)] \dots \dots \dots [3.12]$$

$$\phi_i(r) = (Lk^\phi_i/2) [M_i(r) - (b/2) (\nabla_r - 2) V_i(r)] \dots \dots \dots [3.13]$$

These equations may be solved for two important boundary conditions. Assuming the finite series expressions and then inserting the series expressions into the governing equation for solving the free edge boundary conditions viz. $V_i(0) = V_i(m) = 0$, the equations are:

$$V_{ik} = - \frac{S_k P_{ik} + (\tau_i/e) C_k M_{ik}}{2(\tau_i C_k^2 + S_k^2)} \dots\dots\dots [3.14]$$

$$w_i(r) = \sum_{k=0}^{m-1} w_{ik} \cos \frac{k\pi(r-1/2)}{m} \dots\dots\dots [3.15]$$

$$\theta_i(r) = \sum_{k=1}^m \theta_{ik} \sin \frac{k\pi(r-1/2)}{m} \dots\dots\dots [3.16]$$

By utilizing the homogeneous solution and adding the effects of the loads and the boundary shears for solving the simply supported boundary condition along the joint lines $r = 0$ and $r = m$ we have the following expressions for the total effects.

$$V_i(r) = \sum_{k=0}^m (V_{ik} + V_{ik}^b V_{ik}^h) \sin \frac{k\pi r}{m} \dots\dots\dots [3.17]$$

$$w_i(r) = \sum_{k=0}^{m-1} (w_{ik} + V_{ik}^b w_{ik}^h) \cos \frac{k\pi(r-1/2)}{m} \dots [3.18]$$

$$\theta_i(r) = \sum_{k=0}^m (\theta_{ik} + V_{ik}^b \theta_{ik}^h) \sin \frac{k\pi(r-1/2)}{m} \dots [3.19]$$

The above equations developed by Lee have the advantage of giving a solution to multi-beam slab problem without recourse to time-consuming open-form method or to continuum analogies. Lee's mathematical model is simple, and the solutions are well suited for computation.

3.5. Deflections of Slab Elements:

3.5.1. Deflection of one-way floor system [4]:

In designing prestressed concrete structures the deflection under short-time service loads may often be the governing criteria in the determination of the required dimensions and amounts of prestress. A simply supported slab deflects upward under the action of the prestressing force and downward under the action of the transverse loads. The deflection may be defined with respect to two different reference lines : (a) the position of the element before the release of prestress or (b) the position of the element just before the application of load. The deflections of prestressed concrete elements are considered under two engineering definitions : (a) short-time deflection, and (b) long-time deflection.

Short-time deflections may be defined as those occurring instantaneously under the application of any internal or external force.

Long-time deflections refer to those existing at some time interval after prestressing or loading operation.

3.5.2. Short-time deflections:

The variables affecting the short-time deflections of a prestressed concrete element are : (a) the magnitude and distribution of the load, (b) the length of the span, (c) the dimensions and configuration of the cross-section, and (d) the quality of the concrete mixture. More specifically, the effect of critical variables may be summarized by the magnitude of the strain or stress gradient or the curvature at a section and the variation of this quantity along the span. The curvature at a particular section is defined by

$$\phi = \frac{\epsilon_b - \epsilon_t}{h} = \frac{M}{E_c I} \dots\dots\dots [3.20]$$

in which tensile strains are positive and compressive strains are negative.

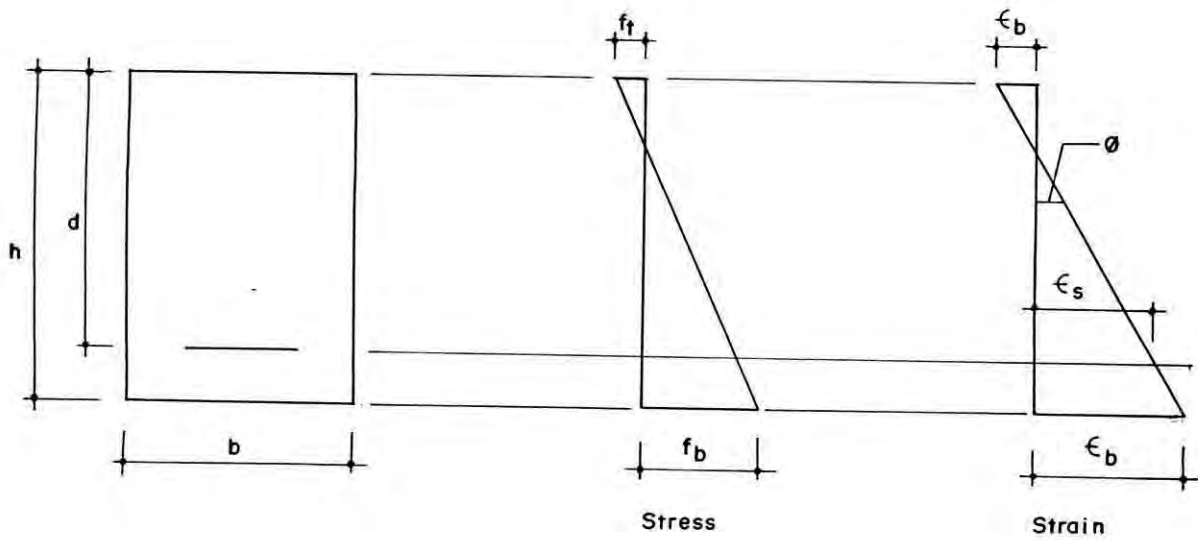


Fig.3.8. Stress and strain distribution immediately after application of the prestressing force.

In most cases the variations in the amount of prestressing steel affect the short-time deflections due to negligible transverse loads. The variations in the prestressing force do not affect the short-time changes in deflection at all, provided the concrete and the steel strains increase linearly with stress, as long as the element remains uncracked. The changes in the curvature or in the deflection of the slab caused by the prestress and the transverse load may be determined by superposition. Considering the uniformly loaded prestressed element, the curvature distribution on application of the load is as shown in Fig. 3.9. The curvature distribution in Fig.3.9. can be divided in two parts:

- a. a rectangular distribution caused by the straight tendon (Fig.3.9c), and
- b. a parabolic distribution (Fig.3.9d) caused by the uniform transverse load.

Both these curvature distributions will change with time. The deflections corresponding to these two imaginary systems are shown in Fig.3.10. Curve A shows the variation with time of the deflection caused by the prestress while curve B indicates the same variation for the transverse load. To determine the net deflection, the imaginary deflections caused by the prestress and transverse load can be added as shown in the Fig.3.10 by the broken curve. How much the element deflects and whether it deflects upward or downward all depends on the relative effect of the prestress and of the transverse loads.

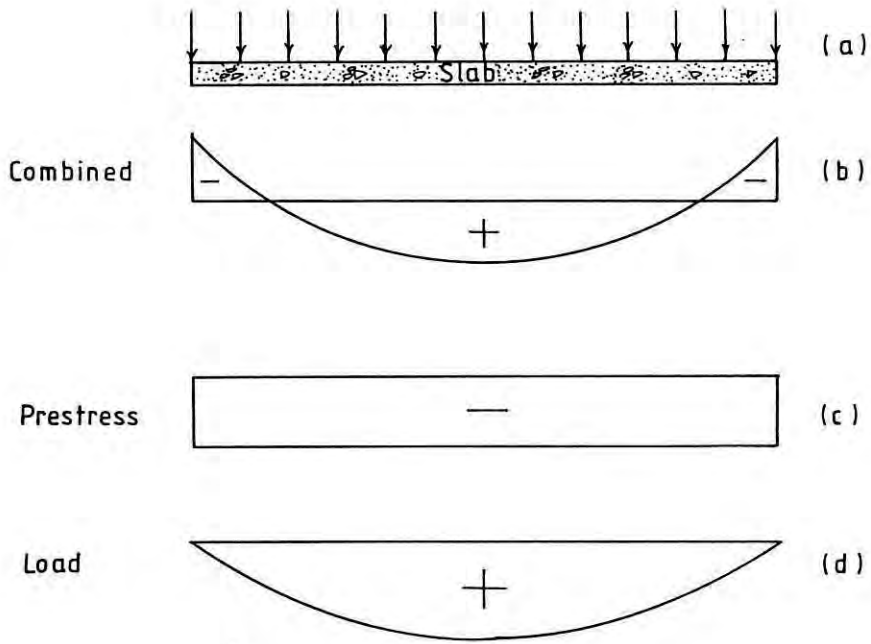


Fig.3.9. Variation of curvature with span.

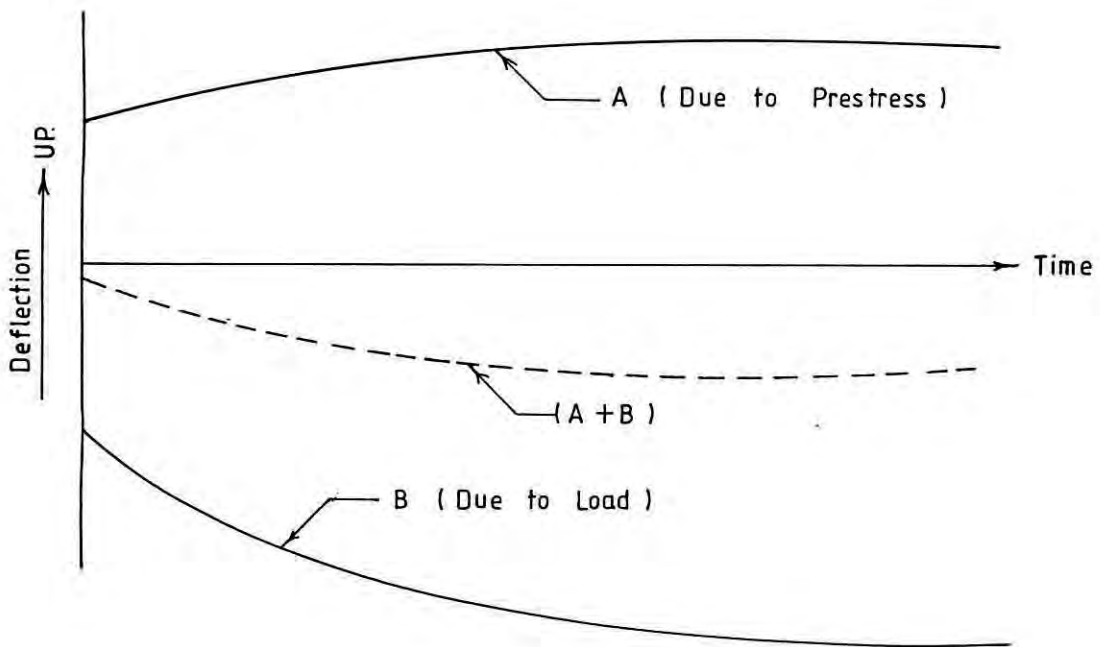


Fig.3.10. Deflection versus time due to prestress and load.

3.5.3. Deflection of two-way floor system [5]:

In deflection calculations for two-way systems, the size and shape of the slab panel, the conditions of supports, and the nature of restraint at the panel edges, should be taken into consideration. More over, what would be the slab moment of inertia to be used for deflection calculations ? That is an important question. According to the suggestion given by Branson [10], the effective moment of inertia being the weighted average of the moment of inertia of the gross concrete section as well as the cracked transformed section. The influence of creep and shrinkage is incorporated through use of multiplying factor, to be applied to calculate immediate deflection.

If stress levels are low, so that the normal assumptions made for the solution of the thin plates with small deflections are satisfied, the classical methods of analysis can be used to predict the deflections of slabs carrying distributed or concentrated loads.

The deflection of a thin, rectangular plate of uniform thickness can be expressed by the Lagrange equation.

$$\frac{\partial^4 w}{\partial x^4} + 2 \frac{\partial^4 w}{\partial x^2 \partial y^2} + \frac{\partial^4 w}{\partial y^4} = \frac{q}{D} \dots\dots\dots [3.21]$$

For a given loading condition $q = f_1(x,y)$, and the supporting conditions, the deflection $w = f_2(x,y)$ can be found by integrating Eq.3.21.

Due to complexities and limitations of the classical methods several attempts had been taken to device, simple but reasonably accurate methods, to obtain slab moments and deflections. In 1904, Marsh [11] suggested the replacement of uniformly loaded continuous slab panel by a grid work of cross-beams. The applied load is assumed to be divided the beams spanning in the short direction, A , and the long direction, B . By applying the requirement of equal vertical deflection at the center of panel, Marsh concluded that fraction of the uniformly distribution load q to be carried by the beam strips in the short direction was

$$r_s = B^4/[A^4 + B^4] \dots \dots \dots [3.22]$$

While the remaining load $(1-r_s)q$ was carried by the beam strips spanning in the long direction.

This result is approximate because it neglects the presence of torsional moments in the slab.

In 1952, a related method known as the "analogous gridwork method", was presented by Ewell, Okubo, and Abrams [12], represented a significant improvement over the crossing beam method considering the influence of torsional moments.

In this method, the slab is first divided into strips in each direction. These slab strips are then replaced by equivalent beams. The beam strips are assumed to be interconnected at their crossing points, the flexural and torsional properties of the beams are those of the corresponding slab strips. At each joint of the grid of beams, flexural and torsional stiffness factors are found in the usual way, finding the bending or torsional moment associated with a unit rotation of the near end of the member, the far end being fixed. Distribution factors for each member are defined as the ratio of member stiffness to total stiffness at the joint. Using the end moments so obtained, the vertical reactions at each joint are found. These represent "auxiliary forces" required to hold the gridwork in the displaced configuration for which the starting moments are found. The total moments, torques, and vertical reactions at each joint are found by adding the contributions associated with each joint displacement and the total reactions are equated to the actual external joint loads. In this way, a set of simultaneous equations is created, in terms of the arbitrary joint displacements. These equations are solved for these unknown displacements. Then actual bending and twisting moments as well as displacements may easily be found.

The finite element method provides a powerful tool for the analysis of concrete slab systems when computer facilities are available. By finite element analysis, the slab is divided into a number of subregions, or finite elements. These are generally triangular, rectangular or quadrilateral in shape. They are considered to be interconnected only at discrete points called the nodes; these are usually at the corners of the individual

elements. Within each subregion defined by the element grid, the continuous displacement quantities are expressed in terms of a finite number of displacements or degrees of freedom at the nodes. For a rectangular plate bending element having 12 degrees of freedom

$$\{ A \} = [K_m] \{ D \} \dots \dots \dots [3.23]$$

where $\{D\}$ is a 12x1 column vector consisting of vertical displacements and rotations about each horizontal axis at each of the four corners, $\{A\}$ is a 12x1 column vector consisting of transverse forces and bending moments at the nodes, and $[k_m]$ is a 12x12 element stiffness matrix relating nodal forces and corresponding nodal displacements.

3.6 Distribution of Flexural Stresses in Simply Supported Rectangular Prestressed Slab:

In a prestressed concrete section under service load, as the external bending moment increases, the magnitude of C, and T remains practically constant, while the lever arm (a) lengthens almost proportionately. Since the location of T remains fixed, in a prestressed section the location of C varies, as the bending moment changes. Thus, when $M = 0$, $a = 0$, and C coincide with T.

Once the magnitude of T is known, the value of lever arm a can be computed for any value of external moment. Then the location of C can be determined.

The stress distribution throughout the entire prestressed section may be determined by the elastic as well as plastic theory. If C coincides with the top or bottom kern point, the stress distribution will be triangular, with zero stress at bottom or top fiber, respectively. If C falls within the kern, the entire section will be under compression and if it falls outside the kern, some tension will exist. When C coincides with c.g. of concrete, stress distribution will be uniform over the entire concrete as shown in Fig.3.11.

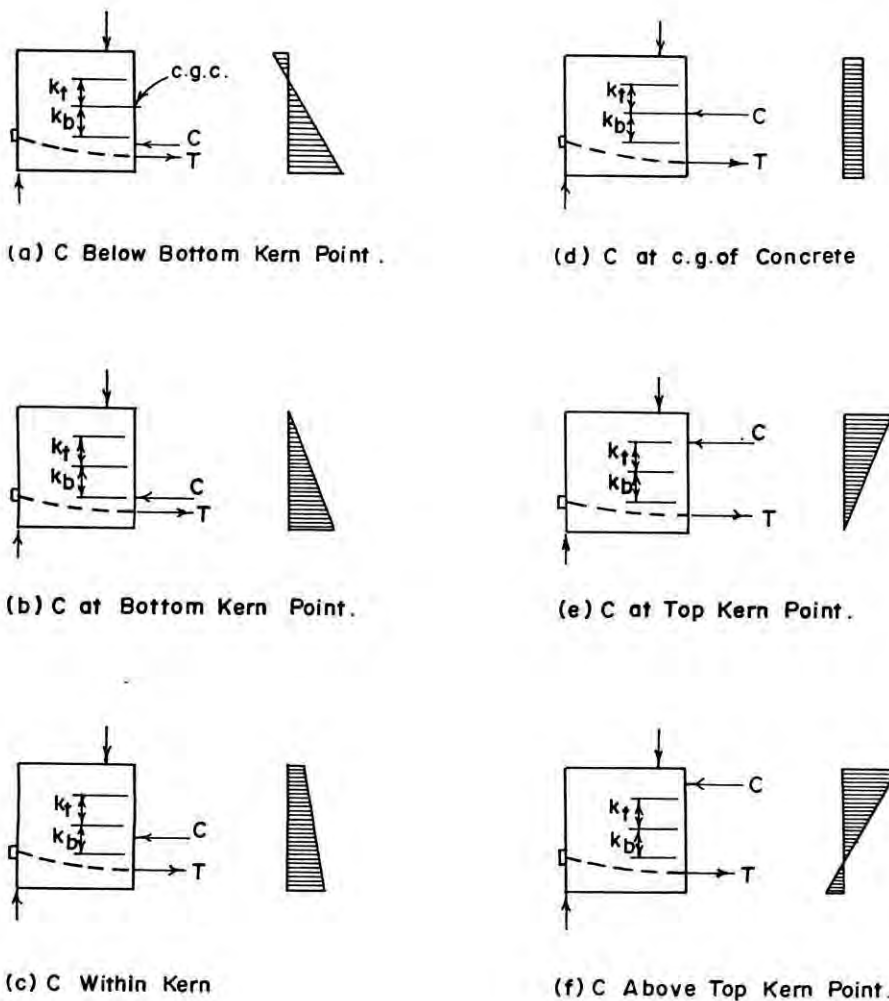


Fig. 3.11. Stress distribution in concrete by the elastic theory.

CHAPTER 4

LABORATORY INVESTIGATION

4.1. General

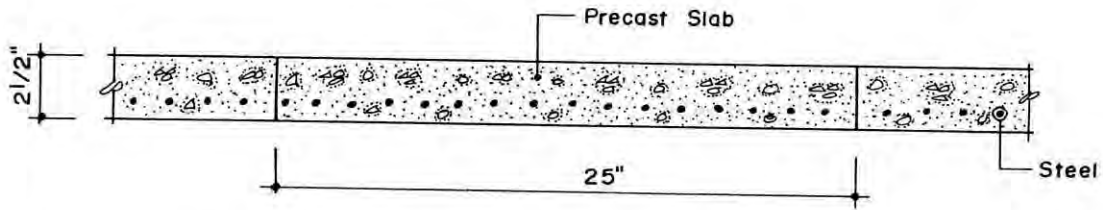
The investigation essentially included the experimental stage of the research study because the structural performance of a member is influenced by the properties of its constituent materials. This stage may be sub-divided into three phases.

The first phase is concerned with the determination of physical properties of aggregates, reinforcements for prestressing and design of concrete mix, specific gravity, absorption, unit weight, fineness modulus of coarse aggregates, yield strength and modulus of elasticity of prestressing wire, compressive strength and split cylinder strength of concrete .

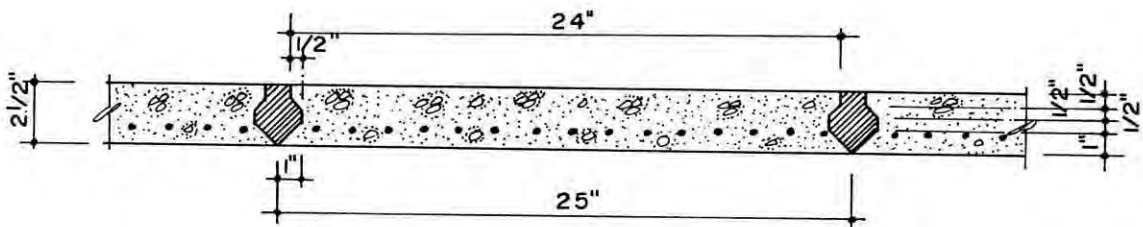
The second phase is concerned with the fabrication and casting of slabs. The jobs involved in the second phase were stretching the prestressing wires to a required stress, anchoring the wires with anchor beam, fitting & fixing the mould in position along casting bed, casting the slabs along with associated cylinders, curing and finally cutting of prestressing wires.

The third phase is concerned with the testing of specimens to investigate the relevant behaviors of interest : This phase was

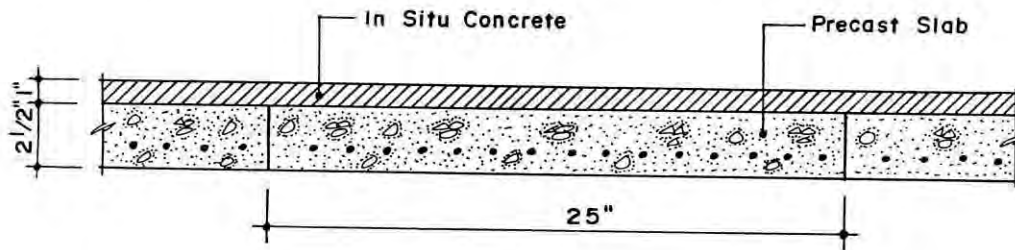
again subdivided into four series of tests, involving a total of nineteen simple span rectangular slab panels of 2'-1" in width, 8'-6" in length, and 2.5" in thickness, as shown in Fig.4.1.



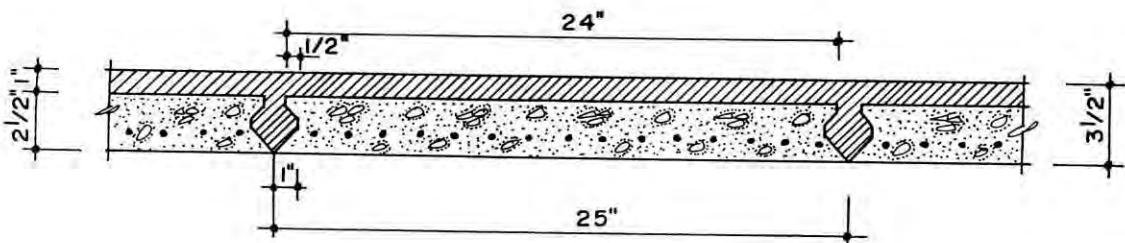
I. Prestressed Concrete Slab Without Shear Keys & Without Topping .



II. Prestressed Concrete Slab With Shear Keys & Without Topping .



III. Prestressed Concrete Slab Without Shear Keys & With Topping.



IV. Prestressed Concrete Slab With Shear Keys & With Topping.

Fig.4.1. Types of slab panels used in Laboratory Investigation.

Four types of slab panels were selected for Investigation:

- I. specimens without shear keys without topping.
- II. specimens with shear keys without topping.
- III. specimens without shear keys with topping.
- IV. specimens with shear keys with topping.

The type-I included only one specimen while rest of series included six specimens for individual test.

The casting of the specimens were conducted on the casting bed, using long-line method, of Housing and Building Research Institute, Dhaka and all the tests were conducted in the concrete laboratory of the Civil Engineering Department of Bangladesh University of Engineering and Technology, Dhaka.

4.2. Properties of Cement:

Ordinary Portland cement was used for all test specimens. Specification and properties of cement are as follows :

Table.4.1. Some physical properties of cement.

1.	Brand Name	Indo
2.	Country Origin	Indonesia
3.	Initial Setting Time	2 hours 45 minutes
4.	Final Setting Time	3 hours 27 minutes
5.	Normal Consistency	22%
6.	Specific Gravity	3.15
7.	Unit Weight	85.60
8.	Compressive Strength(3 days)	2016 psi.
9.	Compressive Strength(7 days)	2502 psi.

4.3. Properties of Aggregates:

4.3.1 *Coarse aggregate :*

Manually crushed, local variety of first class bricks were used as a coarse aggregate for preparation of concrete in this investigation. The 3/4" down graded brick chips were used and initially sieved through 1" to No.4 sieves. The aggregates passing 1" sieve size and retained on sieve no. 4 were stored for casting. The absorption, specific gravity, unit weight and fineness modulus of coarse aggregate were investigated as per ASTI recommendation. The grading and other properties of coarse aggregate are shown in table 4.2 and 4.3 respectively.

Table 4.2. Grading of coarse aggregate.

Sieve No./ Mesh opening	Wt-Retained In gms.	Percentage Retained(%)	Cumulative % Retained (%)
1"	-	-	-
3/4"	1460	9.18	9.18
3/8"	11647	73.20	82.38
#4	2325	14.61	96.99
#8	480	3.01	100.00
#16	-	-	100.00
#30	-	-	100.00
#50	-	-	100.00
#100	-	-	100.00

F.M of Coarse Aggregate = 6.88

4.3.2. Fine aggregate :

Ordinary available coarse sand named Sylhet sand passing sieve No.4 were used as fine aggregate.

The specific gravity, unit weight and fineness modulus of the aggregate were investigated as per ASTM recommendation.

Table 4.3. Some physical properties of coarse aggregate.

Sl. No.	Description	Unit
1.	Specific Gravity	1.80
2.	Fineness Modulus	6.88
3.	Unit Weight(SSD)	75.20 lbs.
4.	Water Absorption	12.16%

The grading and other properties of fine aggregates are shown in the table 4.4 and 4.5.

Table 4.4 Grading of fine aggregate.

Sieve no./ Mesh opening	Wt-Retained in gms.	Percentage Retained(%)	Cumulative % Retained (%)
#4	-	-	-
#8	10	2.0	2.0
#16	16	9.6	11.6
#30	176	35.2	46.8
#50	218	43.6	90.2
#100	44	8.8	99.2
#200	-	-	-
Pan	4	0.8	100.0

F.M of Fine Aggregate = 2.50

4.4. Design of Concrete Mix:

"Design of concrete mix is defined as the process of selecting suitable ingredients of concrete and determining their relative quantities with the object of producing as economically as possible concrete of certain minimum properties, notably consistency, strength and durability". As there is no specific standard method for the designing of high strength concrete with brick aggregates, the ACI method for proportioning concrete mix [23] was followed for a trial mix.

Table 4.5. Some physical properties of fine aggregate.

Sl. No.	Description	Unit
1.	Specific Gravity	2.59
2.	Fineness Modulus	2.50
3.	Unit Weight (SSD)	94.80 lbs.
4.	Water Absorption	0.92%

On the basis of the test results of the trial mix the ratio of cement, sand and aggregates were finally selected by weight to be of 1: 1.86 : 2.11. The mix design was designed to attain a nominal cylinder crushing strength of 4,000 psi at 28 days. The example of mix design is presented in Appendix-1.

The water cement ratio was 0.5 to maintain the slump of 1 ".

The cylinder crushing strength are presented in Table 4.6.

4.5. Compressive Strength and Modulus of Elasticity of Concrete:

Performance of a structure under load, to a great extent, depends on the stress-strain characteristics of the material from which it is made and under the kind of stress to which the material is subjected to. Mainly the concrete is used to resist compression, and hence its compressive stress-strain curve is of primary interest.

Table 4.6. Cylinder crushing strength.

Sl. No.	Date of casting	Date of testing	Age in days	Load in Tons	f' _c in psi.
1.	12.10.89	15.10.89	3	26.0	2060.00
2.	-do-	-do-	3	26.0	2060.00
3.	-do-	19.10.89	7	38.0	3011.00
4.	-do-	-do-	7	42.0	3328.00
5.	-do-	26.10.89	14	38.0	3011.00
6.	-do-	-do-	14	30.4	2377.00
7.	-do-	02.11.89	21	40.0	3169.00
8.	-do-	-do-	21	41.0	3249.00
9.	-do-	09.11.89	28	48.0	3803.00
10.	-do-	-do-	28	47.0	3724.00
11.	-do-	-do-	28	47.0	3724.00

To determine the stress-strain relationship of concrete standard 6"x 12" test cylinder was subjected to direct compression and strain in the cylinder was measured by compresso-meters. To avoid concentration of stress due to roughness of surfaces, rubber strips were placed at top and bottom surfaces of test cylinder.

Physical properties of brick aggregate are different from those of standard aggregates. Modulus of Elasticity of brick aggregate concrete is, obviously, different from stone aggregate concrete. The modulus of Elasticity at 50% f'_c was observed to be around 2.905×10^6 psi. The stress-strain relationship is given in the Fig. 4.2.

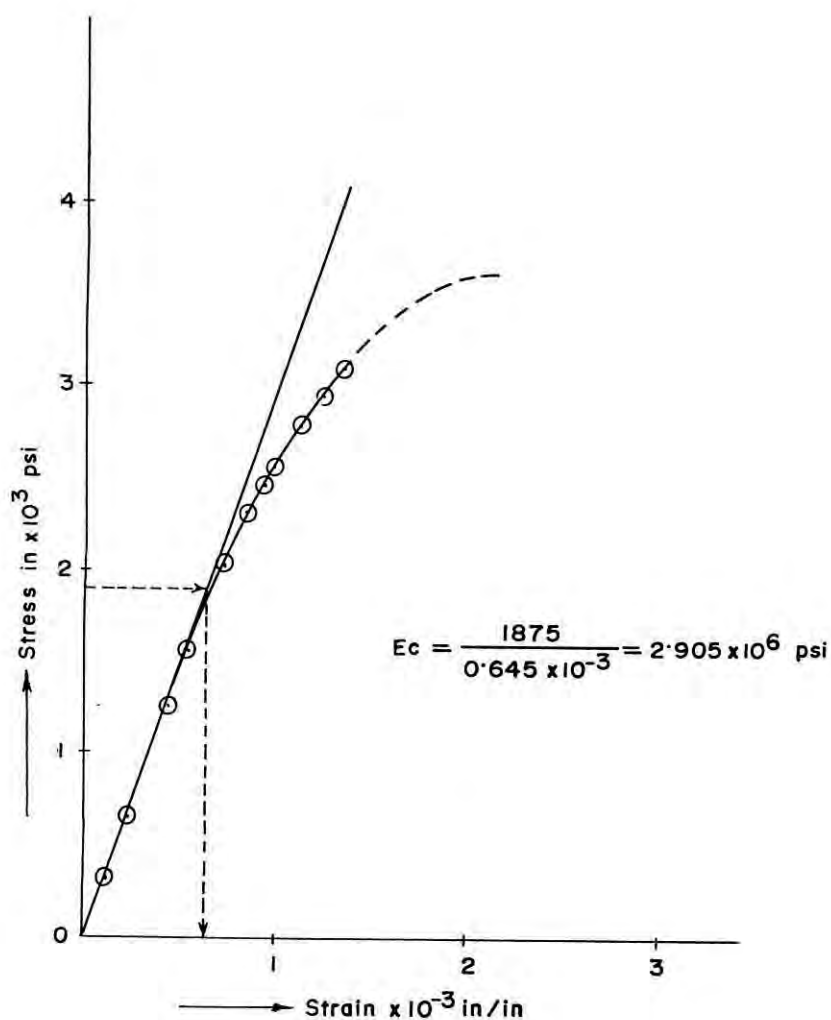


Fig.4.2. Stress-strain curve of concrete.

4.6. Split Cylinder Test:

Split cylinder test or Brazilian test (ASTM C 496-71) is an indirect method of measuring tensile strength of concrete. The results of split cylinder tests are generally assumed to be closer to actual tensile strength of concrete than the results obtained by direct tension test or of modulus of rupture.

Three cylinders of standard dimensions were used to find the split cylinder strength. The cylinder was placed with its axis horizontal on the platform of machine. Rubber strips were placed along the axis between the specimen and platform. The load was applied parallel to the transverse axis of the specimen. The cylinder was loaded to failure by splitting along the vertical diameter.

4.7. Properties of Reinforcement:

Cold-drawn low-carbon (mild) steel wires of nominal 4 mm ϕ were used as prestressing reinforcement. This type steel wires are available in the local market and actual area of wires were used for computation.

Three specimens were cut from the coil and were tested as per ASTM A 370-77 recommendation in order to determine the ultimate strength, percentage elongation and modulus of elasticity. The stress-strain diagram obtained from the test results is shown in Fig. 4.3.

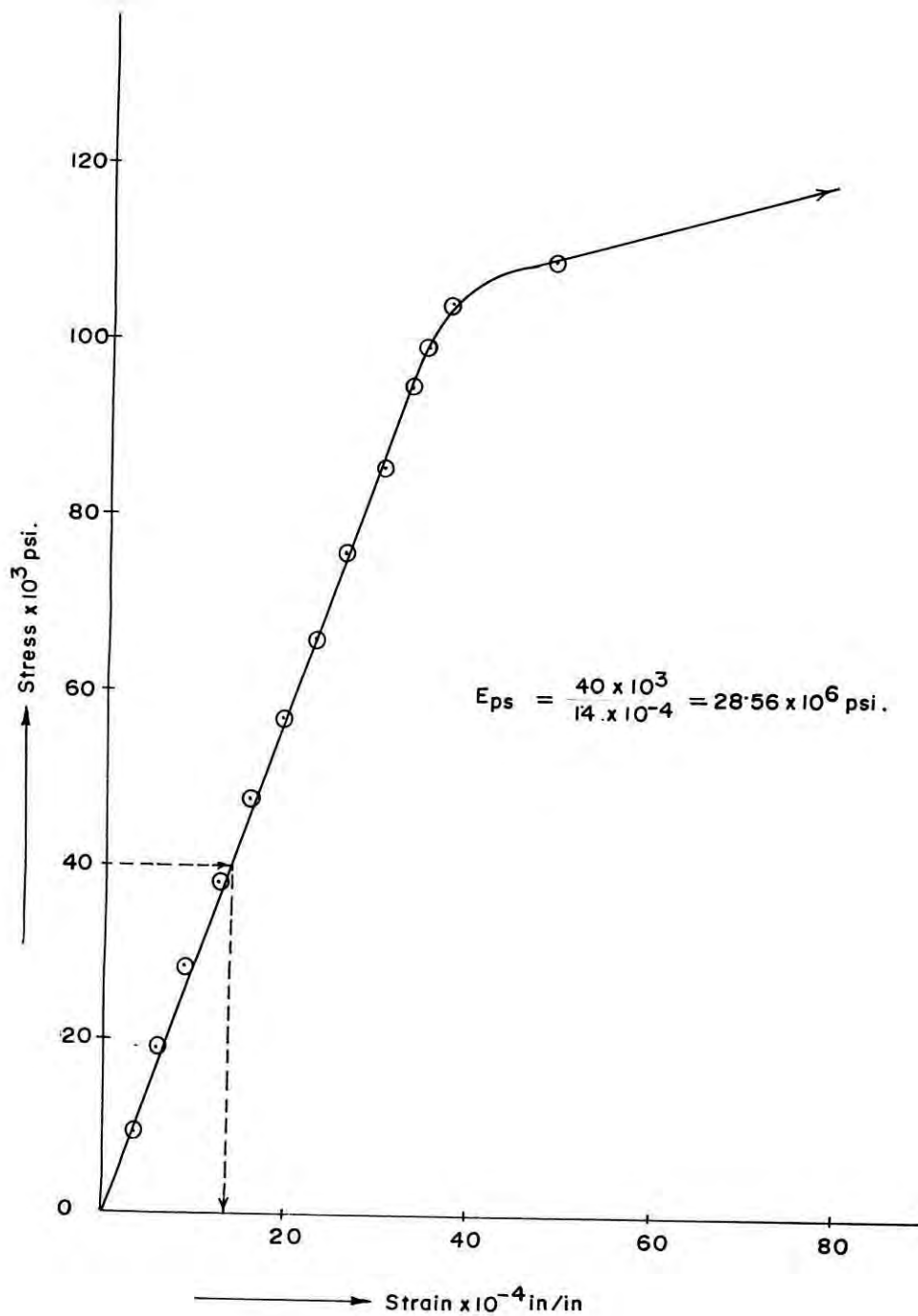


Fig.4.3. Stress-strain curve of cold-drawn steel.

4.8. Construction of the Test Slabs:

Two wooden moulds were prepared for casting the prestressed concrete slabs. The dimensions of the moulds were such that the prestressed slab panels of sizes 25" x 102" x 2.5" could be made. The moulds were also fitted with the arrangements to provide the shear keys as designed for.

A total of 19 rectangular pretensioned prestressed slab panels were constructed for testing. Nominal cross-section of these slabs were 25" by 2.5". Each panel had a total length of 102" for an effective span of 96". The longitudinal prestressing reinforcement were provided by 16 numbers of 4 mm ϕ of cold-drawn low carbon steel wires for slab panels to be tested without any topping. The slab panels with topping were reinforced by 12 numbers of 4 mm ϕ of cold-drawn low-carbon steel wires.

The slab panels were designed following the elastic method allowing no tension in concrete [1]. Examples of design of test slabs are presented in Appendix-2.

The arrangement of the reinforcements for the test slabs are shown in Fig.4.1.

The pretensioning work was performed by utilizing the long line method. The wires were anchored against anchor beam with the help of grips and colloids situated at one end of prestressing bed. Stretching of wires was done one wire at a time, from the other end of the prestressing bed by a electrically operated jack of 1000 kg capacity. At the stressing end, a grip was slipped on each wire. Another grip was slipped on the wire after

the wire being passed through the opening of claw of the stretching machine. The wire was then locked against the of claw of machine. The stretching machine was then switched on for operating and machine was automatically stopped when it reached the predetermined force, fixed on the control dial before being used for operation. The stressed wire was anchored against anchor beam by means of grip and colloid. After the gripping of the wire had been completed the machine was switched on for pushing backward to release the wire. In that way all the wires were stretched one by one and anchored against the anchor beams.

The concrete was mixed in a 6 cubic feet capacity drum type mixer. Prior to batching, the coarse aggregate was soaked in water for 24 hours and moisture content of the both coarse and fine aggregates were measured. According to designed mix ratio, the measured quantity (by weight) of aggregates, cement and water were fed into the mixer machine. The mixing was continued for approximately 2 minutes . Slump was then measured to make sure about proper consistency of concrete mix.

Before pouring the concrete mix, the level and position of the wires and formwork in bed were checked. The inner faces of the formwork were lubricated to facilitate the removal of the formwork. Concrete was then poured into the formwork and was compacted with plate vibrator. Specimens of 6"x 12" cylinders were cast along with the test slabs.

After 24 hours of casting, curing of the slabs was started and continued for several days. After attaining the 70% of the crushing strength of concrete the prestressing wires were cut.

The slab panels were then removed from the casting bed for stacking and kept open to sky for natural curing. Generally, the testing was performed after 28 days of age.

4.9. Fabrication of Testing Platform:

There was a limitation of testing facility for testing the slab panels arranged as floor slab. It was therefore essential to develop a loading frame in the concrete laboratory of BUET as shown in Fig. 4.4, and Fig. 4.5. The loading frame was designed to withstand uniformly distributed load upto 720 pound per square foot. A rexin bag covering the top surface of the slab was used for applying the uniformly distributed load on slab. Water line from the overhead tank of civil Engineering building of BUET was introduced to the pipe which was controlled by gate valve to regulate the amount of water delivered to pressure bag for inflation of the bag that exerted the predetermined uniform pressure directly to slab to be tested.

A water manometer was arranged to measure the pressure developed inside the pressure bag utilizing the Pascal's law of fluid. Load could be removed by releasing the out let valve. With the arrangement described, the load on the slab could be controlled and measured to the nearest of 2 to 3 psf.

The method of loading described above proved to be highly successful and appeared to be an excellent loading method for obtaining uniform distributed loads on testing slabs . Strip loading, loading over small areas or uniform loading over the entire slab can be readily accomplished by this technique.

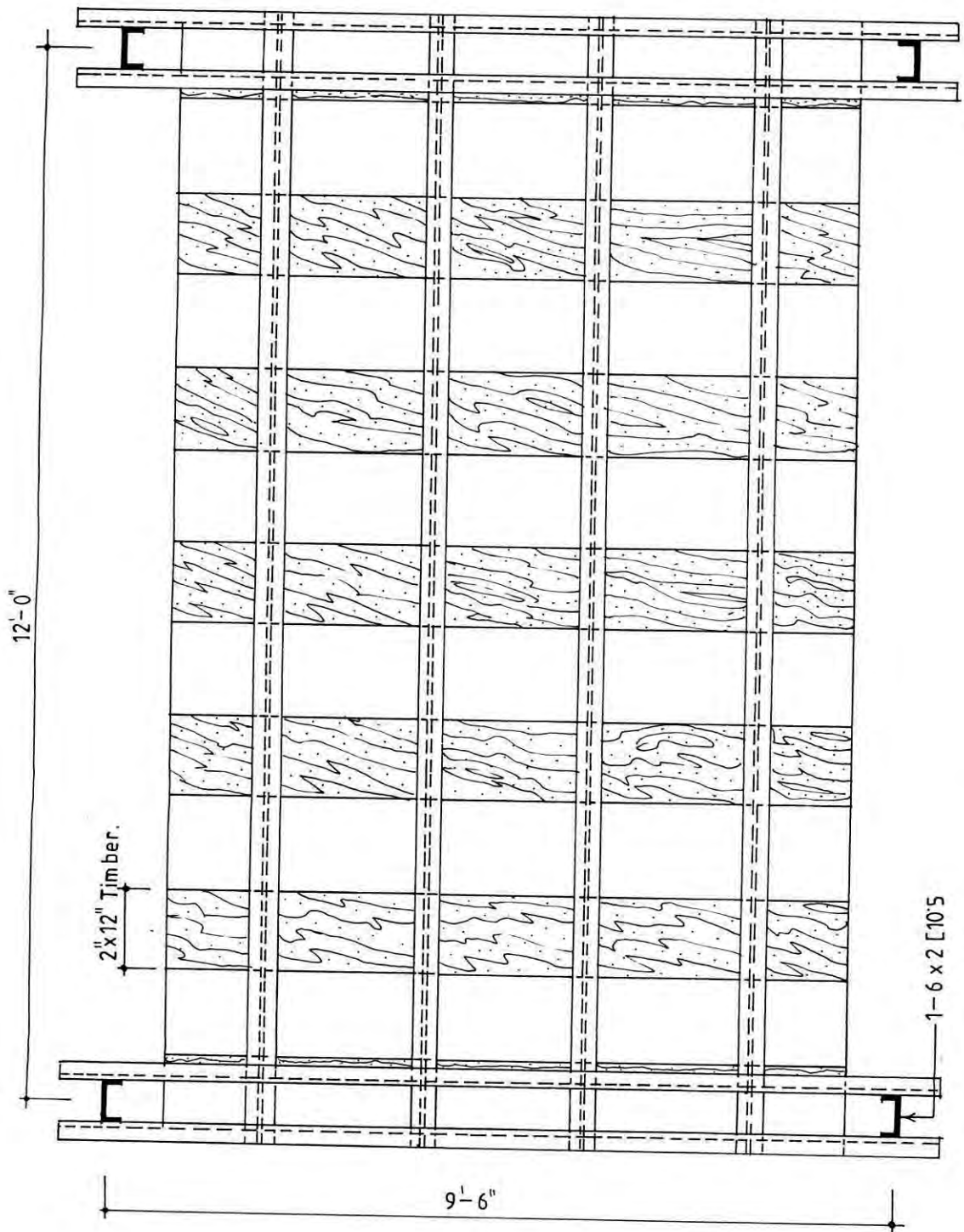


Fig.4.4. Plan of reaction frame for testing the slabs.

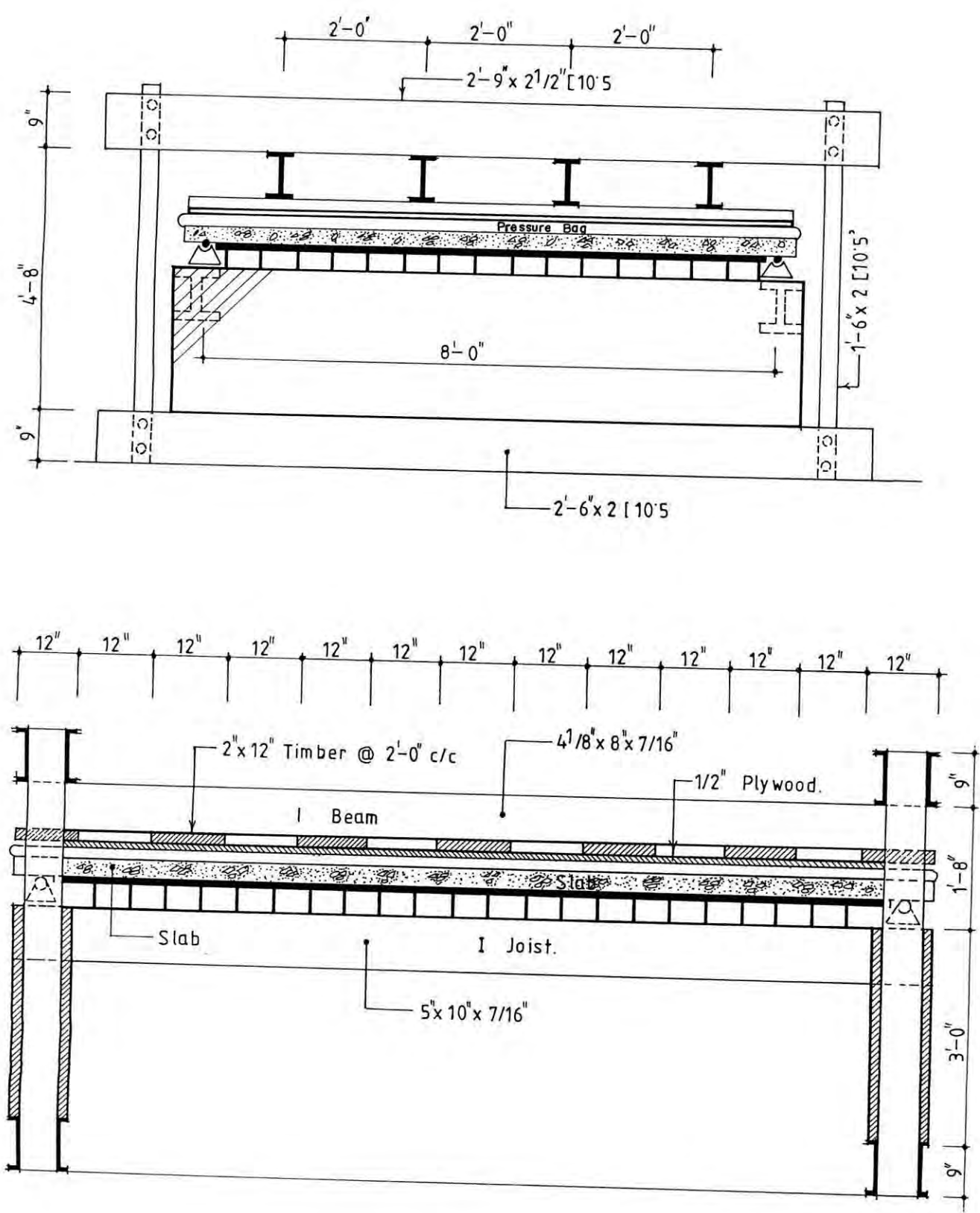


Fig.4.5. Sections of reaction frame in Fig. 4.4.

4.10. Testing of Slabs:

As described in the Art. 4.1 the tests had been performed in four types.

Firstly, considering the slabs without shear key and without topping, slab designated by Type-I, as shown in the Fig. 4.6.

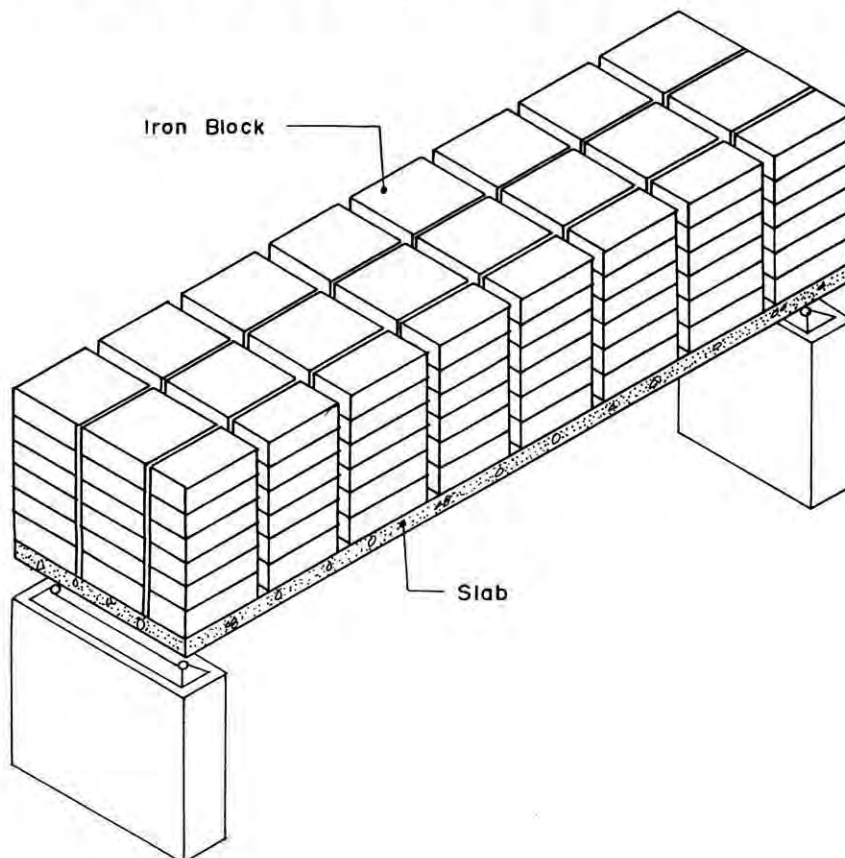


Fig.4.6. Setup arrangement of slab Type-I.

The aforesaid slab was subjected to uniformly distributed load applied at the top surface of the entire slab, in BUET concrete laboratory , by the iron block. One end the slab was rested on steel block and other end was rested on roller arranged support with 1" diameter steel rod. Both the supported ends were rested on the masonry wall placed 8'-0" apart center to center. Details of the arrangements are shown in the photograph of test setup (Fig. 4.7).

The bottom surface of the test slab was white washed to facilitate visual observation of the propagation of cracks. Three deflectometers having smallest division of 0.001" were employed to measure the deflections of the slab. One of them was placed at the central span of the slab and other two were located at the quarter span of the slab as to obtain the profile of deflection along the center line of the slab. Deflectometer readings were recorded at each incremental loading.

Cracks were deeply marked with a soft pencil upon their formation on the bottom surface and the load intensity at which those were formed was noted beside the cracks.



Fig.4.7. Photograph of test setup of slab Type-I.

The slab panels of rest three types were lifted and placed side by side in position on the loading platform as shown in Fig. 4.5. After casting work of shear key gaps and/or topping, as required for individual test type, was completed the slabs were subjected to uniform loading applied at the top surface of the entire slab by inflation of the pressure bag over the slabs. The photograph of the test setup is shown in Fig. 4.8.

82253

The bottom surface of the test slabs was white washed for each individual test to facilitate visual inspection of the propagation of cracks formation on the bottom surface of the said slabs. Eight deflectometers having smallest division of 0.001" were employed to measure the deflections of the respective points of the slabs. The positions of the deflectometers are shown in Fig. 4.9. Deflectometer readings were recorded at each loading increment. The cracks were deeply marked and load intensity at which those were formed was noted beside the cracks. The incremental loadings and respective deflectometer readings are presented in Appendix - 3.

4.11. Testing of Cylinders:

The three cylinders cast along with each of the test slabs were tested under axial compression to determine the ultimate compressive strength (f'_c) of the concrete. The remaining three were tested under diametrical compression to find the split cylinder tensile strength (f'_{sp}).

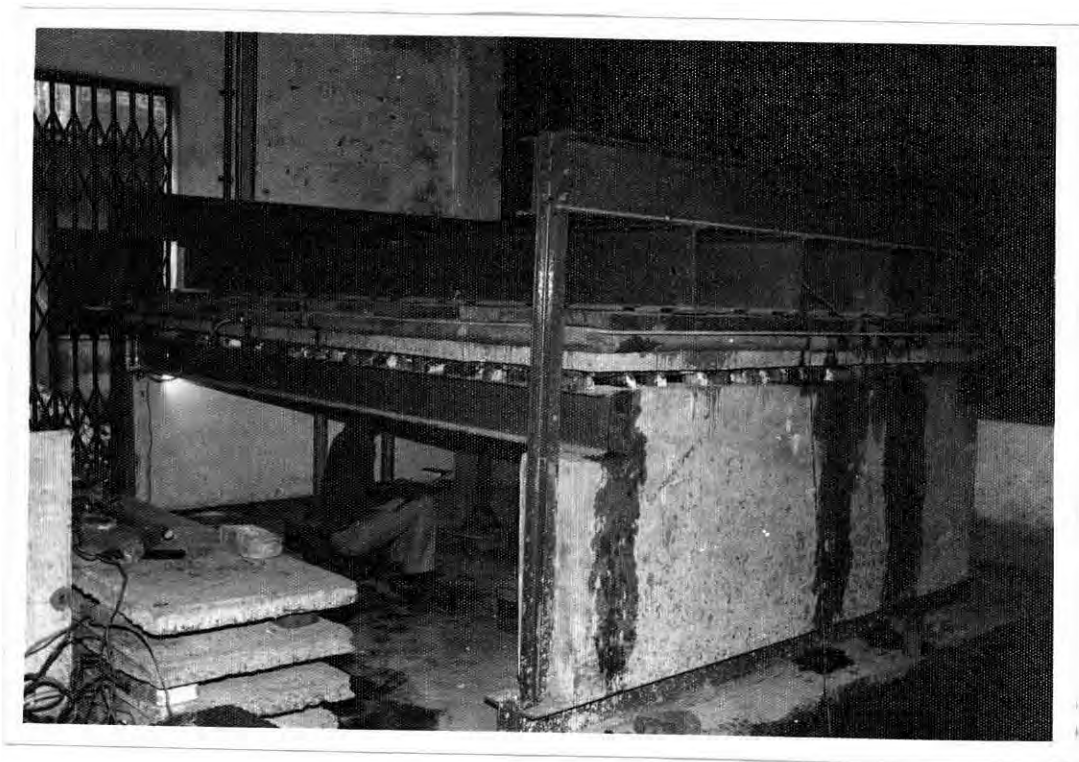


Fig.4.8. Photograph of test setup of slabs Type-II, Type-III & Type-IV.

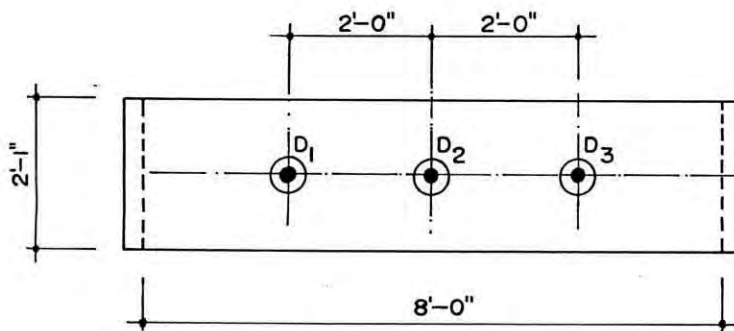


Fig.4.9a. Locations of deflectometers for slab Type-I.

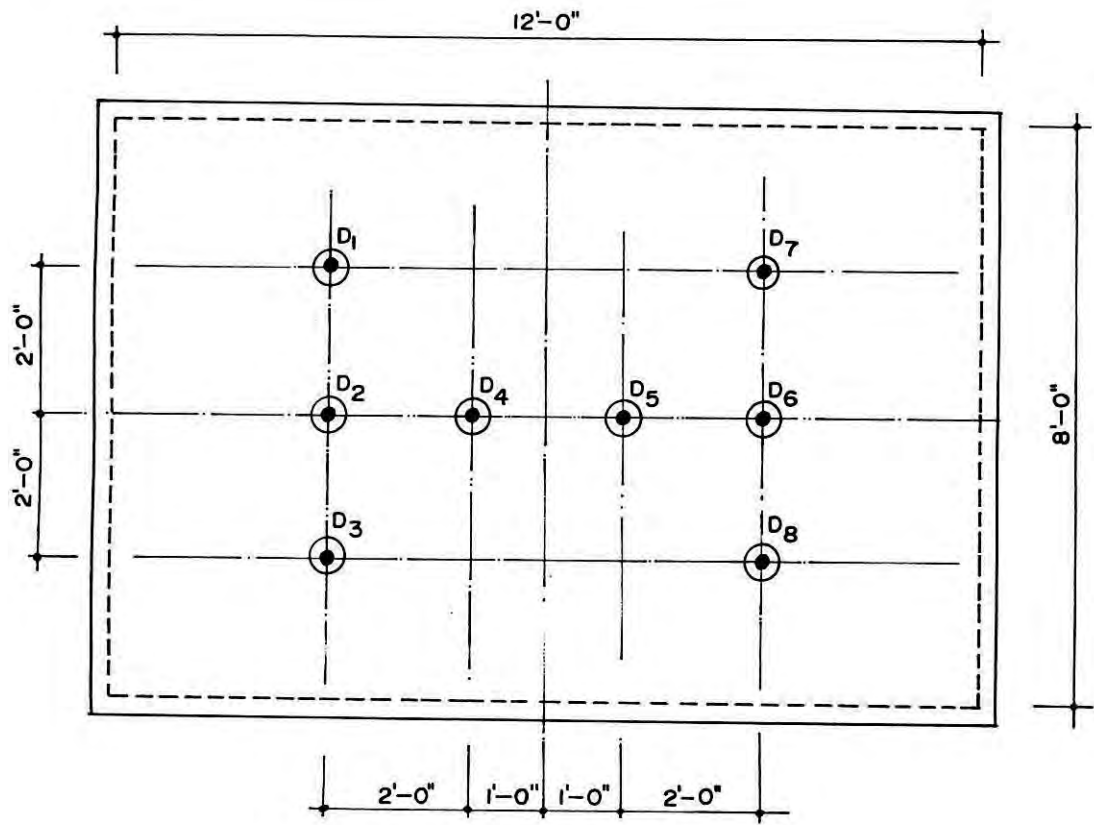


Fig.4.9b. Locations of deflectometers for slab Types-II,III & IV.

CHAPTER 5

TEST RESULTS

5.1. General:

A total of four types of prestressed concrete slab, with low-carbon steel as reinforcement, were tested under uniformly distributed load. Method of application of uniformly distributed load was discussed in the Art.4.10. Efforts were made in the test program in order to observe the effects of shearkeys and topping on (a) the cracking load, (b) ultimate load, (c) the cracking pattern, and (d) the deflection.

The specific observations of interest during the test had been recorded and is being presented in coming articles of this chapter.

5.2. Test Results:

The ultimate load, flexural cracking load and deflections at the selective locations under different load intensities had all been observed, and noted in a systematic manner during the test. Propagation of cracks were marked using magnifying glass. For an easy grasp of the overall performance of the slabs, the test results are presented in a tabular and graphical form. A general description of the contents of the different tables containing various test data seems necessary and is furnished below :

Table 5.1. Properties of test slabs.

Slab Types	Overall depth in inch	Panel Width in inch	Total Slab Dimension in inch.		f'_c in psi.	f'_{sp} in psi.
			Sh.dir.	Lg.dir.		
Type-I	2.5	25.0	25.0	102.0	3750.0	345.0
Type-II	2.5	25.0	102.0	150.0	3763.0	337.0
Type-III	3.5	25.0	102.0	150.0	3763.0	339.0
Type-IV	3.5	25.0	102.0	150.0	3724.0	332.0

Table 5.2. Some properties of concrete of the test slabs.

Slab Types.	$\sqrt{f'_c}$ in psi.	$F'_{sp} = f'_{sp} / \sqrt{f'_c}$	Unit wt in pcf.
Type -I	61.24	5.63	127.0
Type -II	61.34	5.49	128.0
Type -III	61.34	5.53	128.0
Type -IV	61.02	5.44	125.0

Table 5.3. Experimental cracking and ultimate loads of test slabs.

Slab Types.	Visual cracking Load Pf in psf.	Ultimate Load Pu in psf.	Ratio Pf/Pu
Type -I	146.0	271.0	0.54
Type -II	124.0	309.4	0.40
Type -III	124.0	325.5	0.38
Type -IV	137.0	336.0	0.41

5.3. Load Deflection Record:

The deflections of the critical sections of test slabs were recorded at a regular interval of increasing load with deflectometers (graduated in 0.001" divisions) placed at the eight different critical points at the bottom surface of the

test slabs. The readings of the deflectometers were recorded in accordance with the incremental loads.

5.4. Cracking Pattern:

In the test program, only the flexural type of cracks was observed on the bottom surface of the test slabs.

The flexural cracks, caused by the flexural tension, were usually observed in the zone of maximum bending moments and was accentuated by deflection or by the presence of local weakness in the slab sections. In the prestressed concrete slabs, the prestressing introduces a compressive stresses of certain magnitude and distribution in the concrete. As the external load was applied in the incremental basis, the internal compression due to the prestressing was gradually neutralized and at a certain point the stress at the bottom fiber of a simply supported rectangular slab was zero. With further increment of load, tensile stress was developed at the bottom fiber, and when strain due to tensile stress exceeded a critical value flexural cracks appeared. Before cracking of slabs, the strain in concrete due to tension and compression was observed proportional to the distance measured from neutral axis. The first crack was formed at about 38% - 54% of the ultimate load and propagated horizontally and vertically as the applied load increased. Flexural cracks, as observed, initiated in the type - I of the test slab in the center point of the mid span. As the load increased the aforementioned cracks propagated horizontally as well as vertically, from the center point to the edges of the mid span of the test slab as shown in Fig.5.1.

For the rest three types of the test slabs the first flexural cracks were appeared in the joints of the two adjacent slab panels located at the central point of the test slabs. A little increment of load the cracks propagated along the mentioned joint to the supporting edge of the slab. This could happened because the joint was the weakest point as compared with the whole slab system. Further increased load the cracks were observed in the mid portion of the short span. As the load was increasing the cracks were propagated as shown in the figures 5.2 to 5.4. From the cracking patterns of the slabs (Type-II, Type -III and Type -IV) the behavior of the test slabs had tendency to behave like two-way floor system.

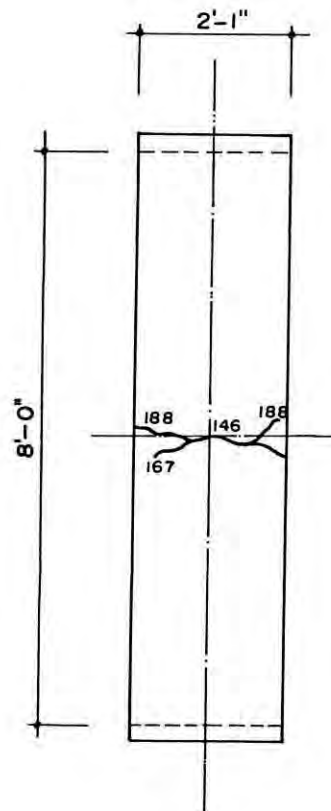


Fig.5.1. Crack patterns of slab Type - I.

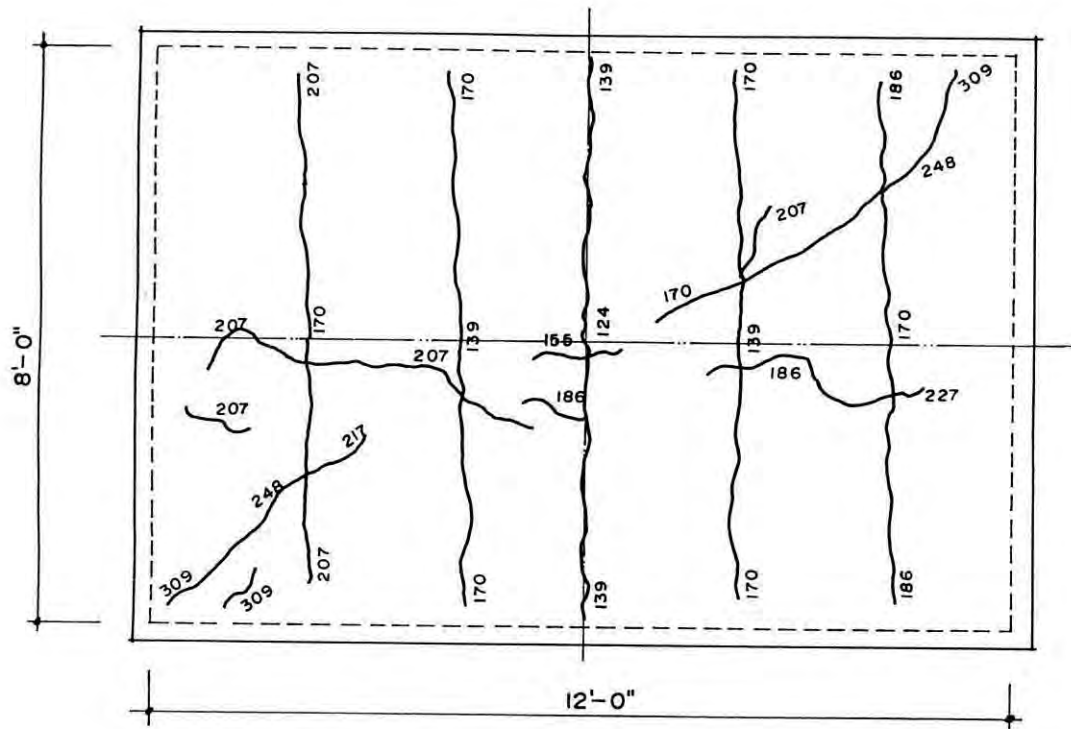


Fig.5.2. Crack patterns of slab Type -II.

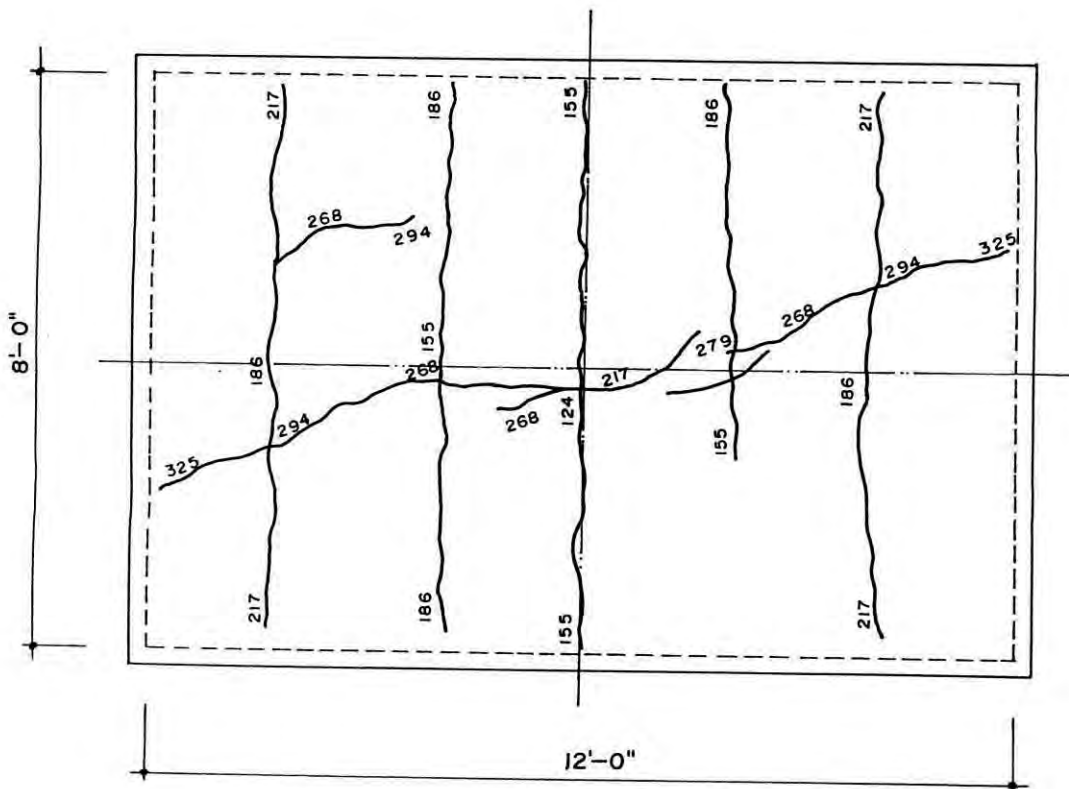


Fig.5.3. Crack patterns of slab Type -III.

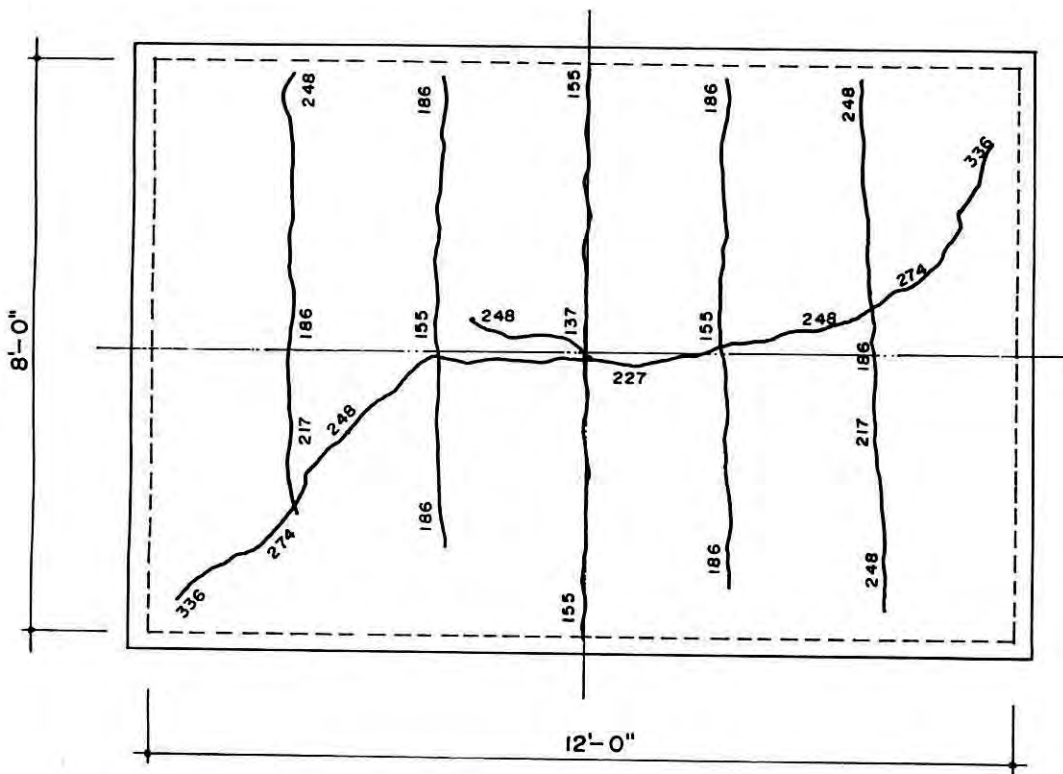


Fig.5.4. Crack patterns of slab Type -IV.

CHAPTER 6

ANALYSIS AND DISCUSSION OF TEST RESULTS

6.1. General:

The research study was aimed to investigate the relevant slab behaviors based on laboratory testing of slab. For this purpose, slabs were arranged in four types, namely :

Type - I: specimens without shearkeys & without topping.

Type - II: specimens with shearkeys & without topping.

Type -III: specimens without shearkeys & with topping.

Type - IV: specimens with shearkeys & with topping.

The information obtained in laboratory investigation are presented in Chapter 5, which are analyzed and discussed in the following articles.

6.2. Moment-curvature Relationship:

In order to develop the moment-curvature relationship for all stages of the loading, it was necessary to analyze the slab under the load upto failure. The stages of analysis are explained below:

Prestressing force only : In this stage it is assumed that the only force acting on the test slabs is the prestressing force which is applied by prestressing wires with an effective prestress f_{sc} . Since the weight of the slab is always present, the

prestress will be affected. The weight of the slab causes the concrete fiber at the level of the wires to lengthen, thus increasing the prestress slightly. However, for simplicity, it is assumed that f_{sc} does not include the effect of the weight of the slab.

Zero strain in concrete at level of steel : Considering the applied moment that produces such magnitude of strain in concrete at the level of steel so that finally the strain in the concrete becomes zero as desired for this step of calculation.

Cracking moment : To estimate the cracking moment which is the end point of uncracked section analysis. Upto this point the moment-curvature curve responds the linear elastic behavior, and is always associated with the modulus of rupture for concrete.

Top fiber strain 0.001 : No more elastic behavior exists beyond the cracking point of the slab. A non - linear relationship exists in this range. The top fiber strain at cracking is estimated to be as 3.94×10^{-4} in/in which is less than 0.001 in/in.

This step requires trial process for estimation of moment along with corresponding curvature for the top fiber strain 0.001 in/in.

Top fiber strain 0.002 : Similar way, as in d, the moment along with the curvature can be estimated.

With the steps stated above, a moment - curvature relationship may be plotted with moment representing Y - axis and that of curvature representing X - axis showing range from no load on the slab to the load corresponding to failure of the slab. M - ϕ curve is illustrated in the Fig. 6.1, and an example of developing the moment - curvature relationship is presented in Appendix -4.

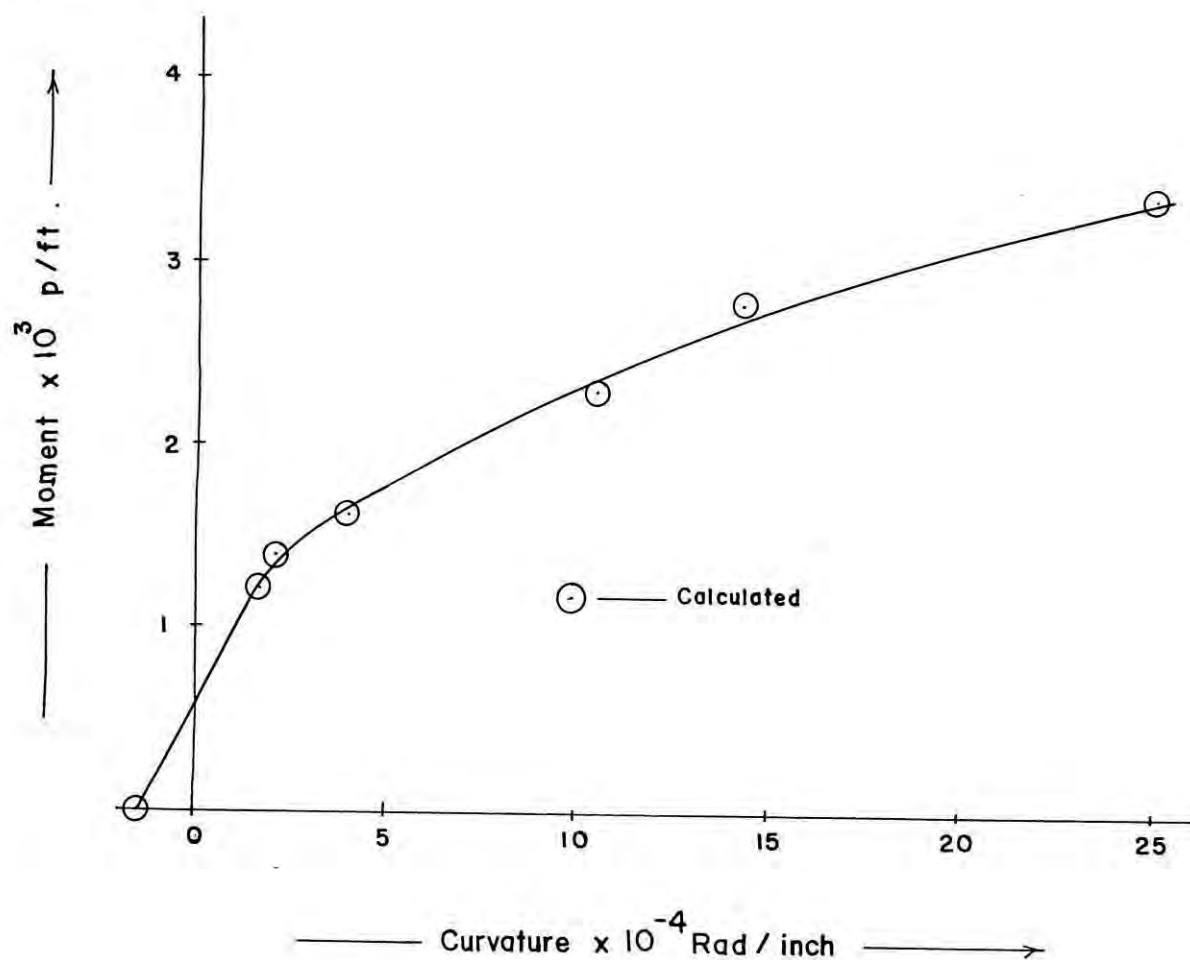


Fig.6.1. M - ϕ curve.

6.3. Load - deflection Characteristics:

The behavior of the slab, refers mainly to the variation of deformations in the slab as the load is increased to the level

when slab fails in a particular way. To study the pattern of deformations, the comparison between the theoretical and experimental deflection was studied.

6.3.1. Theoretical calculation of deflection for one-way slab:

Upto the cracking load, the theoretical estimate of the deflection is associated with the elastic calculation. Upto this point the load - deflection relationship is linear.

A prestressed concrete element develops deformation under the influence of two usually opposing effects, the prestress, and the superimposed load on it, which includes the self weight of the element, and total live load. The amount of deflection produced at a section by prestress only is given by the elastic formula:

$$w = \frac{Mx}{2E_c I} [L - x] \text{ or } \frac{Fex}{2E_c I} [L - x] \dots\dots\dots [6.1]$$

The equation of deflection produced by the superimposed uniformly distributed load is given by:

$$w = \frac{q}{24E_c I} [L^3x - 2Lx^3 + x^4] \dots\dots\dots [6.2]$$

An example showing calculation of deflection using the above Eqs. 6.1 and 6.2 is presented in Appendix - 5.

The above two equations produce a linear relationship and is valid upto the point of cracking of the slab because beyond the point of cracking linear relationship does not hold true.

The non-linear load - deflection relationship beyond the point of cracking may be established with the help of moment - curvature ($M-\phi$) relationship. It is, generally true, that the load-deflection curve for one-way slab will have the same form as that of $M - \phi$ curve.

To determine the load - deflection curve from $M - \phi$ curve, the following steps to be followed :

- a. assumption of load.
- b. drawing of corresponding bending moment diagram.
- c. calculation of curvature at different points upto central span from bending moment diagram.
- d. drawing of curvature diagram.
- e. taking the moment of area of curvature diagram (about the left edge of slab) between the left edge and mid span to get the center point deflection.

Thus calculating the deflection of central span for different amount of load, several points of the load-deflection curve are obtained and then the curve may be drawn with a reasonable accuracy. An example of calculating the points for load-deflection curve are furnished in Appendix - 5, and load-deflection curve is shown in Fig. 6.2.

6.3.2. Theoretical calculation of deflection for two-way slab:

The theoretical calculation of deflection is cumbersome as well as time-consuming. However, slab may be considered as a plate comparing its thickness with the dimensions of its width and

length. The deflection of thin, rectangular plate of uniform thickness carrying distributed load can be solved by the Lagrange equation.

For a known boundary conditions the Lagrange equation [5,6] can be integrated, and after integration the equation becomes:

$$w = \frac{4qa^4}{\pi^5 D} \sum_{m=1,3,\dots}^{\infty} \frac{1}{m^5} \left(1 - \frac{\alpha_m \tanh \alpha_m + 2}{2 \cosh \alpha_m} \cosh \frac{2\alpha_m y}{b} + \frac{\alpha_m}{2 \cosh \alpha_m} \frac{2y}{b} \sinh \frac{2\alpha_m y}{b} \right) \sin \frac{m\pi x}{a} \dots [6.3]$$

where, $\alpha_m = \frac{m\pi b}{2a}$

from which the deflection, of two-way slab, at any point can be calculated by using tables of hyperbolic functions . An example of calculating of deflection of a two-way slab is presented in Appendix - 5.

6.4 Load-deflection Behavior of Slab Type -I:

The experimental deflection of slab Type-I is observed to be linear, and coincides with the calculated theoretical deflection curve upto the 80.0 psf. of superimposed load, as shown in Fig. 6.2.

Beyond 80.0 psf. of superimposed load the experimental deflection curve tends to behave non-linearly, as indicated in the Fig. 6.2 and the deflection can be found to be higher than the elastically calculated deflection.

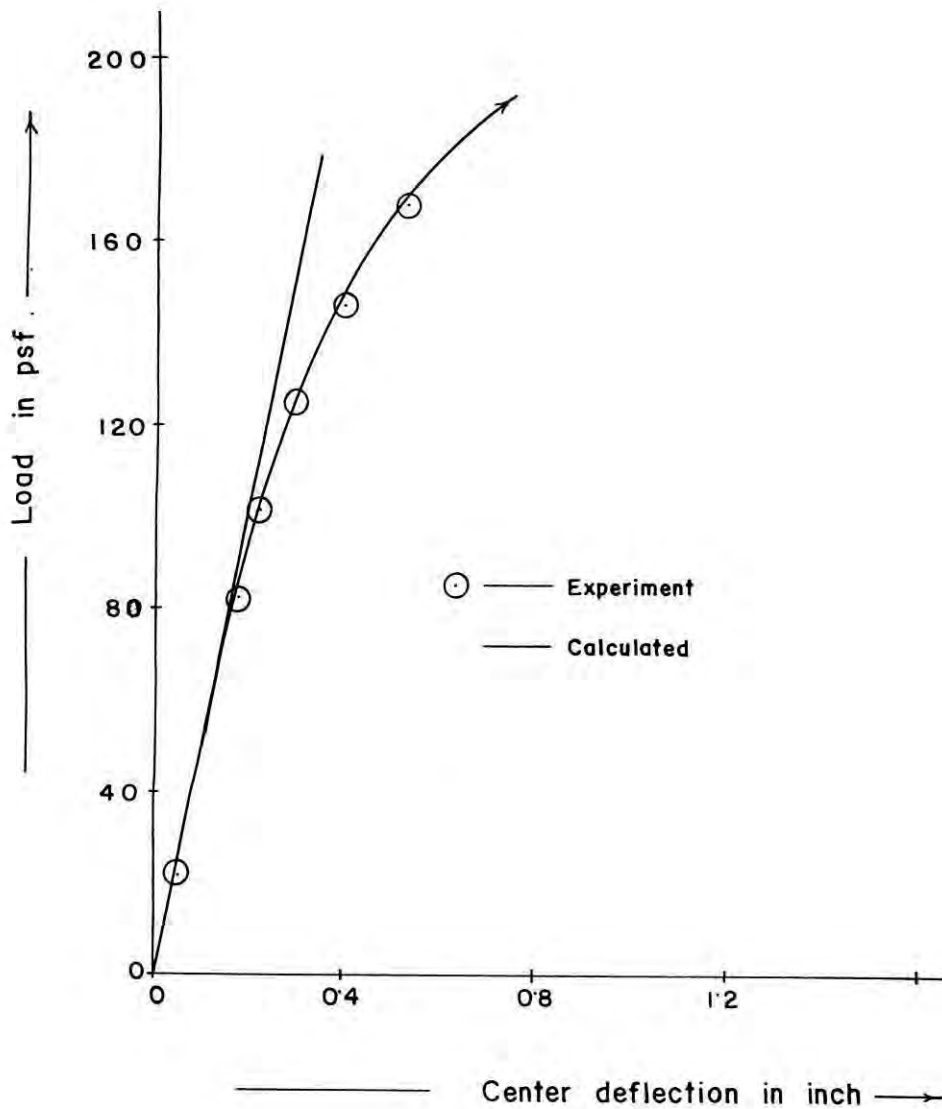


Fig.6.2. Load-deflection curve of slab Type -I (calculated by elastic method).

In this range, deflection calculated by utilizing the elastic theory does not hold true. Hence to correlate the experimental deflected curve with the calculated one, the deflection was computed using the $M - \phi$ curve for all range of loadings, as shown in Fig.6.3.

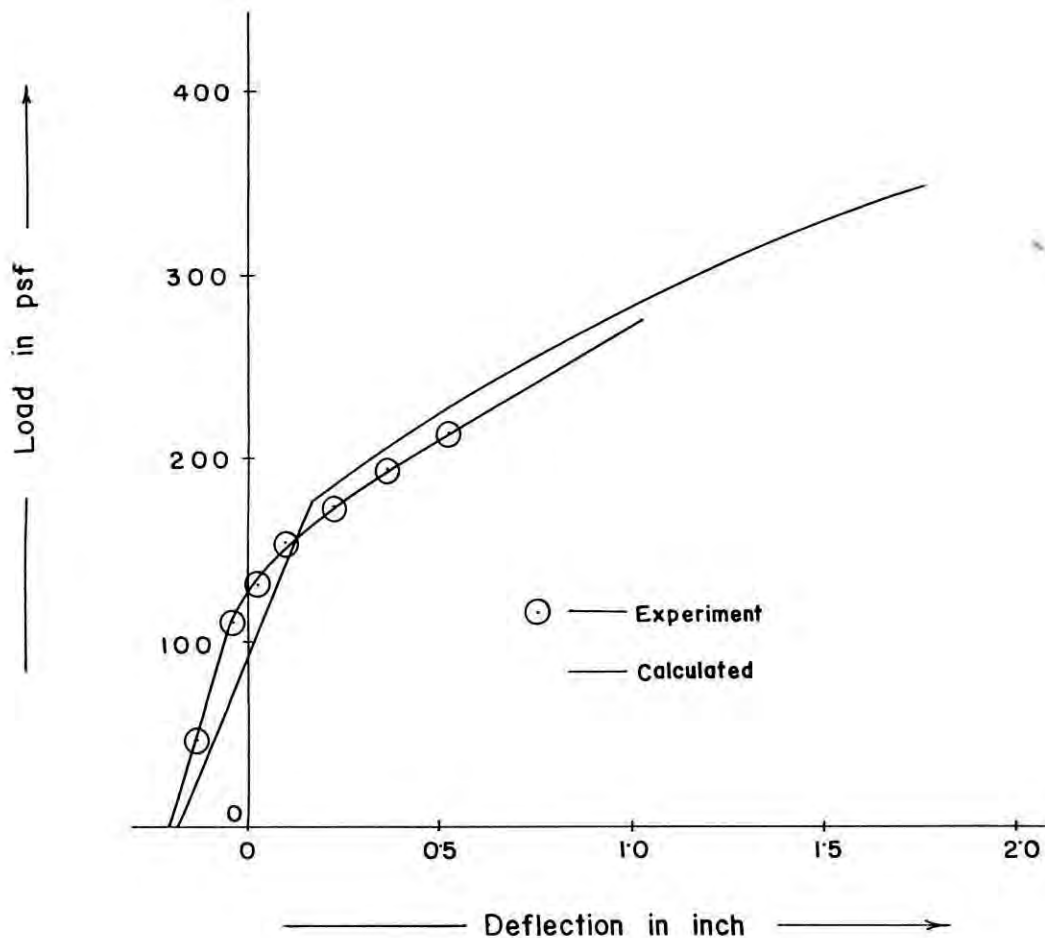


Fig.6.3. Load-deflection curve of slab Type - I (calculated from $M - \phi$ curve).

From Fig.6.3 it can be observed that the locus of the experimental deflected curve is almost parallel to the theoretical deflected curve, and it is smaller than the calculated deflection upto the load of 150.0 psf.

Beyond the load of 150.0 psf. upto failure the experimental deflected curve is also observed to be parallel to the calculated deflected curve, and it is about 10.0% larger than the calculated one. Within the elastic range upto the point of

rupture of the concrete deflections are directly proportional to the loads as expected. Beyond the elastic range the load - deflection curve behaves non - linearly, that is, deflections are no more directly proportional to the corresponding loads.

From the curve shown in Fig.6.3. it is apparent that the prestressed concrete slab Type-I possesses the ductile properties. That is the slab will give ample time of warning before ultimate collapse, as expected in concrete structures.

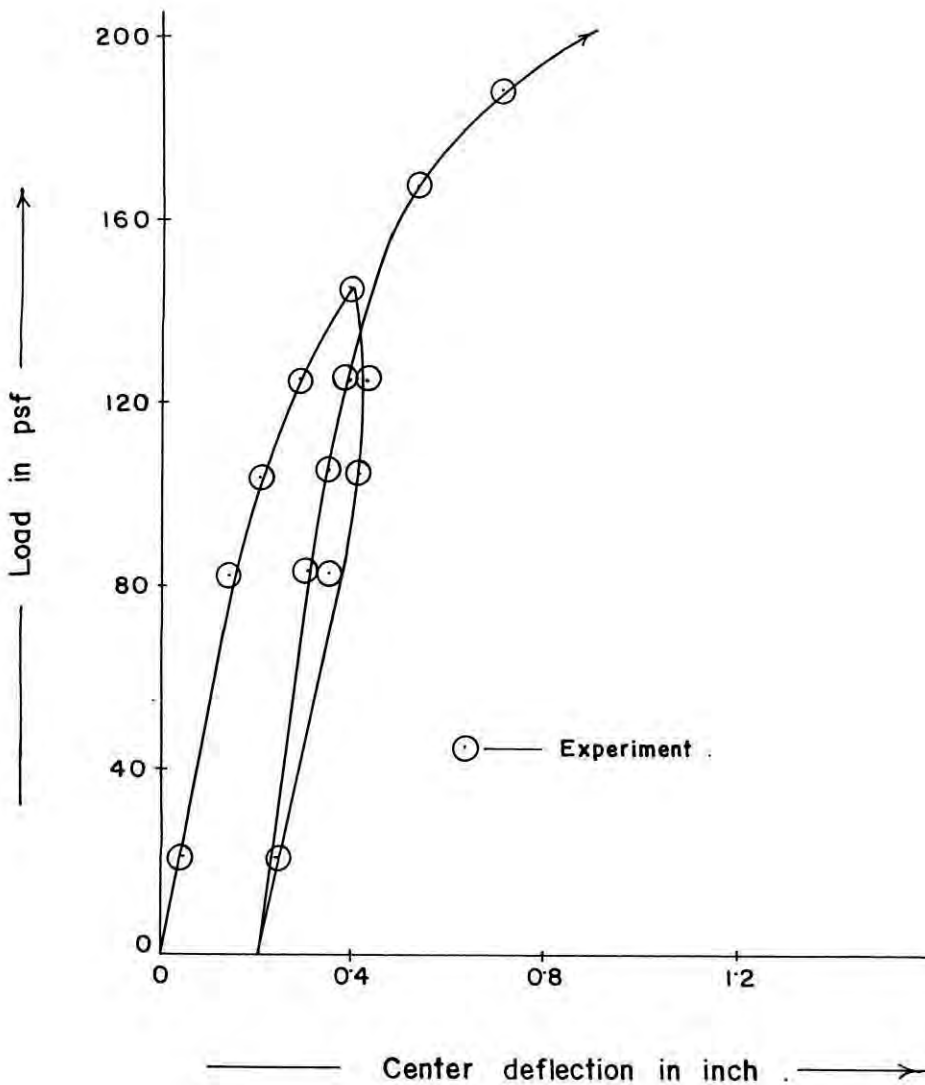


Fig.6.4. Loading and unloading cycle of slab Type -I.

Deflection behavior in loading and unloading cycle is presented in Fig.6.4. In the loading cycle, the load was continued to increase upto 146.0 psf., and then the unloading cycle was begun. Then the slab Type-I was reloaded upto a load of 271.0 psf. The failure was occurred due to the excessive deflection at mid span of the slab.

The slab Type-I was unloaded after being loaded into the plastic range, and hence the elastic part of the strain was recovered, as indicated in Fig.6.4. The plastic strain remains as a permanent increase in length, or permanent set, in the slab. The permanent set was 0.2" and elastic recovery was 0.24".

6.5. Load-deflection Behavior of Slab Type - II:

There were eight points for measuring the deflections of the slab Type-II. The six pieces of precast prestressed slab panels were jointed together by filling gaps between two adjacent slab panels forming a complete slab, so that, the imposed loads on the slab were distributed in both the directions. The load - deflection behavior of the slab is presented, for simplicity, in three load versus deflection curves, namely:

- a. Load versus deflection curve for the deflected points 1,3,7,8 as shown in Fig.6.5.
- b. Load versus deflection curve for the deflected points 2,6 as shown in Fig.6.6.
- c. Load versus deflection curve for the deflected points 4,5 as shown in Fig.6.7.

The location of different points just mentioned is shown in Fig. 4.9. In Fig.6.5 two curves were drawn along with the experimented deflection curve. Between the two calculated deflection curves one is for one-way slab and other is for two-way slab for the points 1,3,7 & 8.

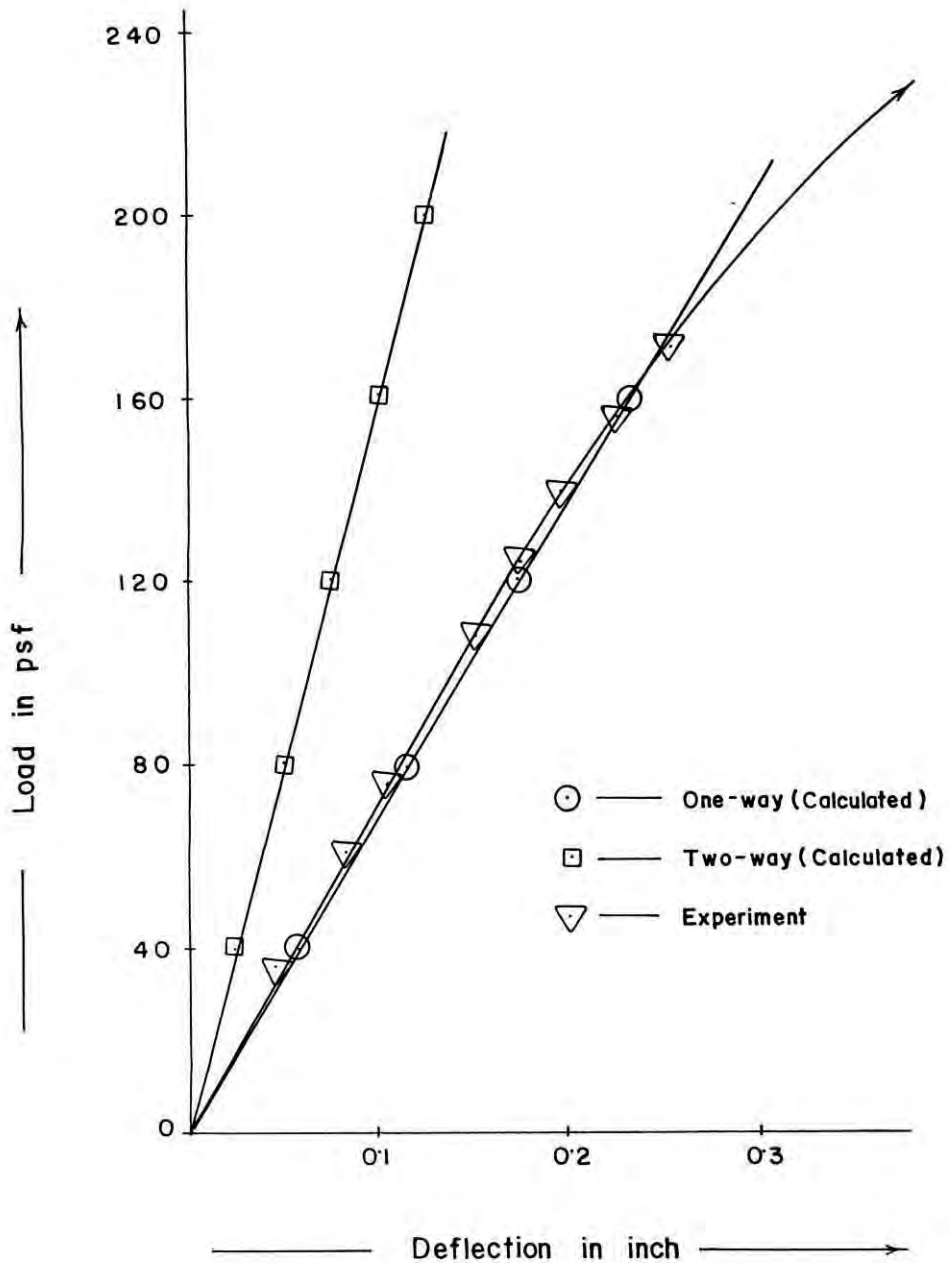


Fig.6.5. Load - deflection curve for the points 1,3,7,8 of Type-II.

The experimental curve can be found to coincide almost with the calculated deflected curve of one-way slab upto the load of 160.0 psf. There after the experimental curve is non-linear. From the figure, it seems that the slab under consideration tends to behave as one - way slab though it was apparently expected that the slab would behave as a two-way slab.

In the Fig. 6.6 similar curves are presented for the slab Type-II but for the points 2 and 6.

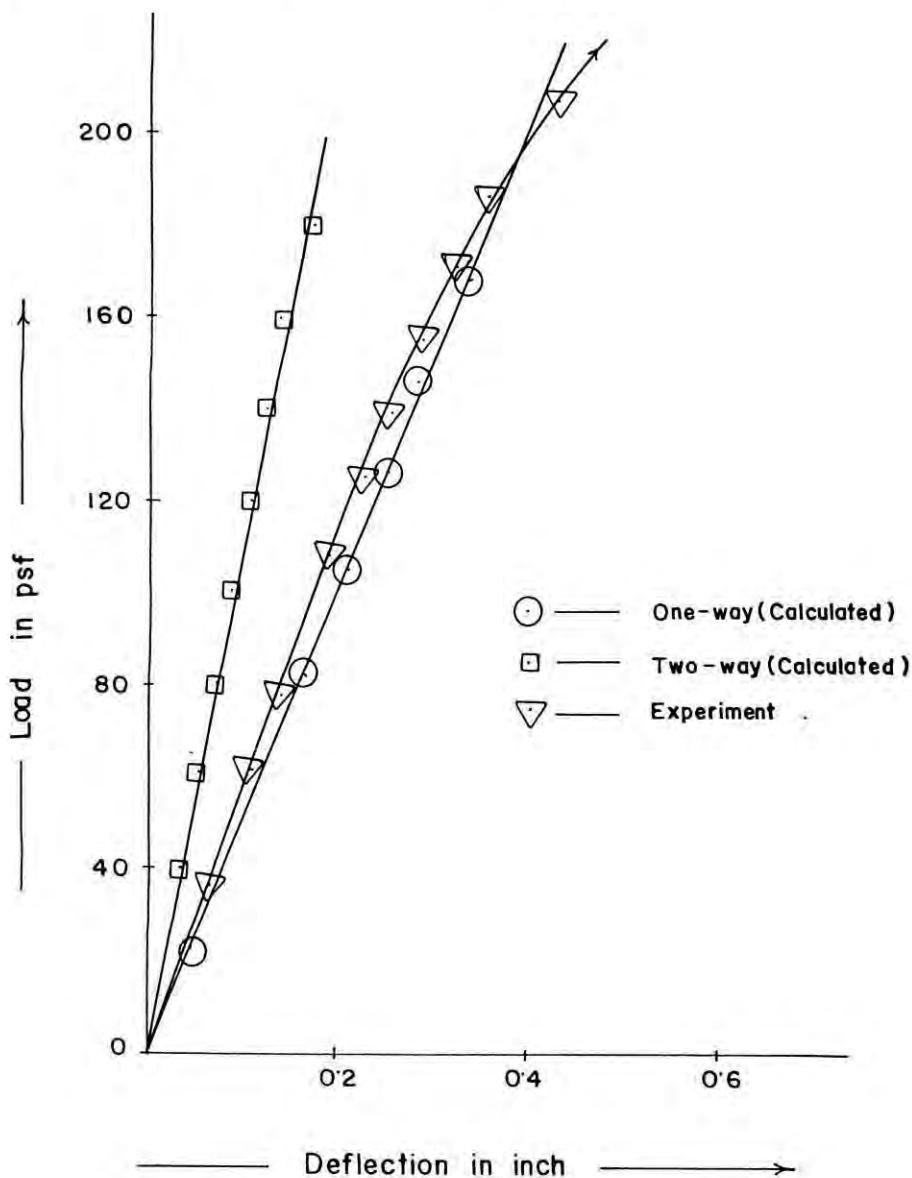


Fig.6.6. Load-deflection curve for the points 2,6 of Type-II.

The curve obtained from experiments can be observed to run parallel to the one-way calculated curve and it can also be observed that the deflections are much higher than that of two-way deflection curve.

The experimental curve in Fig. 6.7 for points 4 and 5 behaves similar to that of points 1,3,7,8, and 2,6 of the slab Type-II.

From the figures, discussed above, it can be concluded that the behavior of the slab Type-II is closely represented by the behavior of a one-way slab.

The slab type II was constructed with the expectation that it would carry the superimposed loads as in a two-way slab system. For that slab arrangement, the locus of the experimental curve would likely to run along with or coinciding theoretically the two-way calculated curve but practically it is observed that the figures 6.5, 6.6 and 6.7, that the experimental curve in each figure coincides with the one-way calculated curve. This phenomenon might happen due to the probable reasons as stated below:

- i. The slab panels were precast and shearkeys were filled in by in-situ concrete. There was every possibility of developing hair cracks (which were not visualized by necked eyes) due to shrinkage of insitu concrete along the shearkeys.
- ii. There might be gaps in between the slab panels and supporting arrangements in some area of slab panels. Owing to incremental increase of superimposed load the untouched

(uncontacted) portion of slab panels were compelled to contact with the supporting systems causing the shear crack along the shearkeys.

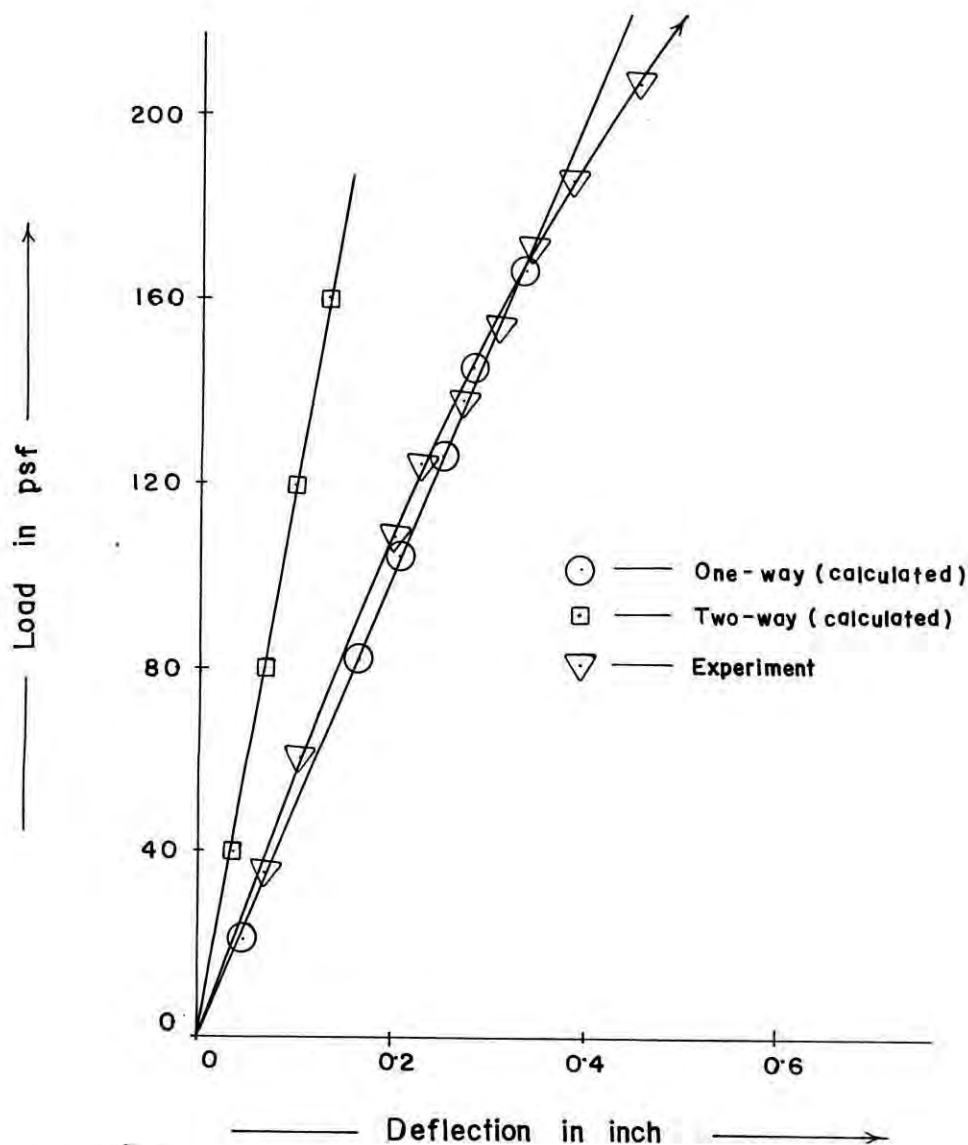


Fig.6.7. Load-deflection curve for the point 4,5 of Type-II.

6.6. Load-deflection Behavior of Slab Type-III:

Slab designated as Type-III, was constructed using six prestressed concrete precast slab panels placed side by side (in Fig. 4.1c) and then casting 1.0 inch thick concrete topping

after placing and leveling each slab panel in position . After proper curing, the slab was tested under uniformly distributed loads applied on the top of the slab using water bag.

To measure the deflections, eight different points were selected and the deflectometers were placed at those points at the bottom surface of test slab (see Fig. 4.9). The curves showing the deflection behavior of the slab are presented in three figures.

Fig.6.8 presents the deflection curves for the points 1,3,7,8 of the slab Type-III. The locus of the experimental curve, upto a loading of 100.0 psf., lies almost midway the calculated curves for one-way and two-way slab. There after the experimental curve gradually bends towards the one-way calculated deflection curve and is non-linear.

At 124.0 psf. load, the experimental deflection is about 23.48% less and is about 68.33% higher than that of calculated value considering one-way and two-way slab action respectively.

Load-deflection relationship for the points 2 and 6 of the slab Type-III are shown in Fig.6.9. The experimental curve upto load of 100.0 psf. is a straight line.

Upto this load range the slab behaved elastically and deflection is directly proportional to the corresponding loads and the locus of the experimental deflection curve lies in between the calculated curves of one-way and two-way slabs but lies slightly towards the one-way curve.

The experimental curve indicates non-linear relationship beyond this load.

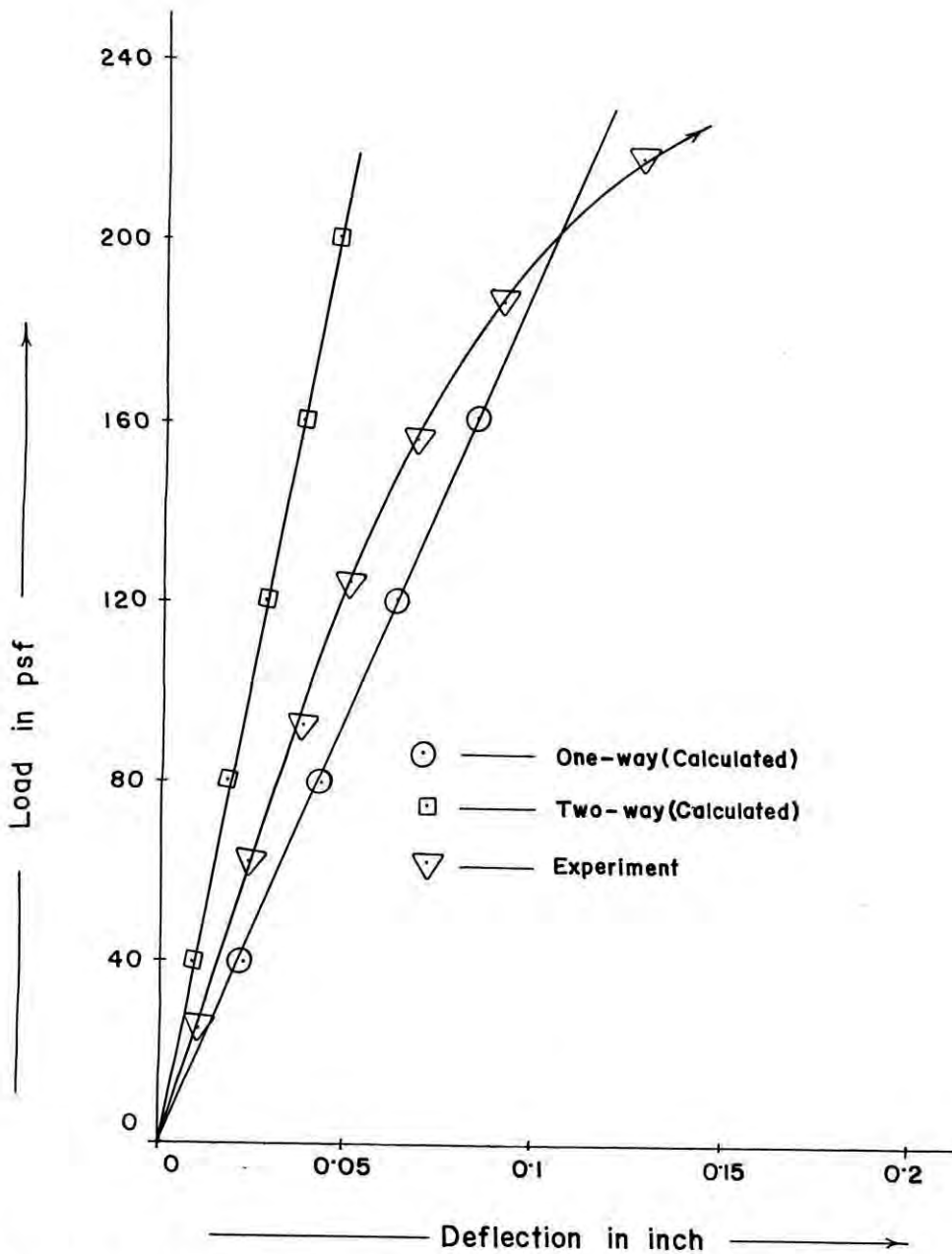


Fig.6.8. Load-deflection curve for the point 1,3,7,8 of Type-III.

From the test slab Type-II, (for points 2 & 6) at 124.0 psf. loading, the experimental deflection is 11.9% less than deflection for one-way slab and 164.29% higher than deflection for two-way slab. The test slab Type-III, the points under

consideration, the experimental deflection is 16.23% less and is about 93.95% higher than that of calculated value considering one-way and two-way slab action respectively.

The deflection curves for the points 4 and 5 of the test slab are presented in Fig. 6.10 and shows similar behavior indicated for other points.

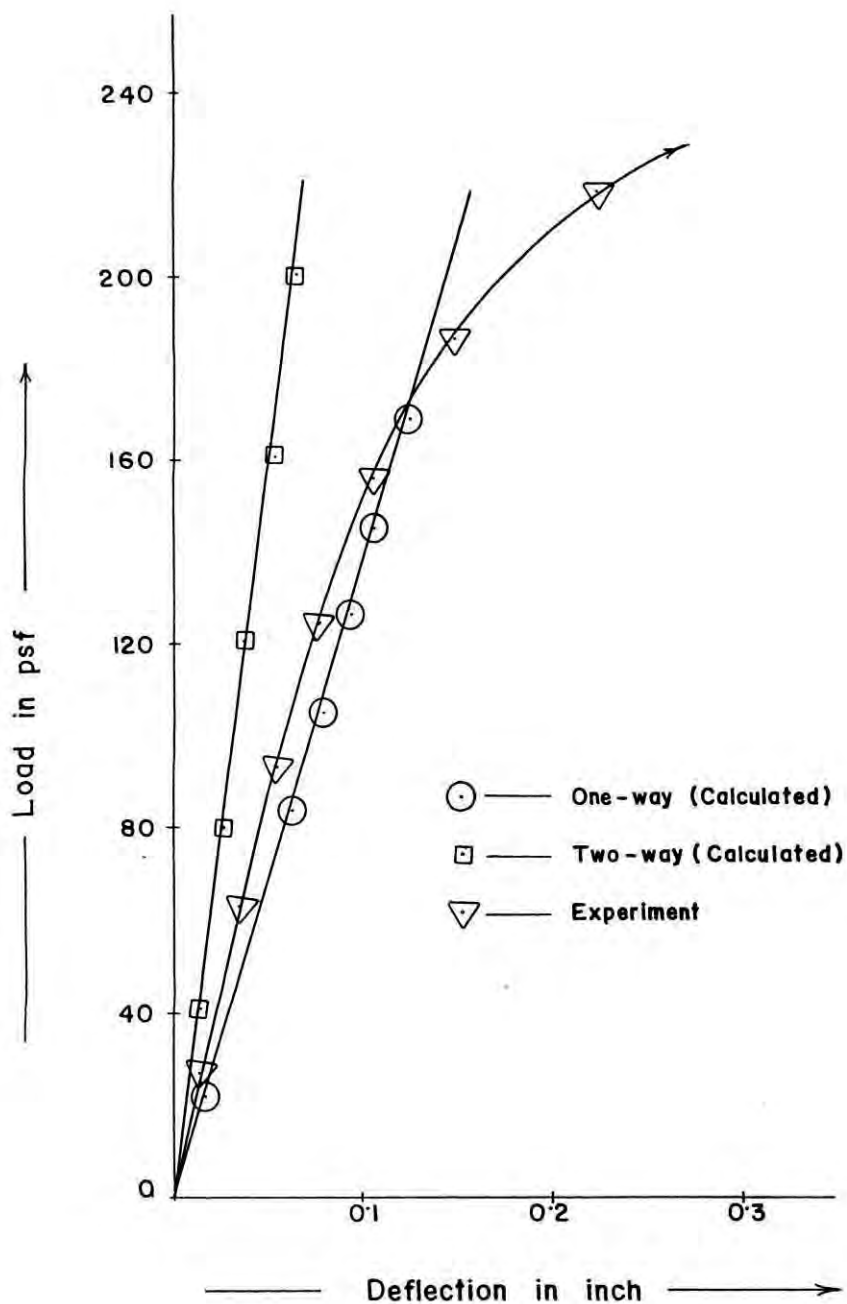


Fig.6.9. Load-deflection curve for the points 2,6 of Type-III.

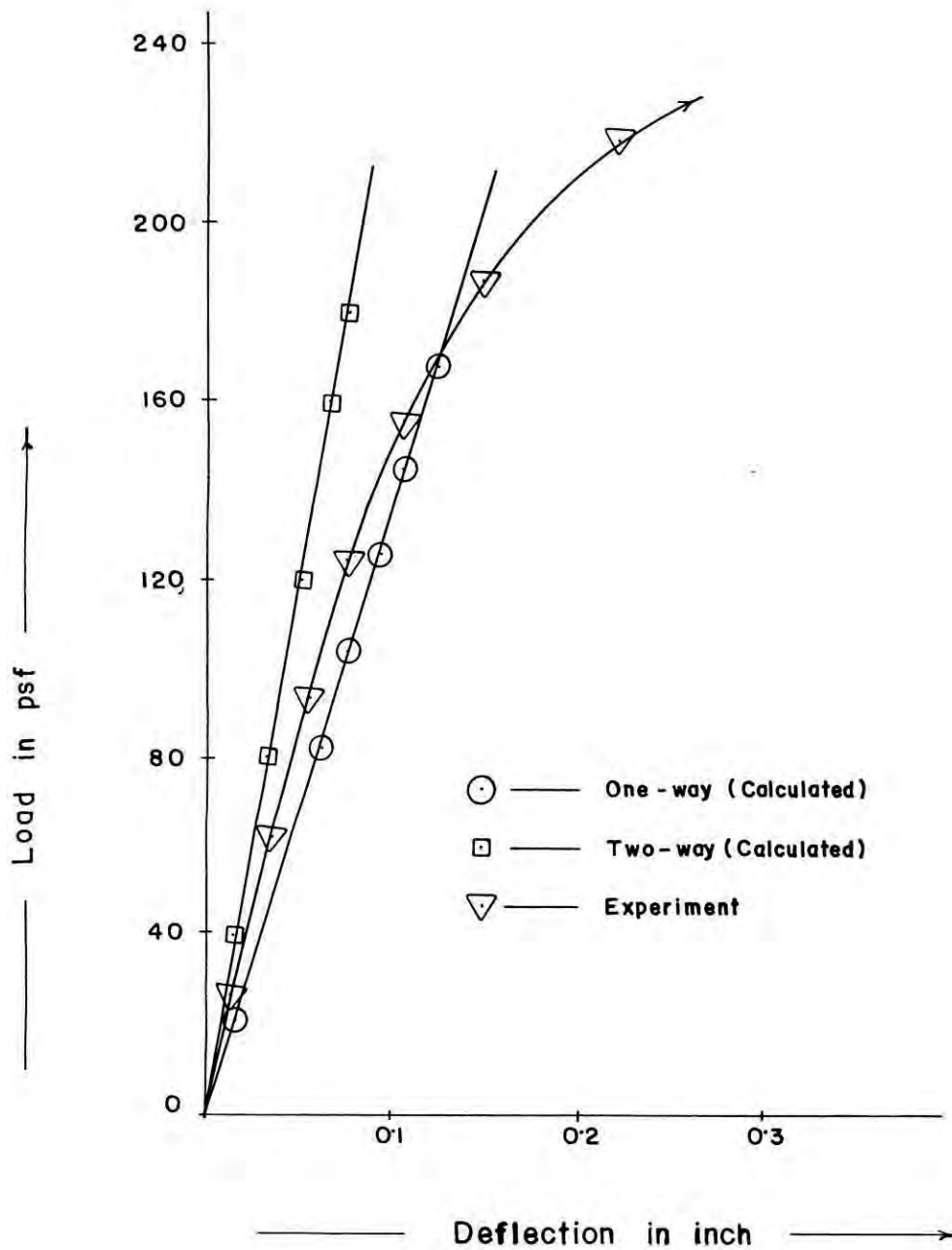


Fig.6.10. Load-deflection curve for the point 4,5 of Type-III.

At 124.0 psf. load, the experimental deflection is about 15.22% less and is 49.0% higher than the calculated value considering one-way and two-way slab action respectively.

6.7. Load-deflection Behavior of Slab Type-IV:

The slab Type-IV is also constructed by placing six precast prestressed concrete slab panels side by side on the loading platform (Fig. 4.1d) and by filling the gaps in between two adjacent slab panels with plain concrete and then placing 1 inch thick plain concrete over the entire area of slab. After proper curing the slab was subjected to laboratory investigation by applying uniformly distributed load using water bag.

Eight different points of the slab were selected and the deflectometers were employed at these locations. The locations of the deflectometers are shown in Fig.4.9. The deflections obtained during testing are presented along with those calculated on the basis of one-way and two-way slab actions.

Three figures are presented for three different groups of points. Each group having similar form of deflection.

Fig.6.11 represents the deflection of the points 1,3,7 and 8 of the test slab. The experimental curve lies, as for slab Type-III, within the two calculated curves and upto the load of about 100.0 psf.

At about 124.0 psf. of loading the experimental deflection is about 32.40% less than and is about 80.0%, higher than the calculated values considering one-way and two-way slab action respectively. Beyond this loading the experimental curve is non-linear and gradually inclines towards the one-way curve.

At about 195.00 psf. load the experimental curve intersects the calculated one-way deflection curve and at a higher load the actual deflection is higher than that calculated based on one-way slab action.

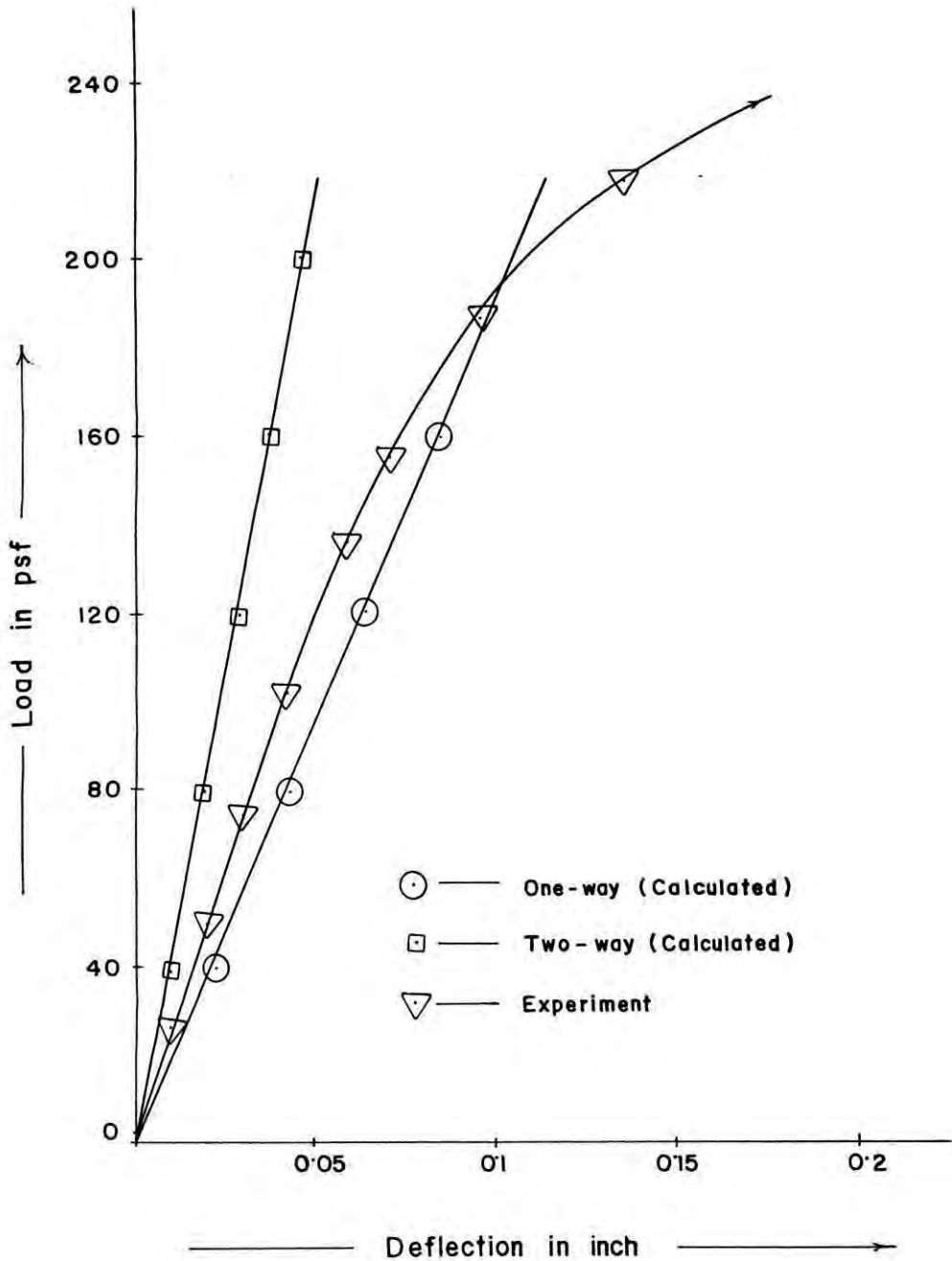


Fig.6.11. Load-deflection curve for the points 1,3,7,8 of Type-IV.

The experimental curve of slab for the points 2 and 6, shown in Fig.6.12, indicates similar behavior. At 124.0 psf. load , the deflection is about 21.11% less than the calculated deflection for one-way , and is about 77.50% higher than the calculated deflection for two-way .

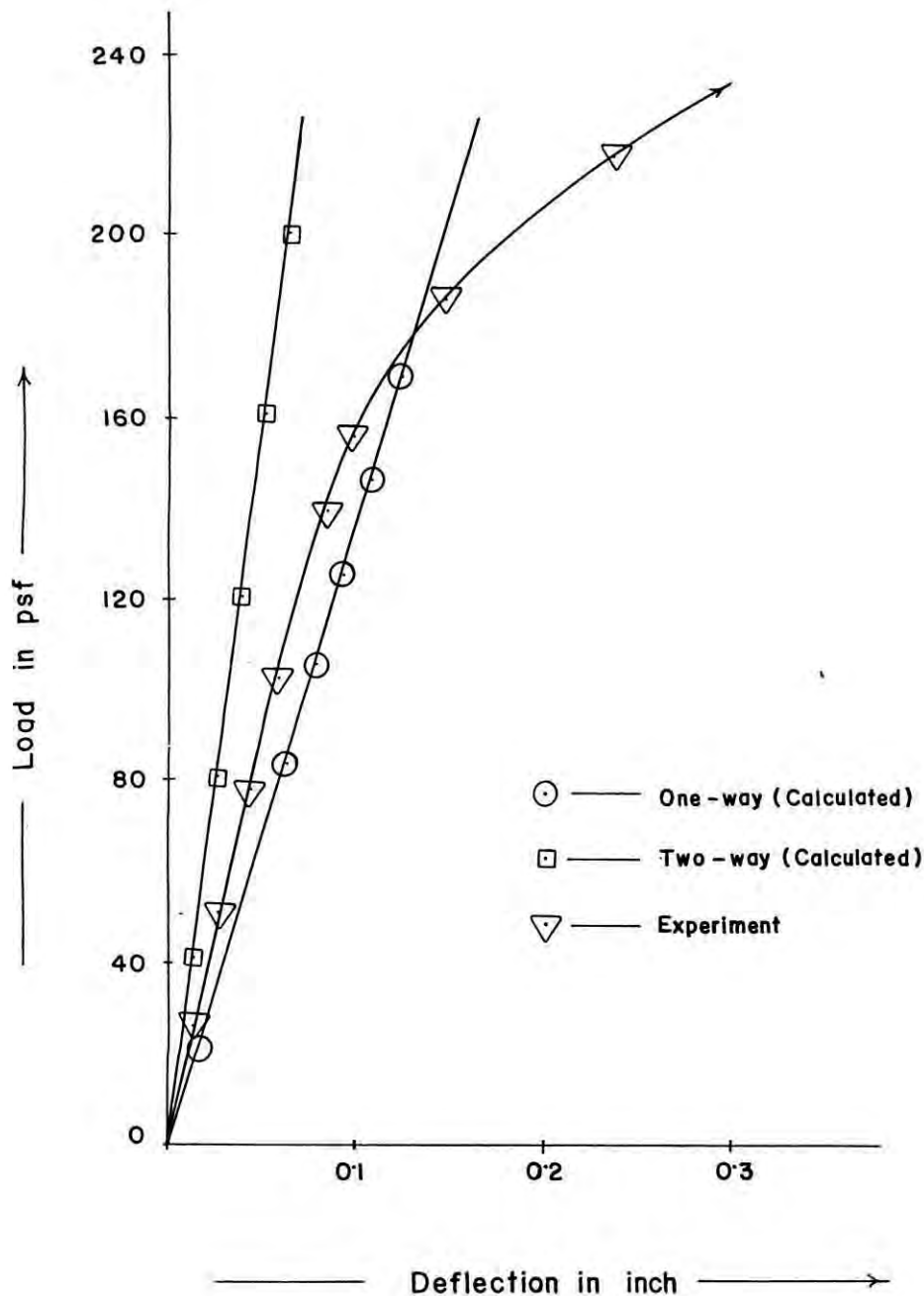


Fig.6.12. Load-deflection curve for the points 2,6 of Type-IV.

Fig. 6.13 presenting deflection curves of the points 4 and 5 for the test slab shows behavior similar to those for other points discussed above.

At 124.0 psf. of loading, the experimental deflection is about 16.67% less and is about 47.16% higher than that of calculated values considering one-way and two - way slab action respectively.

From the study of the load-deflection curves of the three different test slabs it may be concluded that the slab Type-II behaves almost like a one-way slab while test slabs of Type-III and Type-IV deflection lies almost at the middle of the deflection predicted by considering one-way and two-way slab action for a load upto 120.0 psf. At higher load upto 200.0 psf., for slab type III and IV, it is better to use one-way action for deflection precision.

6.8. Discussion on Deflection Profile of Test Slabs:

The deflection profile is the curve plotted from the relationship between span length and deflection. The deflection of the entire span can be plotted in such a way to get the deflected shape of the entire span. The shape of the profile is important for elastic range as well as for plastic range.

The deflection profiles of the test slab Type-I are shown in Fig. 6.14. Two experimental profiles are drawn to compare with the theoretical curves at 83.0 psf., and at 188.0 psf. The experimental profile and calculated profile were drawn for the load of 83.0 psf. are identical to each other. But profiles at

load of 188.0 psf. the experimental profile is much steeper than the calculated one. The profile was drawn for the 83.0 psf.

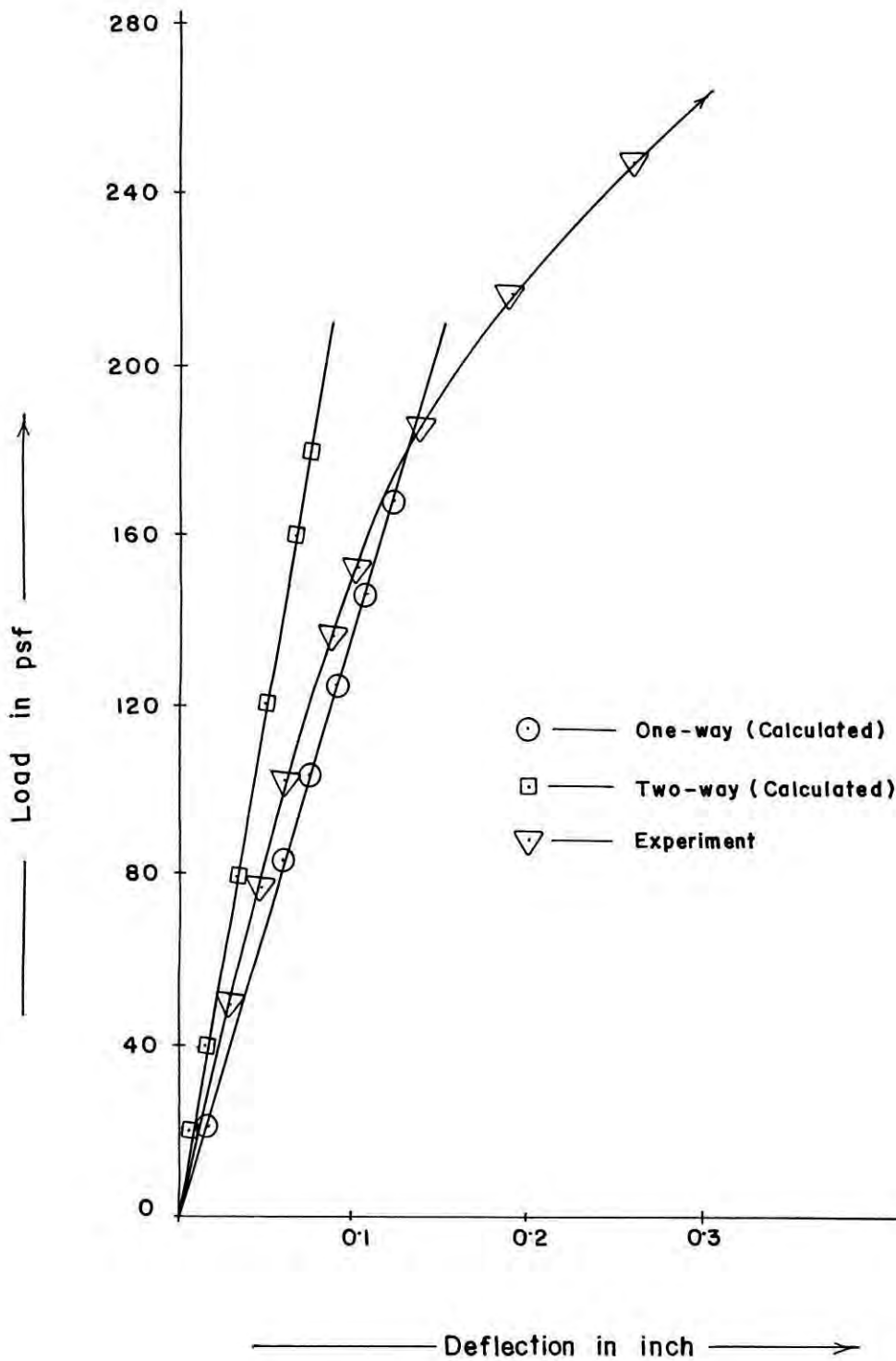


Fig.6.13. Load-deflections curve for the points 4,5 of Type-IV.

load obeys the law of elasticity since no cracking occurred any where in the slab at this stage of loading. The slab was firmly well cracked at 188.0 psf. load the deflections were higher than those given by the elastic theory assuming the section to be uncracked.

Fig. 6.15 represents the deflection profile in short direction of the test slab Type-II. The three curves were drawn at 124.0 psf. load to compare the experimental profile with the theoretical profiles assuming one-way and two-way slab action. The experimental profile for the slab Type-II of the short direction is very much identical with the calculated deflection profile for one-way slab. The experimental profile indicates the deflection at center point is 7.26 % less than that profile for one-way and 121.15% higher than that for two-way slab.

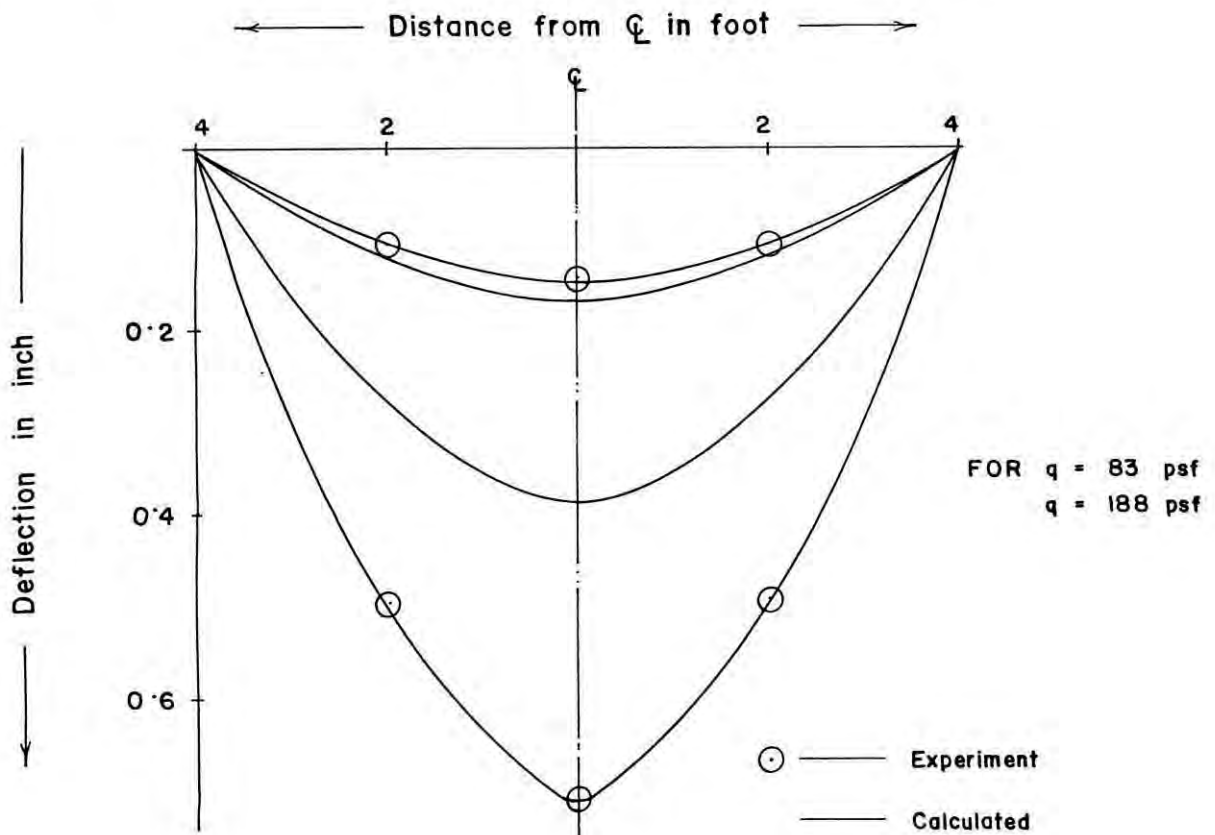


Fig.6.14. Deflection profile of slab Type-I.

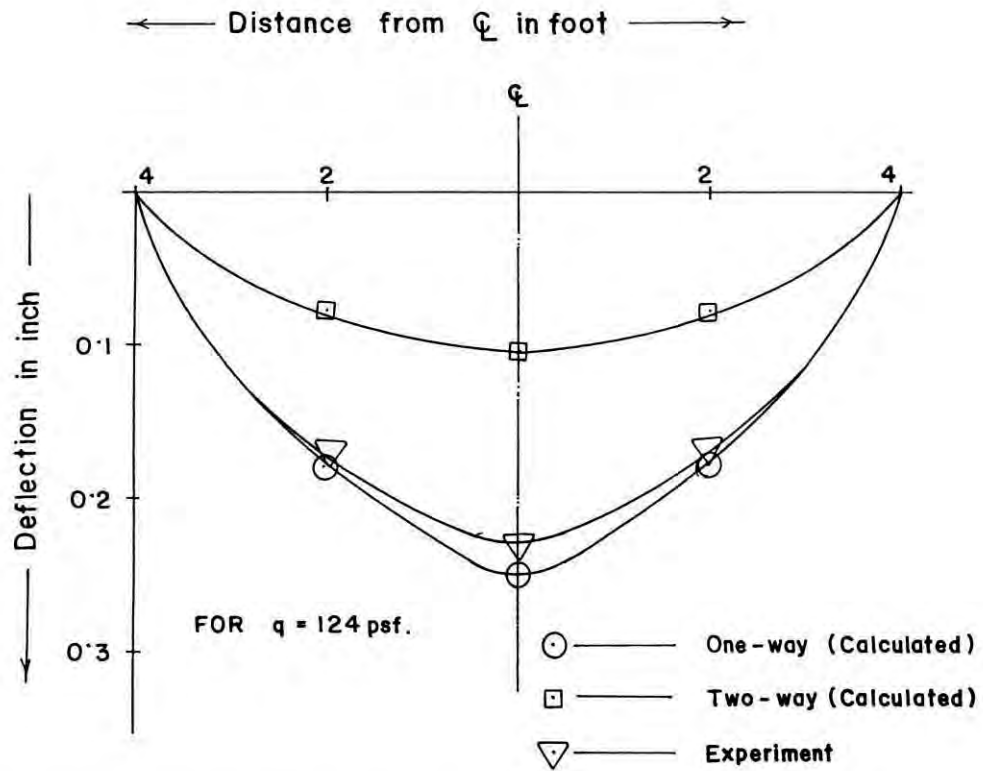


Fig.6.15. Deflection profile of short span of slab Type-II.

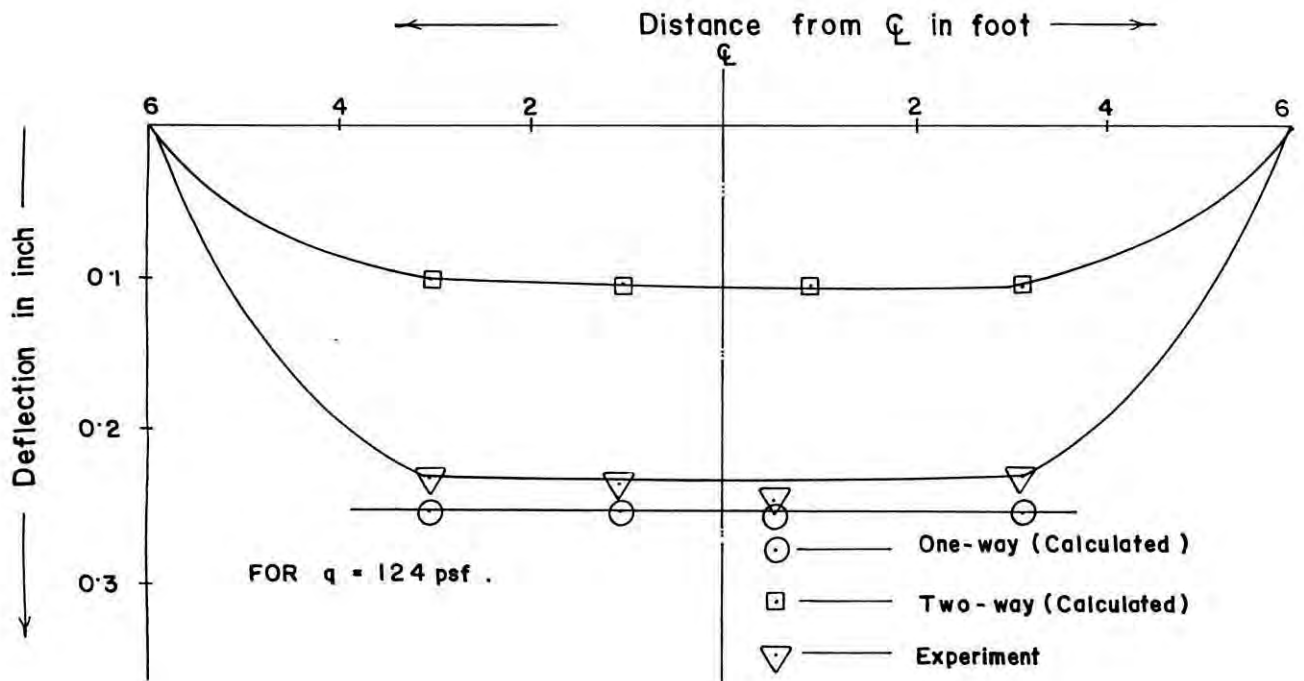


Fig.6.16. Deflection profile of long span of slab Type-II.

In Fig. 6.16 the deflection profiles were drawn along the center line in the long direction of the test slab Type-II. The locus of the observed profile is almost horizontal line in middle half portion.

The experimental profile (Fig.6.16) at the center point is 8.0% less than the calculated profile for one-way slab and 113.0% higher than the calculated profile for two-way slab at 124.0 psf. load. The experimental profile is nearly identical to the calculated profile for one-way slab.

Fig. 6.17 compares the experimental profile in shorter direction of slab Type-III with the calculated profiles for one-way and two-way slab action at a load of 124.0 psf. The locus of the experimental profile is in between and almost at midway the locus of the calculated profiles for one-way and two-way slabs.

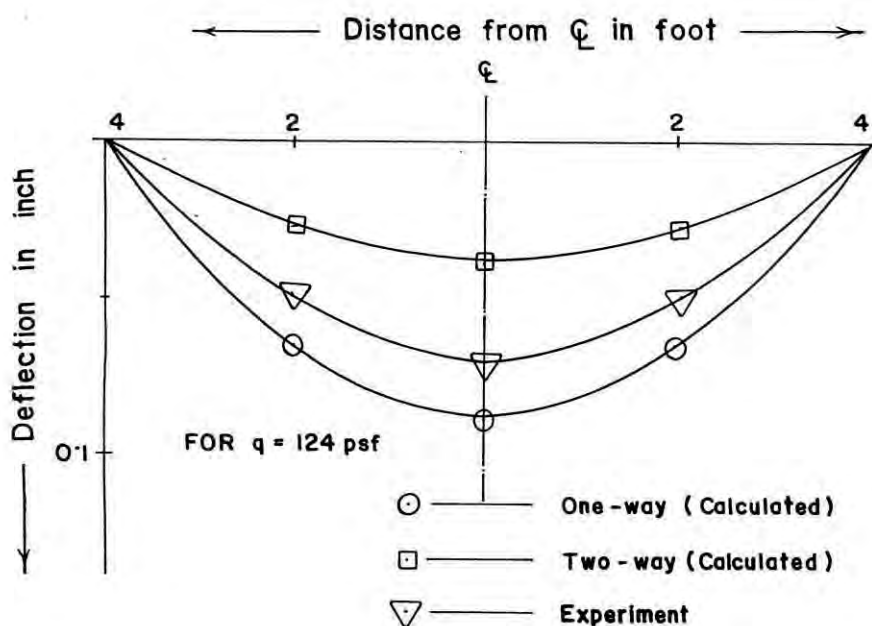


Fig.6.17. Deflection profile of short span of Type-III.

In the Fig.6.18, three profiles were drawn along the center line of the test slab Type-III along the long direction. The locus of the experimental profile is parallel to the profile for one-way slab at a load of 124.0 psf.

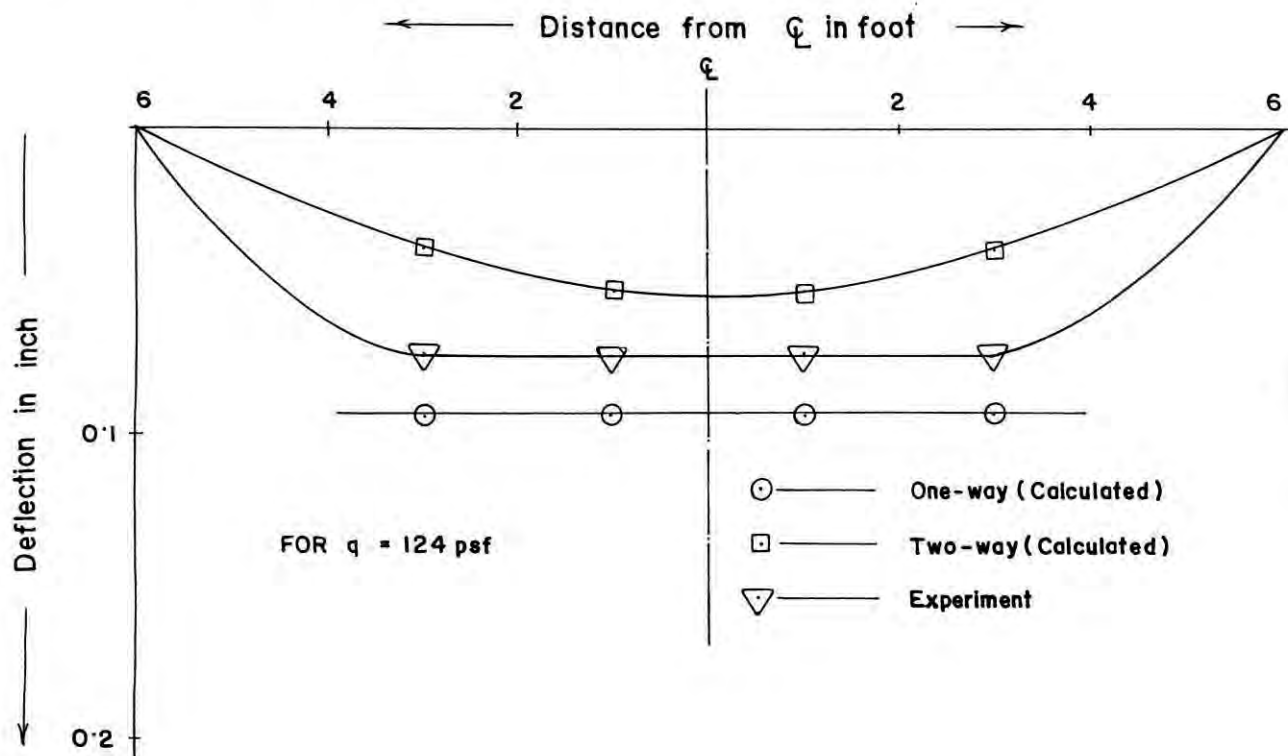


Fig.6.18. Deflection profile of long span of slab Type-III.

Fig.6.19 is representing profiles drawn along the center line of short direction of the test slab Type-IV at a loading of 124.0 psf. The locus of the experimental profile is midway the curves for one-way and two-way slab.

Fig. 6.20 is representing the profiles of the center line along long direction of the test slab Type-IV at a loading of 124.0 psf. The locus of the experimental profile is in between the two profiles drawn for one-way and two-way slabs. It can be observed from the figure that the experimental profile is

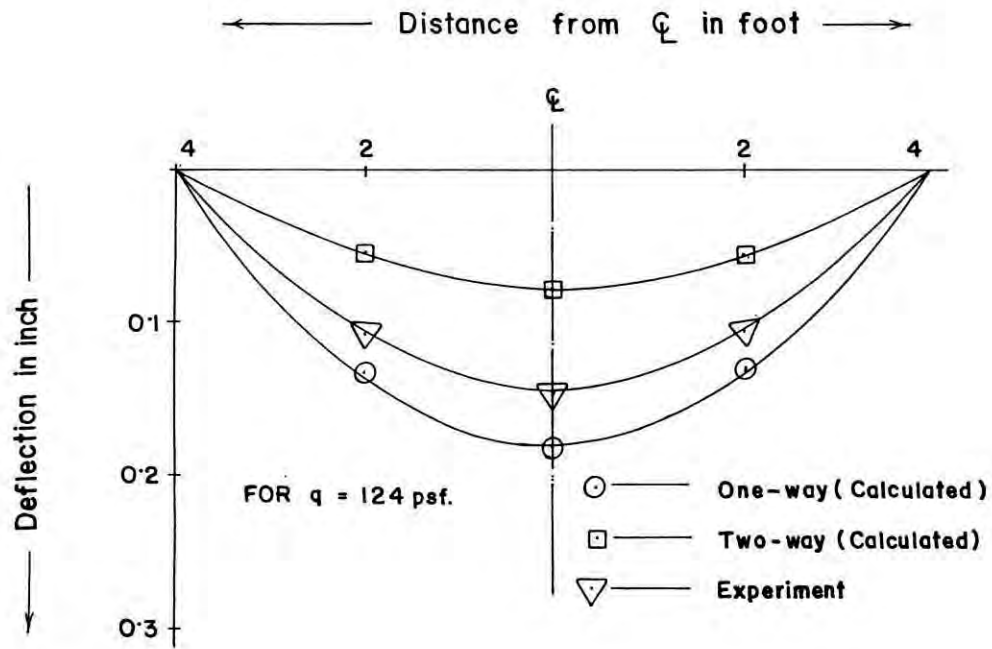


Fig.6.19. Deflection profile of short span of slab Type-IV.

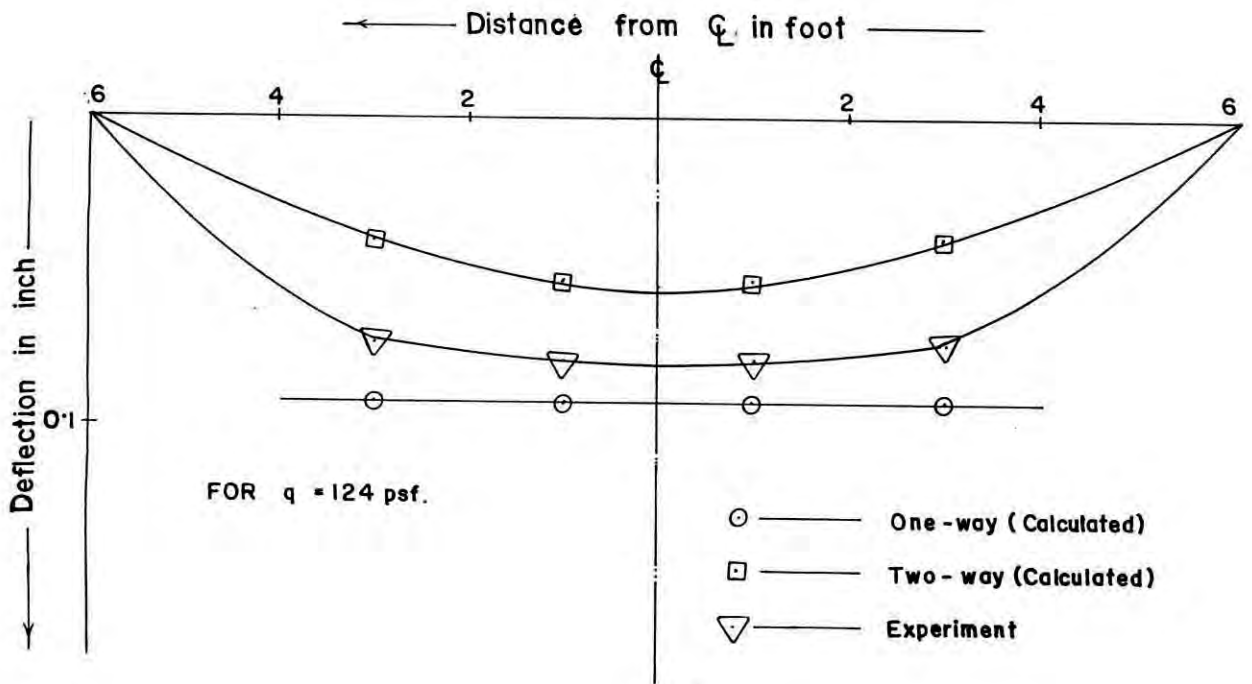


Fig.6.20. Deflection profile of long span slab Type-IV.

intended to be curved instead of being straight as observed for profiles of types-II and III. This indicates that the slab has a tendency to behave like a two-way slab and also indicates that a portion of the load was transferred across the shear keys.

6.9. Cracking Load Characteristics :

In the prestressed concrete flexural members the bending moment producing first hair cracks in the critical zone, can be computed by the elastic theory. Such calculation is based on the assumption that cracking starts when the tensile stress in the extreme fiber of the concrete reaches its modulus of rupture. The modulus of rupture of concrete with crushed brick chips [9] is $9.0\sqrt{f'_c}$.

For slabs Type-I and II, having thickness of 2.5 inch, the cracking moment can be calculated as 1416 lb-ft. & 1417 lb-ft. respectively and the corresponding uniformly distributed loads are about 177.00 psf. resulting the superimposed live load to be 149.0 psf.

The first crack, however, was observed at center point of the mid span of the slab at a live load of 146.0 psf. (Table 5.3) which is much closer to the theoretically calculated cracking load for Type-I.

The arrangement of slab types II , III and IV were such that they were expected to behave like a two-way slab system. But it was observed from the laboratory tests that the first hair

cracks were initiated at the center point of middle shearkeys rather than at maximum moment regions. The first cracks were observed in shearkeys for the slab types II , III and IV at superimposed load of 124.0 psf., 124.0 psf. and 137.0 psf. respectively (Table 5.3). The corresponding flexural stresses at the center points of middle shearkey for the aforementioned slabs can be computed using the following relationship (6),

$$M_y = v \frac{qx(a-x)}{2} - qa^2\pi^2 \sum_{m=1,3..}^{\infty} m^2 [2B_m + (1 - v)A_m] \sin \frac{m\pi b}{a}$$

where,

$$A_m = - \frac{2(\alpha_m \tanh \alpha_m + 2)}{\pi^5 m^5 \cosh \alpha_m}$$

$$B_m = \frac{2}{\pi^5 m^5 \cosh \alpha_m}$$

Using the above relationship the corresponding bending moments acting at the center point of middle shearkeys, for the slab Types-II, III and IV can be computed to be 1884.0 lb-in, 1884.0 lb-in and 2081.0 lb-in respectively. The corresponding flexural stresses are computed to be 151.0 psi, 77.0 psi and 85.0 psi respectively. The computations were presented in Appendix-6. The calculated modulus of rupture , for the above types, are 552.0 psi, 552.0 psi and 549 psi respectively [Appendix-6] .

Thus the experimental rupturing stresses are observed to be much lower than the calculated stresses for the shearkeys. The probable reasons are:

- a. The appeared hair cracks along the shearkeys were not only due to the rotation but shear and rotation would likely to act simultaneously in these sections, (according to Lee [19]).
- b. The slab panels were precast and shearkeys between the panels were filled in by in-site concrete. So, some sort of shrinkage cracks might have been occurred in the shearkeys .
- c. The precast prestressed concrete slab panels were cast in a bed using long line method as discussed in Art. 4.8. There might be uneven surfaces over some areas of the casting bed causing some uneven bottom surfaces in slab elements. These uneven surface might have caused to maintain a gap between the supports of the loading frame and the slabs in particular areas. When these slabs were loaded the uncontacted portions of the slab panels compelled to contact with the support causing shear failure along the shearkeys.

The cracks at the center of the slab Type-II, however, were observed at a live load of 155.0 psf. The experimental cracking load is only 6.0 psf. higher than theoretically calculated one, perhaps due the distribution of some load in the lateral direction of slab panels.

For slabs Type - III and IV, having thickness of 3.5 inch, the cracking moments can be calculated as 2276.0 lb-ft. & 2270.0 lb-ft. (calculation shown in Appendix-6) respectively, and the corresponding uniformly distributed loads are about 284.0 psf. Since the dead load of the slab was 40.0 psf., cracking should be occurred at a live load of 244.0 psf.

In slab Type-III the hair cracks were observed at the center of the slab panel, the maximum moment region, at a live load of 217.0 psf. which is higher than the calculated cracking load of 244.0 psf.

In the location of maximum moment region of slab Type-IV the first crack was observed at a live load of 227.35 psf. The experimental load was higher due to the transmission of load across the gap towards the supports in the long direction.

6.10. Ultimate Load Characteristics:

The failure of a section may start either in the steel or in the concrete and may end up in one or other. The most general case is that of an under-reinforced section, where the failure starts with excessive elongation of steel and ends with the crushing of concrete. A relatively uncommon mode of failure is that of an over reinforced section, where the concrete is crushed before the steel is stressed into plastic range. Hence there is only a limited amount of deflection before rupture, and a brittle mode of failure is obtained. According to the crack-line theory of slab failure, the ultimate capacity of a slab is not reached

until a crack pattern has developed, making the slab unstable.

For slabs Type-I and II, having thickness of 2.5 inch, the ultimate resisting moment can be calculated, by applying Whitney's theory, as 2324.7 ft.-lb. (calculation shown in Appendix-6) and the corresponding total live load at ultimate is 262.60 psf.

For slab Type-III and Type-IV, having the slab thickness of 3.5 inch, the ultimate resisting moment can be calculated as 3000.4 lb-ft. & 3004.0 lb-ft. respectively and the corresponding total live loads at ultimate are 335.00 psf. and 335.50 psf. respectively.

The slab Type-I slab failed at a live load of 271.0 psf. due to excessive deflection of 2.25" at mid span. The cracks were initiated at the center point of mid span and ended on the edges of the slab. However, the experimental ultimate value is very much closer to the calculated ultimate value of 211.0 psf.

The slabs Type-II, Type-III and Type-IV were arranged in such a way that they seemed to be acted as two-way slabs. In all types of the slabs, the first hair cracks occurred in the shearkeys and propagated to the supports as shown in Fig.5.2, Fig.5.3 and Fig.5.4. As the cracks initiated in the center point of the shearkeys and propagated along the shearkeys towards the supports causing the slab panels separated from one another. After separation the panels behaved as one-way slab. The slabs failed as the cracks propagated to the supports causing the slabs unstable.

The experimental ultimate load of Type-II, III and IV were 309.0 psf., 335.0 psf. respectively against calculated loads of 262.0 psf. and 335.0 psf. respectively.

6.11 Cracking Pattern:

In the slab Type-I the flexural cracks were developed in the center point of the mid span at a loading of 146.0 psf. and then, as the load was increased the cracks propagated horizontally towards the edges of the slab (Fig.5.1) at the mid span following the yield - line theory.

In slabs Type-II, Type-III and Type-IV cracks were developed first at the center of the middle shearkey of the slabs and then cracks were propagated along the joints as the joint was the weakest portion of the slab. As the cracks developed in the joints, the panels were separated to one another. On separation between adjacent slab panels the loads in the long direction could not be transferred and hence the slab panels behaved as a one-way slab system. As the load was increased the cracks occurred in the mid span of the short direction and propagated towards the supports.

6.12. Mode of Failure:

Flexural failure was the final mode of failure in the slabs of all types. The cracks were initiated in the maximum moment region and as the load was increased the cracks propagated towards the supports or edges and finally the slabs failed by excessive rotation along the cracks. The cracks were following the patterns established by yield-line theory.

CHAPTER 7

CONCLUSIONS AND RECOMMENDATION FOR FUTURE STUDIES

7.1. Conclusions:

Laboratory tests were conducted on four types of slab system. The slabs were constructed using precast prestressed concrete slab panels of width 25 inch. Analysis and discussion of results obtained in laboratory tests were presented in chapter 6. From the analysis of test results the following conclusions may be drawn:

1. Deflection of the slab without shearkeys and without topping designated as Type-I is predicted accurately by the elastic theory till the slab remains uncracked. After the slab is cracked the deflection is very much identical to that predicted from Moment-curvature relationship.
2. The cracking of slab Type-I was initiated in the maximum moment region and propagated towards edges forming the failure mechanism which is very similar to that predicted by yield - line theory.
3. The cracks were initiated, in central joint of the slab panels of the slab with shearkeys and without topping designated as Type-II, the slab without shearkeys and with topping designated as Type-III and the slab with shearkeys

and with topping designated as Type-IV, and propagated along the joints of the two adjacent panels as the joints are weakest zone of the floor system studied in this work.

4. Load-deflection curve of the slab with shearkeys and without topping, Type-II, coincides with the calculated deflection curve for one-way slab system.
5. For the slab without shearkeys and with topping, Type-III, the deflection curve and the deflection profile was observed to lie around the midway to those calculated for one-way and two-way floor system.
6. The deflection profile of the slab with shearkeys and with topping, Type-IV, is non-linear and lies midway between those calculated for one-way and two-way slab system while it is straight line for the slabs types-II and III and for Type-II it almost coincides with that calculated assuming one-way slab action.
7. Within the service load, the slab without shearkeys and with topping, Type-III and with shearkeys and with topping, Type-IV observed to behave neither like a one-way nor two-way slab system but their behavior lie in between the two system.
8. Cold-drawn low-carbon mild steel can be used for prestressing precast slab panels to be used for constructing a slab without using any formworks.

7.2. Recommendations for Future Studies :

The conclusion stated above were limited by the scope of the tests. It is believed that a wider area in this field remains to be unexplored in order to develop the guide lines for laying the proper code of practice for designers. It should be mentioned therefore, that the investigation on behavior of brick aggregate concrete prestressed with cold-drawn low-carbon mild steel should be continued and all the different characteristics should be studied.

The following recommendations are ,therefore,made for future study of the behavior of prestressed concrete slab panels using brick aggregate concrete and cold-drawn low-carbon mild steel.

1. Influence of low-carbon mild steel using as prestressing reinforcement on the behavior of prestressed concrete slab panels.
2. Influence of brick aggregate on crushing strength of
3. Effect of different types of shearkeys in the joints of the two adjacent slab panels.
4. Influence of applied loading on the slab panels in terms of deflection, cracking and strain characteristics.
5. Effect of thickness of topping over the prestressed slab panels on the behavior of the slabs.
6. Influence of the small diameter reinforcing mesh provided in the topping on the bi-directional efficiency of the slab panels.
7. Influence of the transverse prestressing, as in pseudo slab, on the bi-directional efficiency of the slab panels.

LIST OF REFERENCES

1. Lin, T.Y. and Burns, N.H., "Design of Prestressed Concrete Structures". 3rd. ed., John Wiley and sons inc., 1982.
2. Boquan, S. and Renhu, Y. "Technology Manual on Prestressed Concrete (CWPC)", UNDP/UNIDO Regional Network in Asia-Pacific for Low-cost Building Materials Technologies and Construction Systems, 1984, pp. 4-10 & 139-150.
3. Magnel, G. "Prestressed Concrete", 3rd. ed., Concrete Publications Ltd., 1954.
4. ACI Committee 435, Subcommittee-5 Report, "Deflection of Prestressed Concrete Members", Journal of ACI, Dec. 1963, Title No. 60-72, pp. 1697 - 1727.
5. ACI Committee 435, "Deflection of Two-way Reinforced Concrete Floor Systems" , Manual of concrete Practice, ACI 435.6R-74, pp. 435.6R-1 - 27.
6. Timoshenko, S.P. and Woinowsky-Krieger, S., " Theory of Plates and Shells", 2nd. ed., McGraw - Hill Book Co., 1959, pp. 113-120.
7. Scordelis, A.C., Pister, K.S. and Lin, T.Y., " Strength of Concrete Slab Prestressed in Two Direction", Journal of ACI, Vol.28, No.3, Sept. 1956, Title No. 53-13. Proceedings Vol.53, pp. 241 - 256.
8. Metz, G.A., "Flexural Failure Tests of Reinforced Concrete Slabs", Journal of ACI, Proceedings Vol.62, No.1, Jan. 1985, Title No.62.7, pp. 105-115.

9. Hossain, M.M., "Shear Capacity of brick aggregate concrete beams with Web-Reinforcement", Master's thesis submitted to the Department of Civil Engineering, BUET, Dhaka, Aug. 1986. pp. 63.
10. Branson, D.E., "Design Procedures for computing Deflections", Journal of ACI, Vol. 68, No. 8, Aug. 1971. pp. 555.
11. Marsh, C.F., "Reinforced Concrete", D. Van Nostrand Co., New York, 1904, pp. 283.
12. Ewell, W.W. , Okubo, S. and Abrams, J.I., "Deflection in Grid Works and Slabs" , Trans. ASCE Vol. 117, 1952, pp. 869.
13. Khachaturian, N. and Gurfinkel, G., "Prestressed Concrete", McGraw - Hill Book Co., 1969.
14. Muspratt, M.A., "Behaviors of Simply Supported slabs", Journal of the Structural Division, Proceedings of ASCE, Vol.95, No.ST12, Dec. 1969, pp. 2703 - 2721.
15. Rao, A.S.P., "Direct Minimum Weight Design of Short-span Prestressed Concrete members", Indian Concrete Journal, Vol. 59, No.7. July, 1985, pp. 186 - 192.
16. Somayaji, S. "Prestressed Concrete Flexural Member : Design", Journal of the Structural Division, Proceedings of ASCE, Vol. 108, No.ST8, Aug. 1982, pp. 1781 - 1797.
17. Morris, D., "Prestressed concrete Design by Linear Programming", Journal of the Structural Division, Proceedings of ASCE, Vol. 104, No. ST3, March, 1978.

18. Duberg, J.E., Khachaturian, N. and Fradinger, R.E., "Method for Analysis of Multi-beam Bridges", Journal of the Structural Division, Proceedings of ASCE, Vol. 86, No. ST7, July, 1960, pp. 109 - 138.
19. Lee, D.N., "Analysis of Multi-beam Slabs", International Journal for Solids Structures, Vol. 9, 1973. pp. 495 -506.
20. Cusens, A.R. and Pama, R.P., "Design of Concrete Multi-beam Bridge Decks", Journal of the Structural Division, Proceedings of ASCE, Vol. 91, No. ST5, Oct. 1965, pp. 255 - 277.
21. Morley, C., "The Minimum Reinforcement of Concrete Slabs", International Journal of Mechanical Science, Vol. 8, No.4, April, 1968.
22. Johansen, K.W. "Polyteknisk Forening", Pladeformler, Copenhagen, 1949, pp. 172.
23. A paper on "Materials, Design And Construction of Quality concrete", Prolex Industries Inc., 1964.
24. Guyon, Y., "Prestressed Concrete", Asia Publishing House, Bombay, 1963, Vol. 1, pp. 235-259.
25. Chetty, S.M.K., Rao, A.S.P. and Bhargawa, R.N., "Selection and Design of Prestressed Concrete Sections for Flexure", The Indian Concrete Journal, Reprint No. 61, pp. 1-34.
26. Saether, K., "Direct Design of Prestressed Concrete Members", Journal of ACI, Feb. 1963, pp. 234-242.

APPENDIX - 1

Mix design for Concrete [23]:

1. Required compressive strength of concrete
(at 28 days cylinder strength) _____ 4000 psi.
2. Design strength _____ 4600 psi.
3. Maximum size of coarse aggregate _____ $\frac{3}{4}$ "
4. Specific gravity of coarse aggregate _____ 1.80
5. F.M of coarse aggregate _____ 6.50
6. Specific gravity of fine aggregate _____ 2.59
7. F.M of fine aggregate _____ 2.50
8. Specific gravity of cement _____ 3.15
9. Unit weight of C.A (S.S.D) _____ 75.20 lbs.
10. Unit weight of F.A (S.S.D) _____ 94.80 lbs.
11. Unit weight of cement _____ 85.60 lbs.

Considering the slump to be 1".

From Table 7.4 [23]

Water required _____ 37 gal/cu.yd. or 1.37 gal/cft.

From Table 7.6 [23]

Water-Cement ratio _____ = 0.5

Weight per sack of cement = 110 lbs.

Water required per sack of cement = $55 \text{ lbs}/8.33 = 6.6 \text{ gal.}$

\therefore Cement required = $37/6.6 = 5.6 \text{ sack/cu.yd.}$

Volume of coarse aggregate = 0.64

(From Table 7.7) [23]

Wt. of water per gal./ Wt. of water reqd. per sack of
cement $(62.4/8.33) = 7.5$

Now,

Total volume of cement = $(5.6 \times 110) / (3.15 \times 62.4) = 3.13$ cft.

Volume of water = $37 / 7.5 = 4.94$ cft.

Solid vol. of C. Agg. = $(75.2 \times 27 \times 0.64) / (1.80 \times 62.40) = 11.57$ cft.

Volume of entrapped air = $0.01 \times 27 = 0.27$ cft.

Total vol. occupied by cement, water, C.agg. & air = 19.91 cft.

Volume of fine aggregate = $27 - 19.91 = 7.09$ cft.

Weight of dry sand = $2.59 \times 62.4 \times 7.09 = 1145.85$ lbs.

Materials required (weight basis):

(a) Cement _____ $5.6 \times 110 = 616.00$ lbs.

(b) Water _____ $37.0 \times 8.33 = 308.21$ lbs.

(c) Sand (SSD) _____ = 1145.85 lbs.

(d) Brick chips (SSD) _____ = 1299.45 lbs.

Mix design ratio (weight basis):- 1 : 1.86 : 2.11

APPENDIX - 2

Design of prestressed concrete slabs:

$$f_{pu} = 1,25,000 \text{ psi.}$$

$$f'_c = 3,750 \text{ psi. at 28 days of cylinder strength.}$$

According to ACI code [ACI 318 - 83] permissible stress immediately after transfer of prestress for flexural member

$$f_o = 0.7 f_{pu} = 0.7 \times 125000 = 87,500 \text{ psi.}$$

Effective prestress after deducting lumpsum loss [25% for pretensioning].

$$f_{sc} = 0.75 \times 87500 = 65,625 \text{ psi.}$$

$$f_t \leq 0.45 f'_c = 0.45 \times 3750 = 1687.50 \text{ psi.}$$

$$f_b \leq 0.60 f'_{ci}$$

$$\begin{aligned} f'_{ci} &= \text{taking 75\% strength of concrete at transfer} \\ &= 0.75 \times 3750 = 2812.50 \text{ psi.} \end{aligned}$$

$$f_b \leq 0.60 \times 2812.50 \leq 1687.50 \text{ psi.}$$

Clear span length — 96 inch.

Phase - 1 : (Dead load only):

From span-depth ratio limitations : [one-way solid slab]

$$L/d = 44 \text{ [where } L = \text{span]}$$

$$\therefore d = L/44 = 96/44 = 2.182 \text{ inch. (Say 2.50 inch).}$$

f. Calculating prestress force :

The effective prestress required is, corresponding to a lever arm of $e + k_t = 1.25 - 0.75 + 0.417 = 0.917$ inch.

$$F = M_T / (e + k_t) = 4842 \text{ \#}.$$

$$F_o = 6456 \text{ \#}.$$

g. Computing the required concrete area by :

$$A_c = (Fh) / (f_t c_b) = 8.97 \text{ in}^2.$$

$$A_c = (F_o / f_b) [1 + \{ e - (M_G / F_o) / k_t \}] = 11.80 \text{ in}^2. < 30 \text{ in}^2.$$

$$A_s = 0.074 \text{ in}^2 / \text{'}. \text{ Using } 4 - 4 \text{ mm}\phi.$$

Phase - 2 : Considering the service load (without topping):

a. Load calculation :

Self weight of slab	2.50 x 12.50 = 31.25 psf.
Live load	= 40.00 psf.

$$\text{Total load} = 71.25 \text{ psf. (Say } 71.00 \text{ psf).}$$

b. Moment calculation :

$$M_T = (1/8) \times 71.00 \times 8^2 = 568.0 \text{ \#}.$$

$$M_G = (1/8) \times 31.25 \times 8^2 = 250.0 \text{ \#}.$$

$$M_L = 318.0 \text{ \#}.$$

c. $M_G \geq .20 M_T$, then, large ratios of M_G/M_T governs:

$$F = T = M_T / 0.65h = 4194.0 \text{ \#}.$$

$$A_s = F / f_{sc} = 0.063 \text{ in}^2 / \text{'}.$$

$$F_o = 5592.0 \text{ \#}.$$

d. Calculating the lever arm :

$$e - k_b = M_G / F_o = 0.536 \text{ inch.}$$

$e = 0.536$ inch, indicating 0.536 inch below the bottom kern or 0.297 inch above the bottom fiber.

e. Calculation of prestress force :

The effective prestress required is, corresponding to a lever arm of $e + k_t = 1.25 - 0.75 + 0.417 = 0.917$ inch.

$$F = M_T / (e + K_t) = (568 \times 12) / 0.917 = 7432\#.$$

$$F_o = 7432 \times 87500 / 65625 = 9909\#.$$

f. Computing the required concrete area :

$$A_c = Fh / (f_t c_b) = 8.81 \text{ in}^2.$$

$$A_c = (F_o / f_b) [1 + \{ e - (M_G / F_o) \} / k_t] = 15.04 \text{ in}^2.$$

$$A_s = 0.113 \text{ in}^2. \quad \underline{\text{Using 8 - 4 mm}\phi}.$$

Phase 3 : Considering the service load (with topping) :

a. Load calculation :

Self weight of slab	(2.50+1) x 12.50	= 43.75 psf.
Live load		= 40.00 psf.
		<hr/>
		83.75 psf.

b. Moment calculation :

$$M_T = 1/8 \times 83.75 \times 8^2 = 670 \text{ #'}$$

$$M_G = 1/8 \times 43.75 \times 8^2 = 350 \text{ #'}$$

$$M_L = 670 - 350 = 320 \text{ #'}$$

c. Computing the section properties :

$$A_c = 3.5 \times 12 = 42 \text{ in}^2.$$

$$I = (12 \times 3.5^3) / 12 = 42.87 \text{ in}^4.$$

$$r^2 = I / A = 42.87 / 47 = 1.02 \text{ in}^2.$$

$$k_t = k_b = r^2 (c_b \text{ or } c_t) = 0.582 \text{ inch.}$$

d. Computing the force :

$M_G \leq 0.20 M_T$, then, large ratio of M_G / M_T governs.

$$F = T = M_T / 0.65h = 3634 \text{ \#\"}$$

$$F_o = 4712 \text{ \#\"}$$

e. Calculating the lever arm :

$$e - k_b = M_G / F_o = 0.891 \text{ inch.}$$

$e = 0.891 + 0.582 = 1.473$ inch, indicating $1.75 - 1.473 = 0.277$ inch above the bottom fiber, which is obviously impossible. Suppose that for practical reasons the c.g.s. has to be kept 0.75 inch above the bottom fiber to provide sufficient concrete protection.

f. Calculating prestress force :

The effective prestress required is, corresponding to a lever arm of $e + k_t = 1.75 - 0.75 + 0.582 = 1.582$ inch.

$$F = M_T / (e + k_t) = 5082 \text{ \#\"}$$

$$F_o = F \times (f_o / f_{sc}) = 6776 \text{ \#\"}$$

$$A_{ps} = 0.0774 \text{ in}^2. \text{ Using } 6 - 4 \text{ mm}\phi.$$

g. Checking of stress in concrete area :

when dead load acts only :

$$M_G = 350.0 \text{ \#\"}$$

$$\text{Force acting on slab} = 6 \times 0.021 \times 65625 = 8268.75 \text{ \#\"}$$

Dead load stress :

$$f = 8.268 / 42 + [(350 \times 12 - 8268.75 \times 0.625) / (12 \times 3.5^3 / 12)] \times 1.75 = 196.875 \pm 39.51$$

$$f_{top} = 196.875 + 39.51 = 236.39 \text{ psi (compression)}$$

$$f_{bot} = 196.875 - 39.51 = 157.36 \text{ psi (compression)}$$

APPENDIX-3

Load-Deflection Reading Of Test Slabs.

Load-Deflection Reading of Slab Type-I

Loading Cycle

q lb/sft.	D ₁ in inch.	D ₂ in inch.	D ₃ in inch.	Remarks.
21.00	0.0345	0.0478	0.0342	
83.00	0.1050	0.1450	0.1090	
104.00	0.1540	0.2120	0.1570	
125.00	0.2100	0.2950	0.2140	
146.00	0.2840	0.4010	0.2880	First crack.

Unloading Cycle:

125.00	0.2550	0.4450	0.2540	
104.00	0.2060	0.4200	0.2050	
83.00	0.1590	0.3540	0.1580	
21.00	0.0800	0.2440	0.0800	

Reloading Cycle:

21.00	0.0800	0.2440	0.0800	
83.00	0.1390	0.3340	0.1390	
104.00	0.1920	0.3740	0.1920	
125.00	0.2420	0.4000	0.2440	
146.00	0.2960	0.4360	0.2980	
167.00	0.3810	0.5440	0.3850	
188.00	0.4940	0.7140	0.4980	
271.00		2.2500		Ultimate.

Load - Deflection Reading of Slab Type-II

Pressure in psf.	D ₁ in inch	D ₂ in inch	D ₃ in inch	D ₄ in inch	D ₅ in inch	D ₆ in inch	D ₇ in inch	D ₈ in inch
10.33	0.023	0.027	0.022	0.028	0.031	0.026	0.022	0.022
36.17	0.048	0.067	0.047	0.067	0.081	0.070	0.049	0.045
62.00	0.085	0.112	0.081	0.108	0.123	0.105	0.078	0.078
77.50	0.105	0.148	0.102	0.154	0.172	0.148	0.102	0.102
108.50	0.158	0.192	0.158	0.198	0.209	0.191	0.158	0.156
124.00 (F.C)	0.178	0.230	0.180	0.232	0.242	0.228	0.180	0.179
139.50	0.200	0.254	0.201	0.261	0.292	0.260	0.200	0.200
155.00	0.239	0.290	0.239	0.295	0.327	0.293	0.237	0.236
170.50	0.254	0.319	0.253	0.323	0.363	0.322	0.255	0.253
186.00	0.289	0.355	0.291	0.367	0.404	0.365	0.280	0.280
206.67	0.331	0.429	0.336	0.439	0.482	0.437	0.330	0.325
227.35	0.369	0.481	0.372	0.494	0.545	0.490	0.365	0.363
248.00	0.442	0.521	0.445	0.529	0.592	0.525	0.435	0.434
309.38 (Ult.)								

F.C = First crack.

D₁ = Deflection at point 1.

Load - Deflection Reading of Slab Type-III

Pressure in psf.	D_1 in inch	D_2 in inch	D_3 in inch	D_4 in inch	D_5 in inch	D_6 in inch	D_7 in inch	D_8 in inch
26.00	0.010	0.015	0.010	0.015	0.016	0.016	0.010	0.009
62.00	0.024	0.034	0.025	0.038	0.039	0.035	0.025	0.024
93.00	0.037	0.053	0.037	0.058	0.058	0.054	0.038	0.037
124.0 (F.C)	0.050	0.075	0.050	0.076	0.077	0.076	0.052	0.050
155.00	0.068	0.106	0.067	0.107	0.108	0.107	0.067	0.065
186.00	0.090	0.150	0.091	0.150	0.152	0.152	0.091	0.089
217.00	0.128	0.223	0.128	0.225	0.228	0.225	0.129	0.127
248.00	0.240	0.342	0.241	0.346	0.350	0.343	0.243	0.240
268.00	0.270	0.370	0.275	0.381	0.381	0.372	0.278	0.276
279.00	0.293	0.398	0.295	0.401	0.404	0.400	0.296	0.294
294.00	0.386	0.587	0.387	0.624	0.630	0.589	0.391	0.390
325.5 (Ult)								

F.C = First crack.

D_1 = Deflection at point 1.

Load - Deflection Reading of Slab Type-IV

Pressure in psf.	D ₁ in inch	D ₂ in inch	D ₃ in inch	D ₄ in inch	D ₅ in inch	D ₆ in inch	D ₇ in inch	D ₈ in inch
25.83	0.010	0.013	0.010	0.016	0.017	0.014	0.009	0.010
51.67	0.019	0.026	0.020	0.030	0.028	0.027	0.019	0.020
77.50	0.030	0.043	0.031	0.054	0.054	0.044	0.032	0.030
103.33	0.042	0.059	0.044	0.060	0.060	0.060	0.042	0.040
136.92 (F.C)	0.060	0.083	0.061	0.089	0.090	0.085	0.061	0.059
155.00	0.071	0.096	0.073	0.102	0.103	0.097	0.073	0.070
186.00	0.096	0.146	0.097	0.139	0.138	0.146	0.097	0.095
271.00	0.137	0.232	0.138	0.190	0.192	0.233	0.139	0.136
274.00	0.280	0.301	0.281	0.330	0.332	0.301	0.286	0.282
336.00 (Ult)								

F.C = First crack

D₁ = Deflection at point 1.

APPENDIX-4.

Moment Curvature Computation:

$$f'_c = 3750 \text{ psi.}$$

Limiting strain at ultimate = 0.003 in/in.

$$f_{pu} = 1,25,000 \text{ psi.}$$

$$f_{sc} = 65,625 \text{ psi.}$$

$$c = 1.25 \text{ inch.}$$

$$A_c = 30.00 \text{ in}^2$$

$$I = 15.625 \text{ in}^4$$

$$e = 0.625 \text{ inch.}$$

$$S = 12.50 \text{ in}^3.$$

$$E_c = 2.905 \times 10^6 \text{ psi.}$$

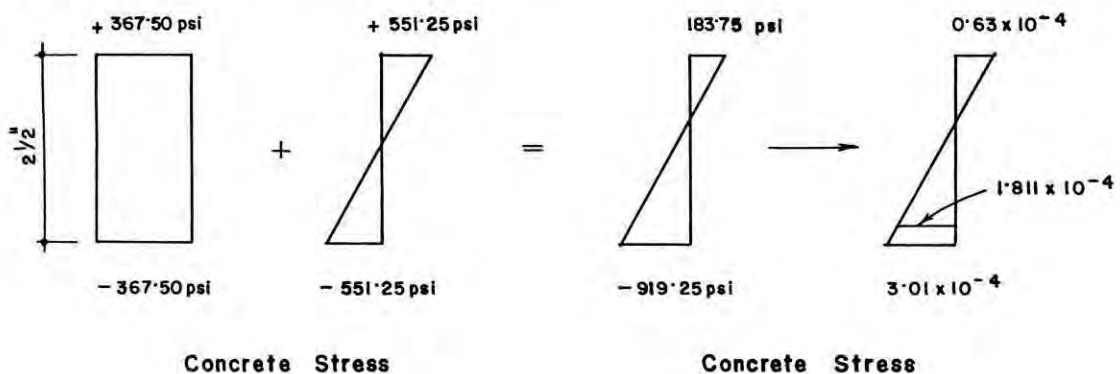
$$E_{ps} = 28.570 \times 10^6 \text{ psi.}$$

$$F = 8 \times 0.021 \times 65,625 = 11,025^\#$$

a. Computing stress and corresponding strain in section at $M = 0$

$$F/A_c = 11,025/30 = -367.50 \text{ psi.}$$

$$F_{cc}/I = \pm 551.25 \text{ psi.}$$



$\phi = \text{curvature} = (0.63 \times 10^{-4} + 3.01 \times 10^{-4}) / 2.5 = -1.457 \times 10^{-4} \text{ rad/in}$
 at $M = 0$.

$\epsilon_{sc} = \text{steel strain at } f_{sc} = 65,625 \text{ psi.}$

$\epsilon_{sc} = f_{sc} / E_{ps} = 2.3 \times 10^{-3} \text{ in/in.}$

b. Zero strain in concrete at level of steel :

An applied moment which produces $\epsilon_{cc} = 1.811 \times 10^{-3} \text{ in/in}$ at the level of steel will cause the strain in the concrete to be zero.

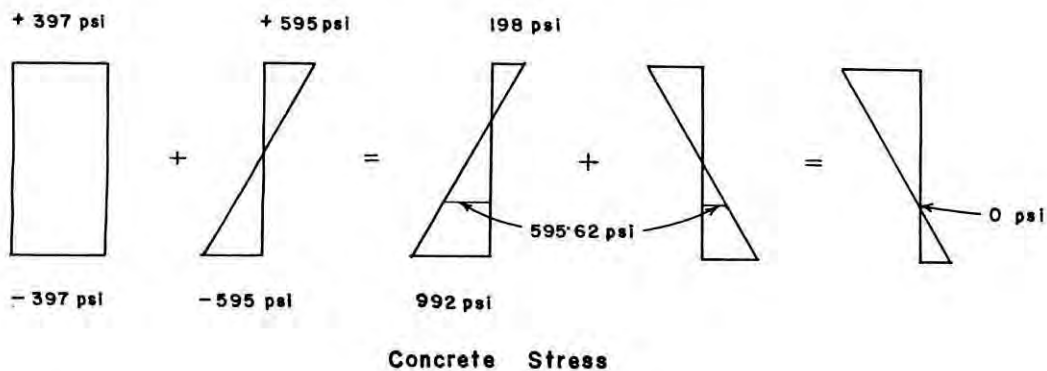
Thus the steel strain will become -

$$\epsilon_{ps} = \epsilon_{sc} + \epsilon_{cc} = 2.3 \times 10^{-3} + 0.1811 \times 10^{-3} = 2.4811 \times 10^{-3}$$

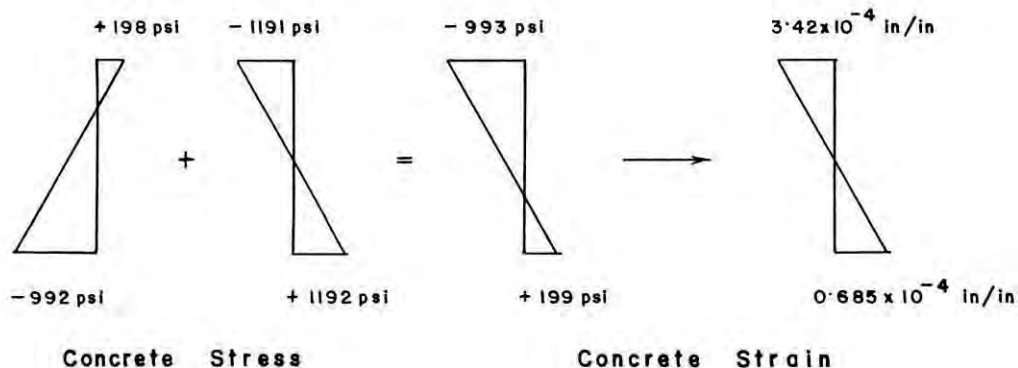
$$f_{ps} = \epsilon_{ps} \times E_{ps} = 2.4811 \times 10^{-3} \times 28.57 \times 10^6 = 70,885.16 \text{ psi.}$$

$$F = 8 \times 0.021 \times 70,885.16 = 11,908.7068 \#$$

Finding the concrete stresses which result from this increased force.



$$M = fI/c = 14890 \# \text{ in} = 1241 \#$$



$$\phi = (3.25 \times 10^{-4} + 0.653 \times 10^{-4}) / 2.5 = 1.64 \times 10^{-4} \text{ rad/in.}$$

From these calculation we have determined a second point in the elastic range of behavior.

$$M = 1241.23 \#.$$

$$\phi = 1.64 \times 10^{-4} \text{ rad/in.}$$

c. *cracking moment level :*

Cracking moment which is the end point for this uncracked section analysis. M_{cr} is associated with $f_r = 9\sqrt{3750} = 551 \text{ psi.}$

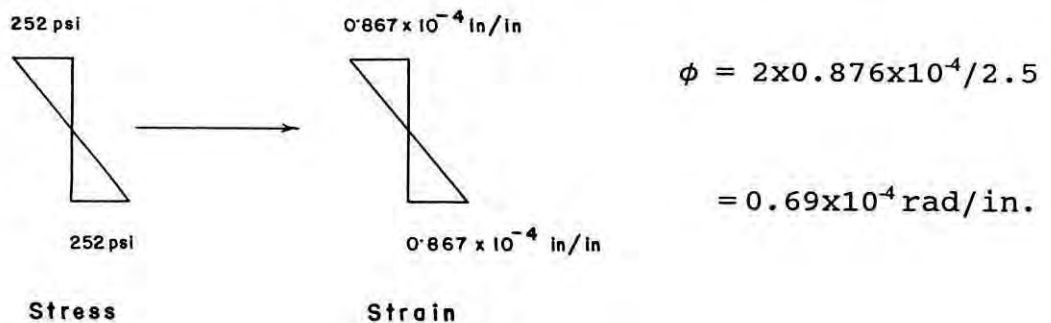
$$\text{Additional tensile stress} = 551 - 299 = 252 \text{ psi.}$$

$$M = \Delta f I / c = (252 \times 15.625) / 1.25 = 3137.5 \#$$

$$M_{cr} = 14890 + 3137.5 = 18027.0 \# = 1402.0 \#$$

$$\Delta f_{ps} = n \times (\Delta M y) / I = 1234.0 \text{ psi.}$$

$$\text{The steel at } M_{cr} \text{ is } f_{ps} = 70,885.16 + 1234.0 = 72119.16 \text{ psi.}$$



$$\phi_{cr} = (1.64 \times 10^{-4} + 0.69 \times 10^{-4}) \text{ rad/in.}$$

$$= 2.33 \times 10^{-4} \text{ rad/in.}$$

d. *at 0.001 top fiber strain :*

The top fiber strain at cracking is

$$\epsilon_c = -3.42 \times 10^{-4} - 0.55 \times 10^{-4} = -3.97 \times 10^{-4} < -0.001 \text{ in/in.}$$

$$\text{From the Fig. 4.2, } \epsilon_o = 0.002 = 2 \times 10^{-3} \text{ in/in.}$$

$$c = 0.9" , \quad \phi = 1.11 \times 10^{-3} \text{ rad/in.} \quad \epsilon_{cc} = 1.08 \times 10^{-3} \text{ in/in.}$$

$$C_c = 12.5 (0.9)^2 \times 3.75 (1.11 \times 10^{-3}) / 2 \times 10^{-3} \times [1 - (1.11 \times 10^{-3} \times 0.9) / 3 \times 2 \times 10^{-3}] = 17.56^k.$$

$$\epsilon_{ps} = 2.48 \times 10^{-3} + 1.08 \times 10^{-3} = 3.56 \times 10^{-3} \text{ in/in.}$$

$$f_{ps} = 101.70 \text{ ksi.}$$

$$T = 8 \times 0.021 \times 101.70 \times 10^3 = 17.23^k. \text{ Ok.}$$

$$x = c [(8\epsilon_o - 3\phi c) / (12\epsilon_o - 4\phi c)] = 0.9 \times [13.003 \times 10^{-3} / 20.004 \times 10^{-3}] = 0.585 \text{ inch.}$$

$$M = C_c [0.975 + 0.585] = 27.39^k. = 2282.80 \#,$$

at $\phi = 1.11 \times 10^{-3} \text{ rad/in.}$

e. with top fiber strain 0.002 :

$$c = 0.75 \text{ inch.}$$

$$\phi = 2.67 \times 10^{-3} \text{ rad/in.}$$

$$\epsilon_{cc} = 3 \times 10^{-3}$$

$$C_c = 12.5 \times (0.75)^2 \times 3.75 \times (2.67 \times 10^{-3} / 2 \times 10^{-3}) [1 - (2.67 \times 10^{-3} \times 0.75 / 3 \times 2 \times 10^{-3})] \times 0.66625 = 23.45^k.$$

$$\epsilon_{ps} = 2.48 \times 10^{-3} + 3 \times 10^{-3} = 5.48 \times 10^{-3} \text{ in/in.}$$

$$f_{ps} = 5.48 \times 10^{-3} \times 28.57 \times 10^3 = 156.56 \text{ ksi}$$

$$T = 8 \times 0.021 \times 156.56 = 26.30^k > C_c.$$

Second trial is required.

$$c = 0.8 \text{ inch.}$$

$$\phi = 2.5 \times 10^{-3} \text{ rad/in.}$$

$$\epsilon_{cc} = 2.68 \times 10^{-3} \text{ in/in.}$$

$$C_c = 25.0^k.$$

$$x = 0.8 [(8 \times 2 \times 10^{-3} - 3 \times 2.5 \times 10^{-3} \times 0.8) / (12 \times 2 \times 10^{-3} - 4 \times 2.5 \times 10^{-3} \times 0.8)] = 0.8 \times (10 \times 10^{-3} / 16 \times 10^{-3}) = 0.5".$$

$$M = C_c (1.1075 + 0.5) = 25 \times 1.6075 = 40.1875^k = 3348.95\#.$$

at $\phi = 2.5 \times 10^{-3} \text{ rad/in.}$

APPENDIX-5

Theoretical Deflection Computation :

a. *One way slab* :

By elastic method :

The equation of deflection produced by the prestress only is given by: $w = (Fex / 2EI)(L-x)$ in.

The equation of deflection produced by the uniformly distributed load: $w = (q/24EI)(L^3x - 2Lx^3 + x^4)$ in.

at $x = L/2$

$$w = (5/384)(qL^4/EI) = 0.013 (qL^4/EI) \text{ in.}$$

at $x = L/4$

$$w = (57/6144)(qL^4/EI) = 0.009277(qL^4/EI) \text{ in.}$$

Deflection at center point :

$$I = bh^3/12 = 42.875 \text{ in}^3$$

$$E_c = 2.905 \times 10^6 \text{ psi.}$$

$$L^4/EI = 29.237$$

$$w_{3.5} = 0.0088793q \text{ in.}$$

$$w_{2.5} = 0.0243645q \text{ in.}$$

Center point deflection for slab of depth 3.5" :

Load in psf.	q in lb/ft.	Deflection in inch.
21	1.75	0.01554
83	6.92	0.06144
104	8.67	0.07698
125	10.41	0.09240
167	13.92	0.12360

Center point deflection for slab of depth 2.5" :

Load in psf.	q in lb/ft.	Deflection in inch.
21	1.75	0.0426
83	3.33	0.1680
104	8.67	0.2110
125	10.41	0.2530
146	10.41	0.2530
167	13.92	0.3386

at 1/4th span of the slab :

$$w = 0.009277343 qL^4/EI$$

$$w_{2.5"} = 0.01736q \text{ in.}$$

$$w_{3.5"} = 0.0063263q \text{ in.}$$

1/4 span deflection for slab depth 2.5" :

Load in psf.	q in psi.	Deflection in inch.
20	1.667	0.0289
40	3.334	0.0578
60	5.000	0.0868
80	6.667	0.1157
100	8.334	0.1446
120	10.000	0.1736
140	11.666	0.2025
160	13.334	0.2314
180	15.000	0.2604

1/4th span deflection for slab depth 3.5" :

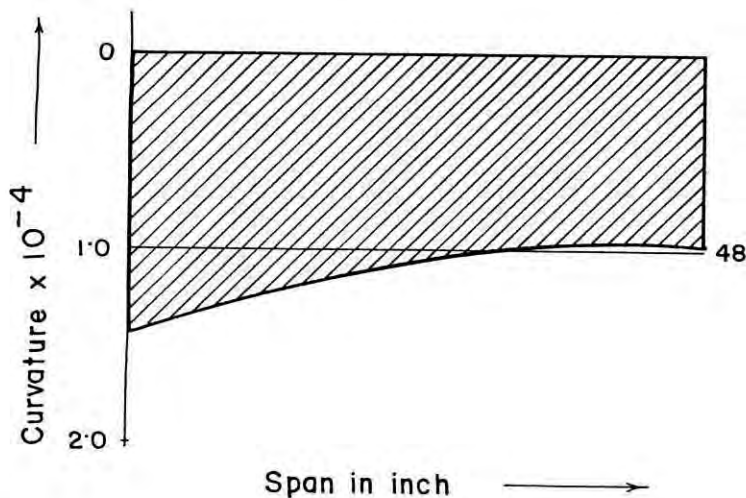
Load in psf.	q in psi.	Deflection in inch.
20	1.667	0.0105
40	3.334	0.0210
60	5.000	0.0316
80	6.667	0.0421
100	8.334	0.0527
120	10.000	0.0633
140	11.667	0.0738
160	13.334	0.0844
180	15.000	0.0949

From moment-curvature curve :

The equation for calculating deflection from M - ϕ curve is given by:

$$w = (\Delta x^2/2) [h_1 + 3h_2 + \dots + (2n-1)h_n]$$

At self weight only:

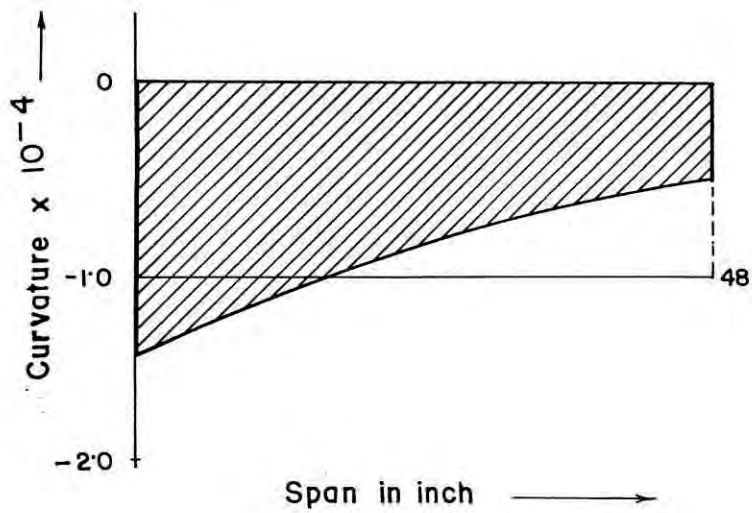


$$\Delta x = 3.2" , \quad \Delta x^2/2 = 5.12 \times 10^{-4}$$

$$w = -5.12 \times 10^{-4} [1.42 + 4.11 + \dots + 27.608]$$

$$= -5.12 \times 10^{-4} \times 232.893 = - 0.11924"$$

At 50 psf. load:

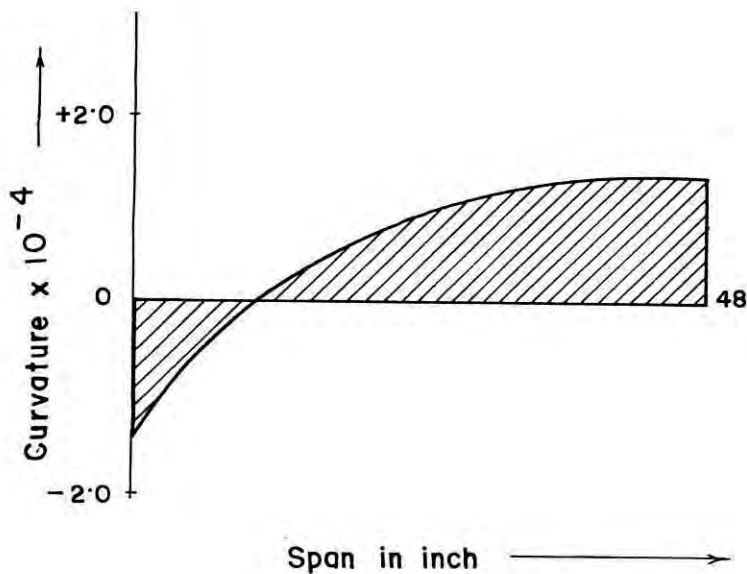


$$\Delta x^2/2 = 5.12 \times 10^{-4}$$

$$w = -5.12 \times 10^{-4} [1.4 + 3 \times 1.32 + \dots + 29 \times 0.525]$$

$$= -0.0845 \text{ inch.}$$

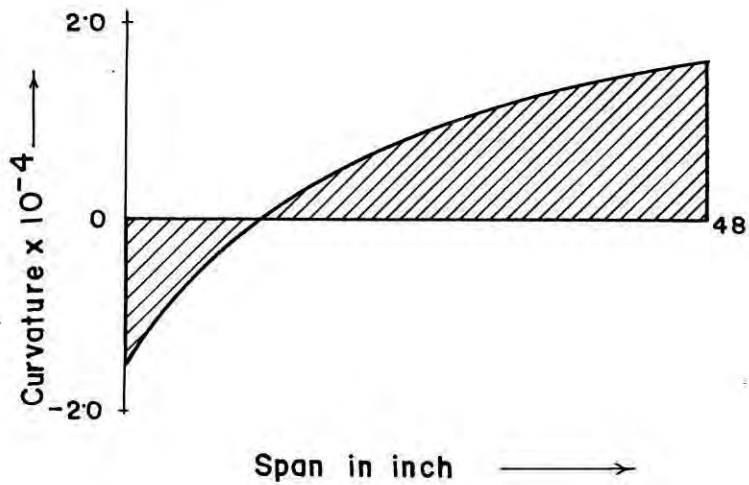
At 114 psf. loads:



$$w = 5.12 \times 10^{-4} [-1.16 - 3 \times 2.04 - \dots + 29 \times 39.44]$$

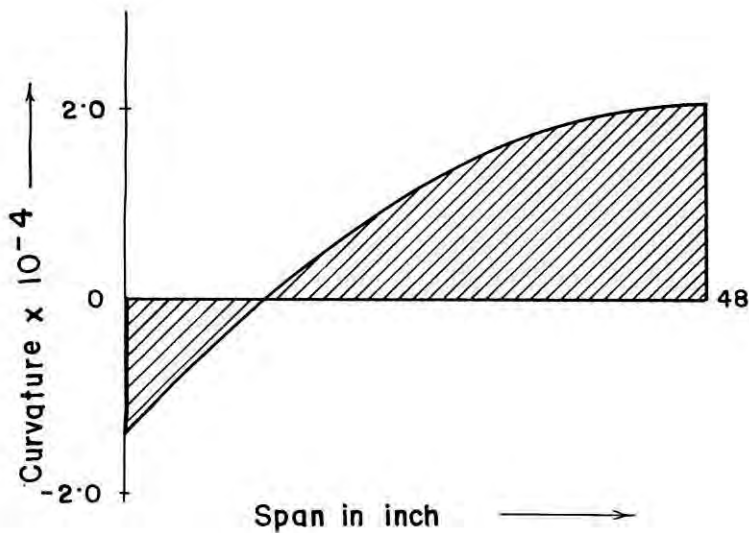
$$= 5.12 \times 10^{-4} \times 231.67 = 0.1186 \text{ inch.}$$

At zero steel strain (155.125 psf.):



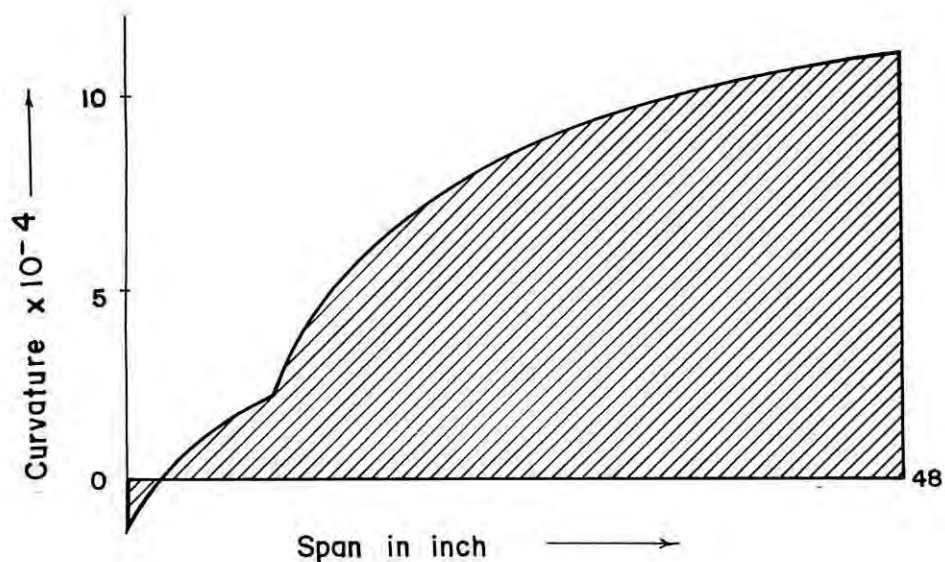
$$w = 5.12 \times 10^{-4} \times 248.07 = 0.127 \text{ inch.}$$

At end point of uncracked section (176 psf.):



$$w = 5.12 \times 10^{-4} \times 335,53 = 0.172 \text{ inch.}$$

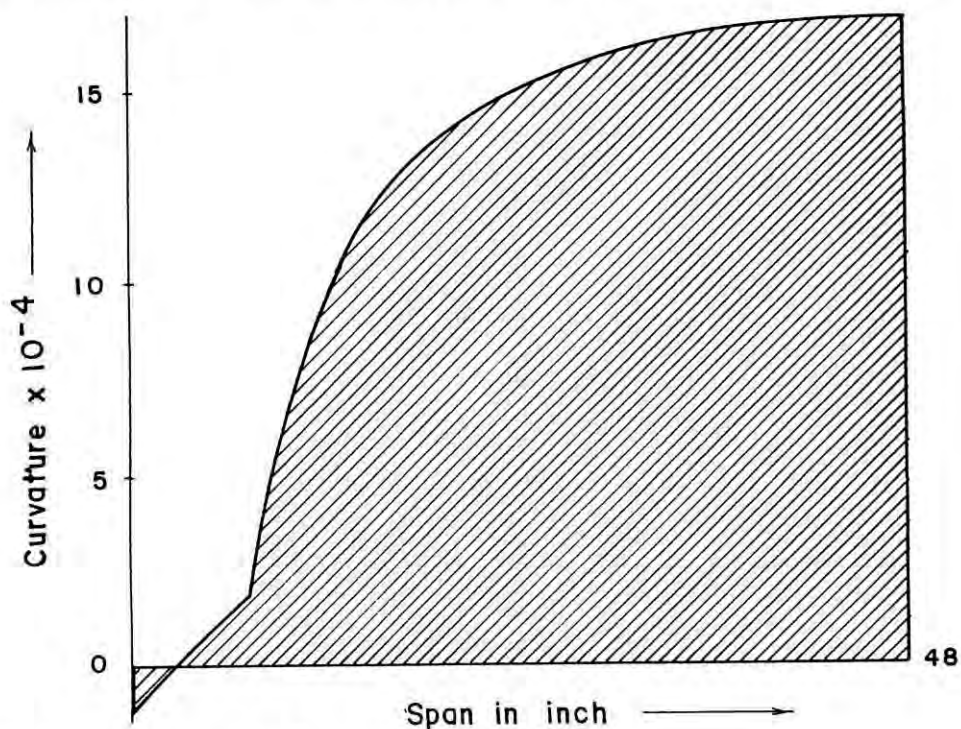
At 0.001 top fiber strain (285.31 psf.):



$$\Delta x = 2.4 \times 10^{-4} \text{ inch}, \quad \Delta x^2/2 = 2.88 \times 10^{-4}$$

$$w = 2.88 \times 10^{-4} [3609.125] = 1.0394 \text{ inch.}$$

At 0.0015 top fiber strain (347.0 psf.):



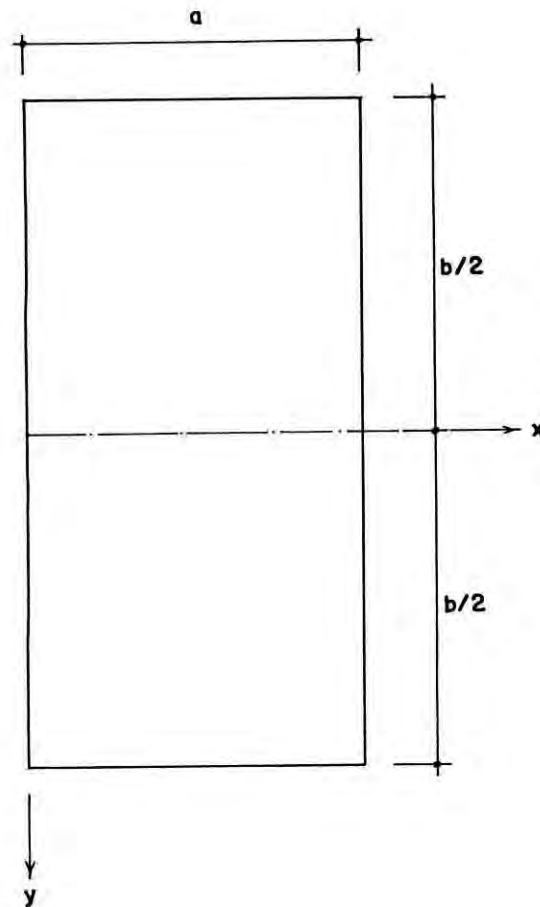
$$\Delta x^2/2 = 2.88 \times 10^{-4}$$

$$w = 2.88 \times 10^{-4} [5987.235] = 1.7243 \text{ inch.}$$

b. two way rectangular slab :

The equation of deflection surface: $\frac{\partial^4 w}{\partial x^4} + 2 \frac{\partial^4 w}{\partial x^2 \partial y^2} + \frac{\partial^4 w}{\partial y^4} = \frac{q}{D}$

where, w is deflection, q is transverse load, D is flexural rigidity of the plate.



$$w = \frac{4qa^4}{\pi^5 D} \sum_{m=1,3,\dots}^{\infty} \frac{1}{m^5} \left(1 - \frac{\alpha_m \tanh \alpha_m + 2}{2 \cosh \alpha_m} \cosh \frac{2\alpha_m y}{b} + \frac{\alpha_m}{2 \cosh \alpha_m} \frac{2y}{b} \sinh \frac{2\alpha_m y}{b} \right) \sin \frac{m\pi x}{a}$$

from which the deflection at any point can be calculated by using tables of hyperbolic function.

where $m\pi b \setminus 2a = \infty_m$

$$b \setminus a = 12 \setminus 8 = 1.5$$

$$a^4 = 84.9346 \times 10^6 \text{ in}^4.$$

$$D = Eh^3 \setminus 12(1 - \nu^2)$$

$$E_c = 2.905 \times 10^6 \text{ psi.}$$

$$h = 2.50" \text{ and } 3.50"$$

$$\nu = 0.15 \text{ (for concrete)}$$

$$D_{2.5} = \frac{2.905 \times 10^6 \times 2.5^3}{12(1 - 0.15^2)} = \frac{45.39 \times 10^6}{11.73} = 3.87 \times 10^6 \text{ #"}^2$$

$$D_{3.5} = \frac{2.905 \times 10^6 \times 3.5^3}{12(1 - 0.15^2)} = \frac{124.55 \times 10^6}{11.73} = 10.59 \times 10^6 \text{ #"}^2$$

Deflections for the points 4, and 5.

When the slab depth is 2.50"

Load in psf.	q in psi.	Deflection in inch.
20	0.139	0.023
40	0.278	0.046
60	0.417	0.069
80	0.555	0.092
100	0.694	0.115
120	0.833	0.138
140	0.972	0.161
160	1.111	0.184
180	1.250	0.207

When slab depth is 3.50"

Load in psf.	q in psi.	Deflection in inch.
20	0.138	0.008
40	0.277	0.016
60	0.416	0.025
80	0.555	0.034
100	0.694	0.042
120	0.833	0.050
140	0.972	0.059
160	1.111	0.067
180	1.250	0.076

Deflections for the points 2, and 6.

When the slab depth is 2.50"

Load in psf.	q in psi.	Deflection in inch.
20	0.139	0.017
40	0.278	0.035
60	0.417	0.052
80	0.555	0.070
100	0.694	0.087
120	0.833	0.104
140	0.972	0.122
160	1.111	0.139
180	1.250	0.157

When slab depth is 3.50"

Load in psf.	q in psi.	Deflection in inch.
20	0.139	0.006
40	0.278	0.013
60	0.417	0.019
80	0.555	0.025
100	0.694	0.031
120	0.833	0.038
140	0.972	0.044
160	1.111	0.051
180	1.250	0.057

Deflections for the points 1,3,7,and 8.

When the slab depth is 2.50"

Load in psf.	q in psi.	Deflection in inch.
20	0.139	0.012
40	0.278	0.025
60	0.417	0.037
80	0.555	0.050
100	0.694	0.063
120	0.833	0.075
140	0.972	0.088
160	1.111	0.100
180	1.250	0.113

When slab depth is 3.50"

Load in psf.	q in psi.	Deflection in inch.
20	0.139	0.005
40	0.278	0.009
60	0.417	0.014
80	0.555	0.018
100	0.694	0.023
120	0.833	0.027
140	0.972	0.032
160	1.111	0.037
180	1.250	0.041

APPENDIX-6

Computation of Cracking and Ultimate Load Capacity.

a. Computation of cracking loads:

$$f_r = 9.0\sqrt{f'_c}, \text{ where } f'_c \text{ is in psi.}$$

For 2.50" depth slab :

$$F = 8 \times 0.021 \times 65625 = 11,025^\#.$$

$$e = 1.25 - 0.75 = 0.5 \text{ inch.}$$

$$I = 15.624 \text{ in}^4.$$

$$c = 1.25 \text{ inch.}$$

$$A_c = 30 \text{ in}^2.$$

For 3.50" depth slab :

$$F = 6 \times 0.021 \times 65625 = 8268.75^\#.$$

$$e = 1.75 - 0.75 = 1.00 \text{ inch.}$$

$$I = 42.875 \text{ in}^4.$$

$$c = 1.75 \text{ inch.}$$

$$A_c = 42.00 \text{ in}^2.$$

$$M_{cr} = Fe + FI/A_c + f_r I/c \dots \dots \dots [1]$$

Maximum bending moment, hence the fiber stress, occurs at the center of the slab (as supported two opposite edges only it acts as simply supported element).

$$M_{cr} = (qL^2)/8 = 8q \dots \dots \dots [2]$$

Types	$f'_c, \text{psi.}$	$f_r, \text{psi.}$	$M_{cr}, \text{ft-lb}$	Cracking load, psf	Cracking live load
I	3750.0	551.00	1416.00	177.00	149.00
II	3763.0	552.00	1417.00	177.00	149.00
III	3763.0	552.00	2276.00	284.50	244.80
IV	3724.0	549.00	2270.00	284.00	244.00

b. Determination of flexural stresses in shearkeys:

The flexural stresses at the centre point of middle shearkeys for the all types of slabs can be computed using the following relationship [9],

$$M_y = v \frac{qx(a-x)}{2} - qa^2\pi^2 \sum_{m=1,3,\dots}^{\infty} m^2 [2B_m + (1-v)A_m] \sin \frac{m\pi b}{a}$$

where,

$$A_m = -\frac{2(\alpha_m \tanh \alpha_m + 2)}{\pi^5 m^5 \cosh \alpha_m}$$

$$B_m = \frac{2}{\pi^5 m^5 \cosh \alpha_m}$$

$$\alpha_m = m\pi b/2a$$

$$\alpha_1 = 2.36$$

$$\alpha_3 = 7.07$$

$$\alpha_5 = 11.78$$

For $m = 1$

$$\tanh \alpha_1 = 0.98$$

$$\cosh \alpha_1 = 102.19$$

$$\pi^5 = 306.00$$

$$A_1 = - 2.76 \times 10^{-4}$$

$$B_1 = 6.39 \times 10^{-5}$$

$$\sin \pi b/a = 1.0$$

$$m^2 [2B_1 + (1 - \nu) A_1] \sin \pi x/a = - 10.68 \times 10^{-5}$$

For $m = 3$

$$\tanh \infty_3 = 0.99$$

$$\cosh \infty_3 = 586.89$$

$$A_3 = - 4.16 \times 10^{-7}$$

$$B_3 = 4.58 \times 10^{-8}$$

$$\sin 3\pi b/a = - 1.0$$

$$\nu q x(a-x)/2 = 148.8^{\#}$$

$$q a^2 \pi^2 = 78325.20$$

$$m^2 [2B_3 + (1- \nu) A_3] \sin 3\pi x/a = + 0.24 \times 10^{-5}$$

For slab Type - II:

$$M_y = 157.0^{\#} = 1884.0^{\#}$$

$$\text{Flexural stress} = 150.70 \text{ psi.}$$

For slab Type -III and Type - IV:

$$M_y = 173.44^{\#} = 2081.0^{\#}$$

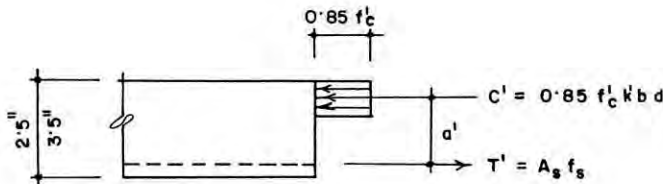
$$\text{Flexural stress for Type -III} = 76.89 \text{ psi.}$$

$$\text{Flexural stress for Type -IV} = 84.96 \text{ psi.}$$

c. Computation of ultimate load:

Assuming that the prestressing steel had sufficient ductility, the slab would reach its ultimate capacity when moment across the entire crack has reached a uniform value equal to the ultimate resisting moment of the section.

An average resisting moment per linear foot of width could be approximated by applying Whitney's theory using a rectangular stress block in the concrete.



$$M' = T'a' = C'a'$$

$$T' = f_{ps} A_s = C' = 0.85 f'_c k'bd.$$

for $b = 12$ inch, $f_{pu} = 125000$ psi.

for $t = 2.50$ inch, $A_{ps} = 8 \times 0.021 = 0.168$ in².

for $t = 3.50$ inch, $A_{ps} = 6 \times 0.021 = 0.126$ in².

The average external moment per ft. of width of slab along the center line crack is given by:

$$M_{cr} = \frac{q \times 8^2}{8} = 8q \dots \dots \dots [3]$$

$$k'd = \frac{f_{ps} A_{ps}}{0.85 f'_c b} = \frac{f_{ps} A_{ps}}{0.85 \times 12 f'_c} = \frac{9.80 \times 10^{-2} f_{ps} A_{ps}}{f'_c}$$

$$M' = T'a' = A_{ps} f_{ps} (d - K'd/2) \dots \dots \dots [4]$$

The ACI code introduces, the flexural strength reduction factor, $\phi = 0.9$, the equation [4] becomes -

$$M' = 0.9 [A_{ps} f_{ps} (d - K'd/2)] \dots \dots \dots [5]$$

Equating the equations [3] and [5]

$$8q = 0.9 A_{ps} f_{ps} (d - K'd/2)$$



For a bonded cable this value is normally taken equal to the ultimate strength of the steel.

Types	K'd in inch	Lever arm in inch	Ultimate resisting moment, M', ft-lb	Total Ultimate load in psf.	Total Live load at Ultimate, q in psf.
I	.548	1.47	2325.00	290.6	262.6
II	.547	1.47	2325.00	290.6	262.6
III	.410	2.54	3000.00	375.0	335.0
IV	.414	2.54	3004.00	375.5	335.5